Techno-economic evaluation of Organic Solvent Nanofiltration separation to recover dewaxing solvent from lube-oil

by

Bella Ann Dorrington

Thesis presented in partial fulfilment
of the requirements for the Degree

of

MASTER OF ENGINEERING
(CHEMICAL ENGINEERING)

in the Faculty of Engineering
at Stellenbosch University

Supervisor

Prof. AJ Burger

March 2020

DECLARATION

By submitting this thesis electronically, I declare that the entirety of the work contained therein is my own, original work, that I am the sole author thereof (save to the extent explicitly otherwise stated), that reproduction and publication thereof by Stellenbosch University will not infringe any third party rights and that I have not previously in its entirety or in part submitted it for obtaining any qualification.

Date: March 2020

PLAGIARISM DECLARATION

1. Plagiarism is the use of ideas, material and other intellectual property of another's work and to present is as my own.

2. I agree that plagiarism is a punishable offence because it constitutes theft.

3. I also understand that direct translations are plagiarism.

4. Accordingly, all quotations and contributions from any source whatsoever (including the internet) have been cited fully. I understand that the reproduction of text without quotation marks (even when the source is cited) is plagiarism.

5. I declare that the work contained in this assignment, except where otherwise stated, is my original work and that I have not previously (in its entirety or in part) submitted it for grading in this module/assignment or another module/assignment.

Student number: ……..

Initials and surname: ……..

Signature: ……..

Date: ……..

ABSTRACT

To recover the solvent from dewaxed lube-oil, classical separations such as evaporation and distillation are typically used. In the past decade separations that consume less energy and utilities have been investigated. One such technology is organic solvent nanofiltration (OSN). OSN is the size-exclusion of species over a membrane. Many studies have shown that OSN separation consumes less energy than evaporation and distillation. However, few have compared the cost of OSN to classical separations. Therefore, the aim of this investigation was to simulate and compare the cost and energy demand of a conceptual OSN unit with classical separation for the recovery of solvent from dewaxed lube-oil. Cost was expressed as the annualised capital plus total operating costs per year. Energy demand is the total energy consumed per volume of solvent recovered.

Max-Dewax was the first and largest OSN membrane unit to recover solvent from lube-oil. For this investigation, a conceptual OSN unit was developed based on Max-Dewax to treat a 480 m^3/h feed containing 19% lube-oil, and 46% methyl-ethyl ketone (MEK) and 35% toluene as solvents. Membrane permeate rates for MEK, toluene and lube-oil were 360, 91 and 1 mm/h. Long-term membrane stability was based on a 28% average decline in flux over a membrane life of 24 months. At an operating pressure of 42 bar, the OSN unit could achieve a 51% recovery of solvent at a 99% purity and average flux of 11 $L/m^2/h$. A sensitivity analysis revealed that specific membrane cost, membrane life, flux decline over membrane life, operating pressure and membrane permeate rates had the biggest influence on the cost and energy demand of the OSN unit.

The solvent remaining in the concentrated product from the OSN unit was further recovered by evaporation and distillation. The complete solvent recovery unit is referred to as hybrid-OSN and could recover 98% solvent at a 99% purity. The simulated cost of the hybrid-OSN unit for a specific membrane cost of 3200 ZAR/m^2 effective area was 127 ZAR/m^3 solvent recovered per year. The energy demand was 177 kWh/m^3 solvent recovered. Compared to a classical separation including only evaporation and distillation, the energy demand of the hybrid-OSN unit was 64 kWh/m^3 less. However, the hybrid-OSN unit was 40 ZAR/m^3 more than the classical separation.

Process simulations revealed that for a membrane cost of 990 ZAR/m^2 and higher membrane permeate rates for MEK and toluene of 540 and 137 mm/h, the energy demand of the hybrid-OSN unit was 140 kWh/m^3 and the cost equal to the classical separation. Extending membrane life to 72 months at a membrane cost of 1600 ZAR/m^2, the cost of the hybrid-OSN and classical separation were also equal. Moreover, for a membrane cost of 630 ZAR/m^2 and 14% decline in flux after 24 months, the energy demand of the hybrid-OSN unit was 163 kWh/m^3 and the cost was equal to the classical separation.

Typical results from process simulations showed that under certain conditions, OSN membranes bare the economic and energy potential to assist classical solvent recovery units. However, the profitability of a hybrid-OSN unit largely depends on the cost of membrane modules and long-term membrane performance such as flux decline over membrane life.

Key words: Organic solvent nanofiltration (OSN), hybrid-OSN, process simulation, solvent recovery, sensitivity analysis.

OPSOMMING

Om die oplosmiddel uit ontwasse smeerolie te herwin, word klassieke skeidings soos verdamping en distillasie tipies gebruik. In die laaste dekade is skeidings wat minder energie en utiliteite gebruik ondersoek. Een so ’n tegnologie is organiese oplosmiddelnanofiltrasie (OSN). OSN funksioneer deur middel van die grootte-uitsluiting van spesies oor ’n membraan. Baie studies wys dat OSN-skeiding minder energie as verdamping en distillasie gebruik. Min het egter die koste van OSN teenoor klassieke skeidings vergelyk. Daarom is die doel van hierdie ondersoek om die koste- en energievereistes te simuleer en ’n konsepsionele OSN-eenheid met ’n klassieke skeiding vir die herwinning van oplosmiddel uit ontwasse smeerolie, te vergelyk. Koste is uitgedruk as die jaarlike kapitaal plus totale bedryfskostes per jaar. Energievereistes is die totale energiegebruik per volume oplosmiddel herwin.

Max-Dewax was die eerste en grootse OSN-membraaneenheid om oplosmiddel uit smeerolie te herwin. Vir hierdie ondersoek is ’n konsepsuele OSN-eenheid ontwikkel gebaseer op Max-Dewax om ’n 480 m^3/h voer, wat 19% smeerolie en 46% metieletielketoon (MEK) en 35% tolueen as oplosmiddels gebruik het, te behandel. Membraan deurlaatbaarheid vir MEK, tolueen en smeerolie was 360, 91 en 1 mm/h. Langtermyn membraanstabiliteit is gebaseer op ’n 28% gemiddelde afname in fluks oor ’n membraanleeftyd van 24 maande. By ’n toegepaste druk van 42 bar, het die OSN-eenheid ’n 51% herwinning van oplosmiddel by ’n 99% suiwerheid en gemiddelde fluks van 11 L/m^2/h behaal. ’n Sensitiwiteitsanalise het ten toon gestel dat spesifieke membraankoste, membraanleeftyd, fluks afname oor membraanleeftyd, toegepaste druk en membraan deurlaatbaarheid die grootste invloed op die koste- en energievereistes van die OSN-eenheid gehad het.

Die oplosmiddel wat in die gekonsentreerde produk van die OSN-eenheid oorbly, is verder herwin deur verdamping en distillasie. Die algehele oplosmiddelherwinningseenheid word na verwys as hibried-OSN en kan 98% oplosmiddel by 99% suiwerheid herwin. Die gesimuleerde koste van die hibried-OSN-eenheid vir ’n spesifieke membraankoste van R3 200/m^2 doeltreffende area was R127/m^3 herwin per jaar. Die energie-aanvraag was 177 kWh/m^3 oplosmiddel herwin. Vergeleke met ’n klassieke skeiding wat slegs verdamping en distillasie behels, is die energievereiste van die hibried-OSN-eenheid 64 kWh/m^3 minder. Die hibried-OSN-eenheid was wel R40/m^3 meer as die klassieke skeiding.

Prosessimulasies het bekend gemaak dat vir ’n membraankoste van R990/m^2 en hoër membraan deurlaatbaarheid vir MEK en tolueen van 540 en 137 mm/h, die energievereiste van die hibried-OSN-eenheid 140 kWh/m^3 was, en die koste gelyk aan die klassieke skeiding. Met vergroting van membraanleeftyd na 72 maande by ’n membraankoste van R1 600/m^2, was die koste van die hibried-

OSN en klassieke skeiding ook gelyk. Verder, vir ’n membraankoste van R630/m^2 en 14% afname in fluks na 24 maande, was die energievereiste van die hibried-OSN-eenheid 163 kWh/m^2 en die koste gelyk aan die klassieke skeiding.

Tipiese resultate van prosessimulasies het gewys dat onder sekere omstandighede, OSN-membrane dieselfde ekonomiese en energiepotensiaal het om klassieke oplosmiddelherwinningseenhede by te staan. Die winsgewendheid van ’n hibried-OSN-eenheid is egter grootliks afhanklik van die koste van membraanmodules en langtermyn doeltreffendheid soos fluks afname oor membraanleeftyd.

Sleutelwoorde: Organiese oplosmiddelnanofiltrasie (OSN), hibried-OSN, prosessimulasie, oplosmiddelherwinning, sensitiwiteitsanalise.

TABLE OF CONTENTS

LIST OF SYMBOLS

A	Area	m^2
α	Persemselectivity	-
b	Membrane permeate rate	mm /h or L /m^2/h
C	Concentrate stream	kg/s or m^3/h
c	Concentration	mol /L
D	Diameter	m
ε	Error	%
η	Efficiency	-
F	Mass flowrate	kg /s
J	Permeate flux	L /m^2/h
m	Rate of flux decline	1/h
N	Number or amount	-
n	Number of years	-
O	Output	-
P	Pressure	Pa
$\Delta\pi$	Osmotic pressure gradient	Pa
ϕ	Recovery	%
Q	Heat duty	kW
R	Membrane rejection	-
R_c	Universal gas constant	J /mol/K
ρ	Density	kg /m^3
t	Time	h
$\dot{V}$	Volumetric flowrate	m^3 /h
v	Molar volume	m^3/mol
W	Work	kW
x	Compositional fraction	-

SUBSCRIPTS

C	Concentrate
F	Feed
FD	Flux decline
FF	Fresh feed
k	Species
MAX	At maximum
MF	Mixed feed
MIN	At minimum
P	Permeate
PC	Preconditioning
R	Retentate
RR	Retentate recycle
SR	Solvent recovery

SUPERSCRIPTS

M	Mass
V	Volume

ABBREVIATIONS

ASW	Aspen simulation worksheet
CS	Carbon steel
Centrif.	Centrifugal
CEPCI	Chemical engineering plant cost index
CI	Capital investment
DP	Differential pressure
EAC	Equivalent annual cost
EUR	Euro

FCI	Fixed capital investment
MOC	Material of construction
MM	Membrane module
MEK	Methyl-ethyl ketone
MW	Molecular weight
MWCO	Molecular weight cut-off
OSN	Organic solvent nanofiltration
PCE	Purchased cost for equipment
PPC	Physical plant cost
PDMS	Poly(dimethylsiloxane)
PTSP	Poly[1-(trimethylsilyl)-1-propyne]
PEI	Polyetherimide
PI	Polyimide
PSE	Process simulation environment
PV	Pressure vessel
SI	Sensitivity index
ZAR	South African rand
SARS	South African revenue services
SEC	Specific energy consumption
SWM	Spiral wound membrane
304 SS	Stainless steel type 304
TAC	Total annualised cost
TMP	Transmembrane pressure
USD	United States dollar

DEFINITIONS

Classical separation: Evaporation or distillation.

Concentrate: Retained concentrated product from a stage. If a recycle-loop is present, the concentrate would be the remaining retentate not recycled.

Concentration polarisation: Reversible, immediate accumulation of retained solutes.

Dewaxed filtrate: Oil product after wax has been removed by means of rotary drum vacuum filtration.

Driving force: Positive pressure difference or chemical potential leading to the transport of species across a membrane.

Effective membrane area: Membrane area available for permeation. It excludes the area occupied by spacers and membrane supports.

Fixed capital investment: Includes the total purchased cost for equipment, the installation thereof and indirect costs for engineering, contractor's fees and contingency.

Flux decline: Decline in average membrane flux over membrane life. Flux decline is the reduction from initial to final membrane flux due to concentration polarisation, membrane compaction and fouling.

Fouling phenomena: Irreversible adsorption, pore-blocking and deposition of solidified solutes occurring over a long period of time.

Hybrid-OSN: Separation unit that includes OSN separation followed by classical separation.

Operating pressure: Applied feed pressure to an OSN unit for membrane separation.

Membrane module: Multiple membrane sheets wrapped within a tubular module.

Membrane skid: Membrane elements contained in pressure vessels that are mounted onto a metal framework.

Membrane stage: Pressure vessels that contain serial membrane modules are arranged in parallel with a retentate recycle loop.

Membrane system: Includes membrane modules and pressure vessels arranged in a stage configuration.

Membrane unit: Includes membrane modules, pressure vessels and additional plant equipment such as pumps, tanks, heaters and instruments.

Oil distillate: Crude oil reclaimed as one of the petroleum fractions produced in conventional distillation.

Permselectivity: Membrane permeate rate of permeating species (i.e. solvents) relative to that of the solute (i.e. the lube-oil).

Physical plant cost: Includes the purchased cost of equipment and the installation (i.e. erection, piping, instrumentation, electrical and process buildings) thereof.

Preconditioning solvent: Clean solvent used to wash out preservative and prepare active membrane layer of newly installed membrane modules.

Retentate: Concentrated product retained on the feed-side of the membrane.

Taper: Reducing the number of parallel pressure vessels per stage towards the end of a membrane system.

Traditional process equipment: Includes well-established process units such as pumps, heat exchangers, evaporators and distillation columns.

Transmembrane pressure: Difference between the operating pressure and permeate pressure over a membrane.

Transport model: Describes the movement of species through a membrane.

CHAPTER 1: INTRODUCTION

The depletion of fossil resources, consequences of climate change and strict environmental regulations are challenging chemical industries to minimise their impact on the environment. In South Africa, 66% of the total energy supply in 2010 was generated from coal combustion (Maleka et al., 2010). In addition, 50% of the industrial energy demand goes towards separation processes (Sholl & Lively, 2016; Maleka et al. 2010).

One example of an industrial separation process is the recovery of dewaxing solvent from lube-oil at a refining plant. Such recovery systems often involve classical separations like evaporation and distillation (Sequiera, 1991; Werth et al., 2017b; Gould et al., 1994; Richter et al., 2001; Pokorny & Speer, 1956). The main contributions toward total energy consumed by said separations are to create a vapour phase during evaporation (Werth et al., 2017b; Peshev and Livingston, 2013) and to supply heat to reboilers during distillation (Micovic et al., 2014). Over the past decade industries have considered incorporating technologies that are less energy intensive (Oatley-Radcliffe et al., 2017). One example of an alternative process that requires no phase change, and therefore becomes less energy intensive, is membrane separation.

Organic solvent nanofiltration (OSN) is a non-thermal, membrane separation that relies on the size-exclusion of species based on their molecular weights (Marchetti et al., 2014). An illustrative description is shown in Figure 1.1.

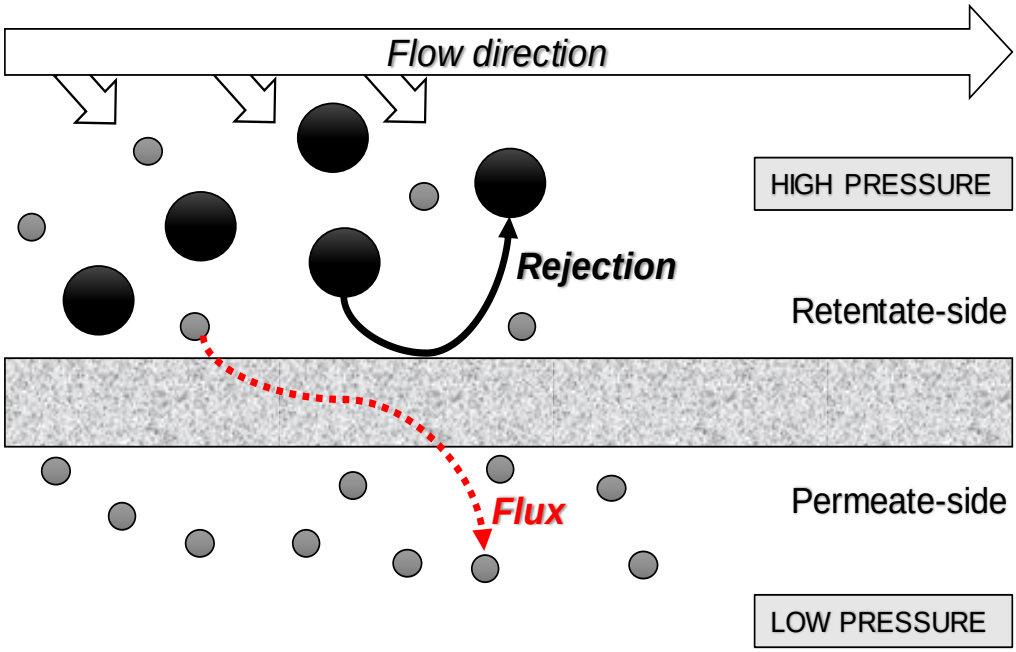

Figure 1.1: Transport phenomena across an OSN membrane. The solvent (●) will permeate through the membrane but the solute (●) will be rejected by the membrane and remain on the feed-side.

Referring to Figure 1.1, the separation performance of OSN membranes is measured in terms of permeate flux and solute rejection. The driving force is a positive pressure difference between the retentate and permeate sides. For a dewaxed lube-oil with a molecular weight of ≥ 350 g/mol dissolved in a solvent mixture of MEK (72 g/mol) and toluene (92 g/mol), the OSN membrane is more likely to allow toluene and MEK to pass through while the lube-oil is rejected (White and Nitsch, 2000). Consequently, the retentate-side becomes more concentrated in lube-oil as the permeate-side becomes richer in solvent. Some studies have measured the flux and rejection of similar feeds by means of bench-scaled experiments with OSN membranes (White and Nitsch, 2000; Kong et al., 2006; Yuan et al., 2014). These studies reported lube-oil rejections of 95 to 97% and permeate fluxes of 11 to 30 L/m^2/h under operating pressures of 20 and 40 bar.

The permeate flux and solute rejection across an OSN membrane can theoretically be predicted using transport models and mass balances. Such predictions have been demonstrated for the enrichment of aromatic streams (White, 2006), purification of a hydroformylation product stream (Micovic et al., 2014), recovery of solvent from non-edible oil (Werth et al., 2017b), the purification of residual solvent recovered from active pharmaceutical ingredients (Darvishmanesh et al., 2011) and the concentration of plant extracts (Peshev et al., 2011). White and Nitsch (2000) and Kong et al. (2006) recommended the solution-diffusion transport model to predict flux and rejection of an OSN membrane to recover dewaxing solvent from lube-oil but did not demonstrate the model's predicting performance.

The first large-scale, commercial demonstration of OSN separation was the implementation of the Max-Dewax membrane unit at the Exxon Mobil Beaumont Refinery (Bhore et al., 1999). The unit was designed for a feed capacity of 480 m^3/day and could recover up to 50% of solvent, thereby debottlenecking the downstream evaporator, distillation columns and lowering total plant energy demand by 20%. In addition, the capital investment of the Max-Dewax unit was only a third of a classical separation operating under the same feed capacity. The success of the project earned it the Kirkpatrick Honor award for chemical engineering achievement in 1999 (Kirkpatrick, 1999). The Max-Dewax unit included prefilters, high pressure feed pumps, multiple membrane modules coupled in series and process control instrumentation.

Similar designs for OSN units have been conceptualised for the purpose of process simulation. These conceptual designs typically involved a high-pressure feed pump, membrane modules coupled in series contained in pressure vessels, and multiple pressure vessels arranged in parallel referred to as a stage (Micovic et al., 2014; Werth et al., 2017b; Peshev and Livingston, 2013). Certain studies included a retentate recycle loop to maintain the permeate rate through a membrane module near the recommended flowrate supplied by the membrane manufacturer (Werth et al., 2017b; Peshev

and Livingston, 2013). Since commercial membrane purification units are well-established for wastewater treatment, many conceptual OSN designs have been based on typical nanofiltration units for wastewater treatment (Oatley-Radcliffe et al., 2017).

A commercial RO unit typically involves a feed intake, pretreatment system, pumps to increase pressure as well as a cleaning-in-place system (Accepta water treatment, 1997; Owen et al., 1995). According to an OSN membrane manufacturer, Evonik, cleaning-in-place is not recommended for OSN (Evonik GmbH, 2017). However, the manufacturer does suggest preconditioning after new OSN membranes have been installed to wash out the preservative that was used to store the membranes in. With regards to pretreatment, prefilters remove scale and wax crystals in the feed that might otherwise damage OSN membranes (Bhore et al., 1999; Gould et al., 1994). However, the conceptual designs developed by Werth et al. (2017b), Micovic et al. (2014) and Peshev and Livingston (2013) did not included these additional processing steps. It would be of interest to add a feed intake, pretreatment step and preconditioning step to develop a more realistic conceptualised representation of an OSN unit at a lube-oil refinery.

One of the many benefits of process simulations is that cost and energy comparisons between for example classical separation and separation by OSN can be performed. OSN separation has shown to be less energy intensive than classical separations for the concentration of plant extracts (Peshev and Livingston, 2013), purification of hydroformylation streams (Micovic et al., 2014), recovery of solvent from non-edible oil (Werth et al., 2017b) and the recovery of solvent from dewaxed lube-oil (Bhore et al., 1999). Although the cost of the Max-Dewax unit was only a third of that of classical separation, conceptualised OSN unit simulations by Micovic et al. (2014) and Werth et al. (2017b) revealed the opposite.

In addition to comparing the cost and energy of different process configurations, a sensitivity analysis can be a useful tool to identify important variables and parameters that will have a significant influence on the energy consumption and cost of a process (Pannell, 1997). Lee et al. (2017) observed that the cost of a membrane unit is sensitive to changes in specific membrane cost and membrane performance. This knowledge is valuable to optimise OSN unit operations.

The implementation of the Max-Dewax unit in 1999 revealed benefits including a reduced cost and energy consumption compared to classical separation. However, the question remains why OSN units for recovering solvent from dewaxed lube-oil is so sparse even though the cost and energy benefits of Max-Dewax are so apparent.

In a technical report on the Max-Dewax unit, it was shown that after a year and a half the permeate rate reduced by 27%. Since its first demonstration in 1999, membrane manufacturers have applied

additional treatment techniques to improve the long-term stability of OSN membranes. Through improving the stability, membranes can be kept on stream for longer durations, thus reducing the cost of membrane replacement. However, these additional treatments increase the cost to manufacture OSN membranes which will in turn increase the capital investment.

The 27% reduction in permeate rate after 18 months suggests that the long-term stability of the OSN membranes of the Max-Dewax unit could be improved through additional membrane treatment. The result is that the capital investment for the Max-Dewax unit might seem less attractive due to the more expensive membrane cost. This could be confirmed if the membrane price of the Max-Dewax unit was known; however, this information was not disclosed. Alternatively, varying the cost, membrane performance and long-term stability of an OSN membrane in a simulation could be used to quantify the influence on overall cost and energy consumption.

The aim of this investigation was therefore to simulate the cost and energy consumption of an OSN solvent recovery unit to compare with classical separations. The aim can be broken down in the following objectives and tasks:

First objective: Simulate the separation across an OSN unit that can maintain a capacity like the Max-Dewax unit. This is achieved through:

- Simulating the separation through a single membrane, and
- Simulating the separation across the entire unit involving multiple membranes.

Second objective: Do a conceptual design of an OSN unit that is like Max-Dewax by including the following equipment:

- Pumps,
- Tanks,
- Membrane modules and pressure vessels,
- Instrumentation,
- Pipes, valves and fittings,
- Filters, and
- Heaters.

Third objective: Estimate the cost of the conceptual OSN unit with regards to:

- The specific energy consumption (SEC),
- The fixed capital investment (FCI),
- Operating cost, and
- Total annualised cost (TAC).

The estimations were followed by a sensitivity analysis to evaluate the impact of changes in assumptions applied throughout the process simulation on cost (TAC) and energy consumption (SEC).

Fourth objective: Compare the estimated cost and energy consumed by a hybrid-OSN unit with classical separation through:

- Simulating the cost (TAC) and energy consumed (SEC) for a solvent recovery process at a lube-oil refinery involving classical separation,
- Simulating the TAC and SEC for a solvent recovery process at a lube-oil refinery involving hybrid-OSN, and
- Using the knowledge gained from the sensitivity analysis to draw further conclusions regarding the potential of hybrid-OSN compared to classical separation for the recovery of dewaxing solvent from lube-oil.

CHAPTER 2: LITERATURE REVIEW

The literature review explores three main areas:

- Conceptual process configurations of classical and OSN solvent recovery units,
- Separation by OSN, and the
- Cost and energy consumption of classical and OSN solvent recovery units.

A brief background of process configurations for the recovery of solvents is provided with a focus on where it takes place, why it is necessary and how OSN could be included. The focus is then shifted towards conceptual process configurations in literature with regards to classical solvent recovery units, OSN and hybrid-OSN units.

In the second section, the reader is provided with a background on permeate flux and solute rejection across an OSN membrane. The section then dives deeper into aspects affecting flux and rejection such as membrane characteristics for different solvent-solute-membrane combinations, transport modelling, long-term membrane performance, the membrane module and finally OSN unit configuration.

The third section provides a discussion on cost and energy comparisons made for classical, OSN and hybrid-OSN solvent recovery units.

2.1 Process configurations of classical, OSN and hybrid-OSN solvent recovery units

Solvent dewaxing of lube-oil is the removal of wax from unrefined oil distillates to improve the lubricating properties and cold-flow qualities of lube-oil (Jones & Pujado, 2006). The removed wax is a mixture of linear alkanes of chain lengths ranging from 17 to 40 carbon atoms (Khan et al., 2006; Mansoori et al., 2003). These wax-forming alkanes are removed by the following steps (Sequeira, 1991; Pitman and Harrison, 1982; Gould et al., 1994):

1. Diluting the oil distillate with an organic solvent to lower the viscosity of the feed,
2. Cooling the mixture down until wax crystals precipitate from the solution,
3. Removing the wax by means of rotary filtration under vacuum conditions, and
4. Concentrating the dewaxed, lube-oil filtrate through recovering the organic solvent which is reused in the first step.

An illustrative description of a typical solvent recovery units by classical separation is shown in Figure 2.1.

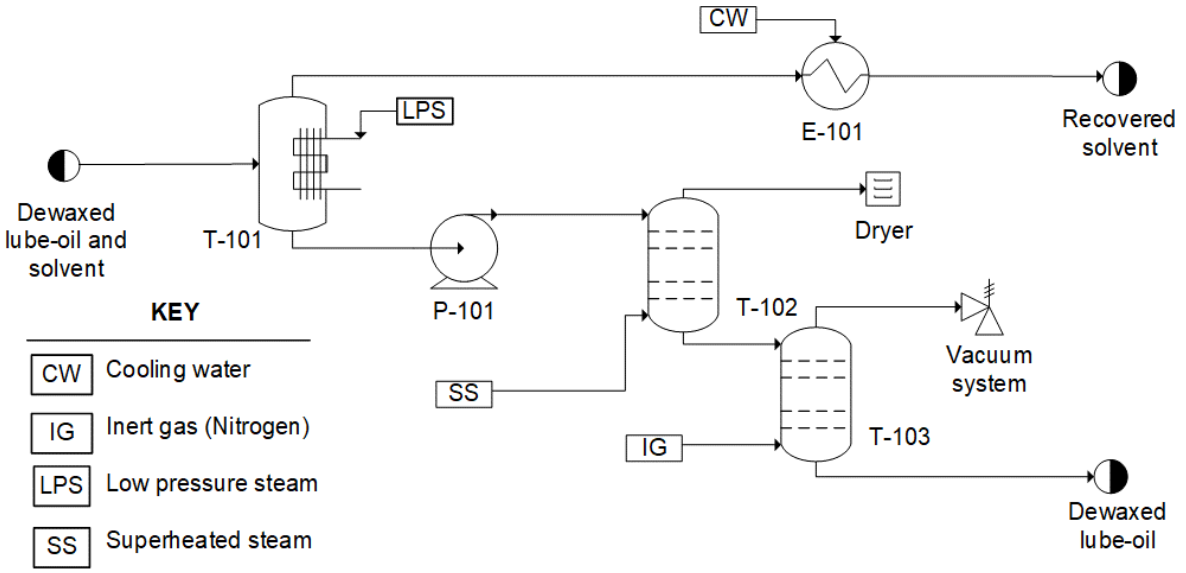

Figure 2.1: A typical solvent recovery unit at a lube-oil refining plant (Sequeira, 1991).

Some of the first solvent recovery units included a steam still, followed by a separating drum to remove entrained water coming from the steam (Pokorny and Speer, 1952). Thereafter, recovery units evolved to include evaporation and distillation for finer separations that could otherwise not be achieved with a single steam still. These more modern units such as the process configuration in Figure 2.1 typically include a series of evaporation steps under low, high and/or vacuum pressure followed by atmospheric steam stripping. The entrained water is finally removed by means of stripping with inert gas under vacuum pressure (Morris and Nixon, 1969; Pitman and Harrison, 1982; Gould et al., 1994; Mansoori et al., 2003; Jones and Pujado, 2006).

Classical separations are energy demanding and can sometimes be the most energy intensive step in an industrial process. In addition, 66% of South Africa's total energy supply is generated through coal combustion (Maleka et al., 2010). Coal is both a finite resource and harmful to the environment when volatile organic compounds from combustion are released to the atmosphere. Sholl and Lively (2016) estimated that membrane separations would consume 90% less energy than separations by distillation. Therefore, it is believed that including non-thermal separations such as OSN membranes could lower the national energy demand and minimise carbon emissions from coal combustion.

The use of separation by OSN to recover solvent from dewaxed lube-oil has been demonstrated through experiments with a polymeric nanofiltration membrane (White and Nitsch, 2000; Kong et al. 2006; Namvar-Mahboub and Pakizeh, 2013; Yuan et al., 2014). The studies demonstrated the viability of OSN to recover organic solvent at a rate of 11 to 30 L/h/m^2 at a solvent purity of up to 99% and operating pressure ranging from 20 to 40 bar.

The Max-Dewax unit was implemented at the Exxon Mobil Beaumont Refinery for a 19% lube-oil, 46% MEK and 35% toluene to demonstrate the benefits of OSN compared to classical separation. Exxon Mobil planned to increase the capacity at their Beaumont refinery by an additional 480 m^3/h. The upgrade meant that the current solvent recovery unit including evaporation, distillation and vacuum stripping, had to be expanded. Two process configurations were taken into consideration to add to the current solvent recovery unit:

1. Classical separation which is the same as the current solvent recovery unit, or
2. An OSN membrane unit.

Through a demonstration it was found that the OSN unit could recover up to 50% solvent at a purity of 99%. Adding the OSN unit to the existing solvent recovery unit reduced the energy consumption for all equipment by 20%. In addition, the capital investment for the OSN unit was only a third of the classical separation.

No more information on the design and operation of the Max-Dewax unit was disclosed. However, the success of Max-Dewax motivated further research on the commercial potential of OSN for the concentration of herbal extracts (Peshev and Livingston, 2013; Darvishmanesh et al., 2011), solvent recovery from active pharmaceutical ingredients (Vanneste et al., 2013), for the refining of non-edible oil (Werth et al., 2017b) and for the purification of hydroformylation product streams (Micovic et al., 2014).

Conceptual process configurations of some classical and OSN units are presented in the following subsections. Firstly, classical separations are discussed which include only classical separation techniques such as evaporation and/or distillation. Thereafter, designs including OSN separation technology is addressed.

2.1.1 Process configurations of classical solvent recovery units

In a patent by Sequiera (1991), a solvent recovery unit was designed for a solvent dewaxing plant at a lube-oil refinery. The unit was previously shown as Figure 2.1 and includes an evaporator under vacuum pressure, followed by a steam stripping column and a vacuum dehydration tower with trayed columns. Similar conceptual process configurations are presented in Figure 2.3 for the following industries:

(a) Solvent recovery from non-edible oil by two-stage evaporation, shown as Figure 2.3a (Werth et al., 2017b).
(b) Concentrating ethanolic plant extracts by means of solvent recovery, shown as Figure 2.3b (Peshev & Livingston, 2013).

(c) Purifying hydroformylation product streams by distillation, shown in Figure 2.3c (Micovic et al., 2014).

The reason for selecting these studies is that the molecular weight of typical solvent dewaxing solvents like MEK (72 g/mol) and toluene (92 g/mol) are within the range of that of the solvents like hexane (86 g/mol), ethanol (46 g/mol) and decane (142 g/mol). Since OSN relies on the size exclusion of species, it is thought that looking at systems where the solvents were close to MEK and toluene would be good for comparison. In addition, each study involved purifying a product or recovering solvent by classical separation only or OSN or hybrid-OSN, estimating the energy demand and/or cost and comparing. It would have been beneficial to compare more closely related processes. The closest study is the Max-Dewax demonstration but the criteria for comparisons between OSN and classical recovery only considered the reduction in overall energy demand and investment capital.

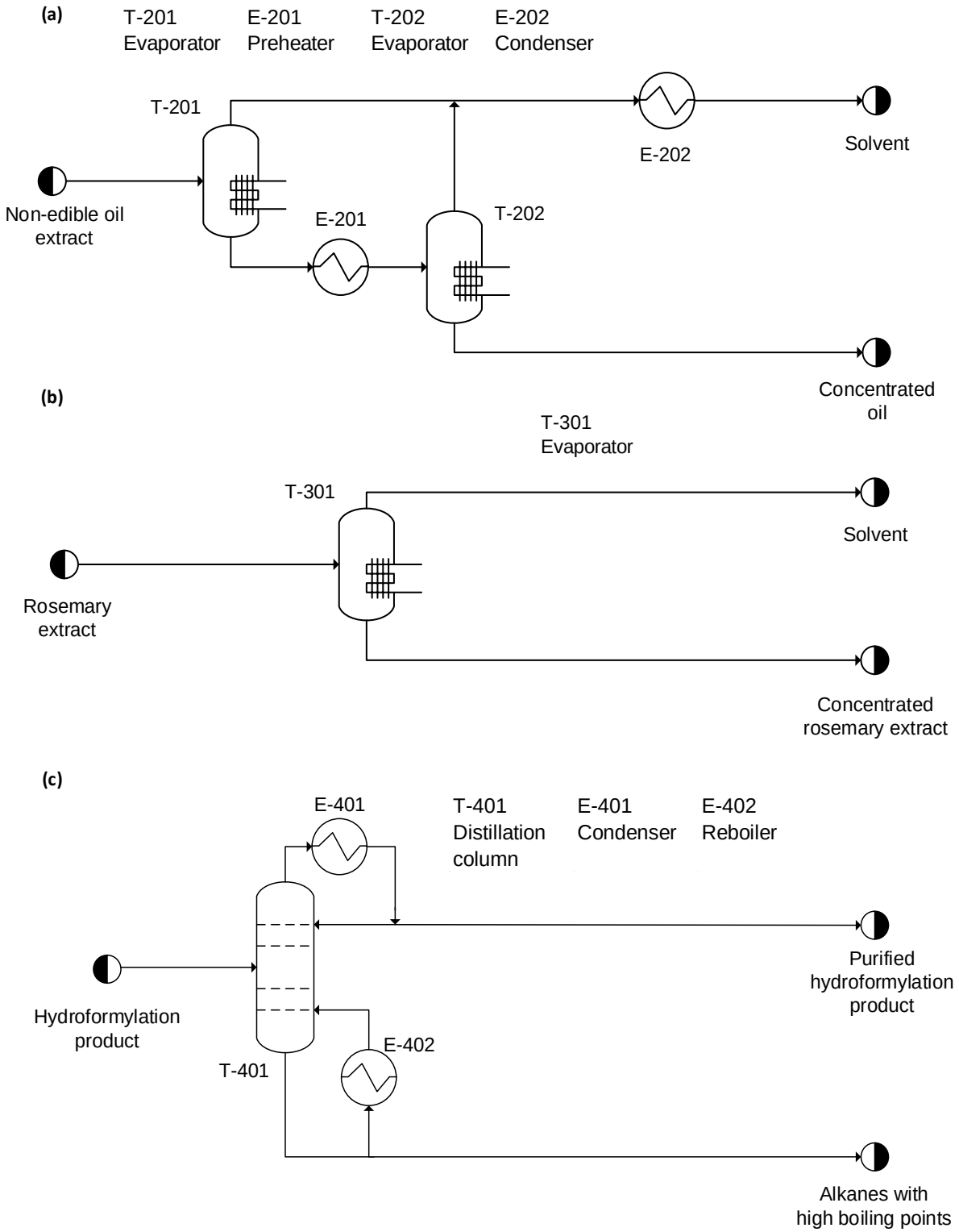

Figure 2.3: Process configurations of classical solvent recovery units to recover (a) hexane from non-edible oil (Werth et al., 2017b), (b) ethanol from an antioxidant ethanolic rosemary extract (Peshev & Livingston, 2013), and to (c) purify hydroformylation streams from alkanes with high boiling points (i.e. heavy boilers) (Micovic et al., 2014).

In Figure 2.3a, hexane is used as a solvent for the refining of non-edible oil and is recovered by a two-stage evaporation under vacuum conditions (Werth et al., 2017b). Similarly, in Figure 2.3b, ethanol is recovered from an antioxidant rosemary extract by means of single stage evaporation (Peshev & Livingston). In Figure 2.3c, a hydroformylation stream is purified from heavy boilers (i.e. undesired products of aldol condensation) by means of atmospheric distillation (Micovic et al., 2014).

An energy and economic analysis were performed for the process configurations in Figure 2.3. The most detailed analysis was for the two-stage evaporation unit in Figure 2.3a. The analysis included total energy consumption, operating cost and capital cost with and without the integration of heat (Werth et al., 2017b). The energy consumption included the energy demand for the evaporators, a preheater and the condenser. The capital cost included the investment cost of all equipment as well as periphery charges for instrumentation, control and piping based on factors. The operating cost was the sum of the cost of steam for the evaporator(s) and preheater, and cooling water for the condenser.

Heat integration is often applied for the recovery of solvent from non-edible oil by two-stage evaporation (Kemper, 2013). For an illustrative explanation, Figure 2.4 demonstrates how a portion of the waste energy from the downstream desolventiser toaster is transferred to the first evaporator.

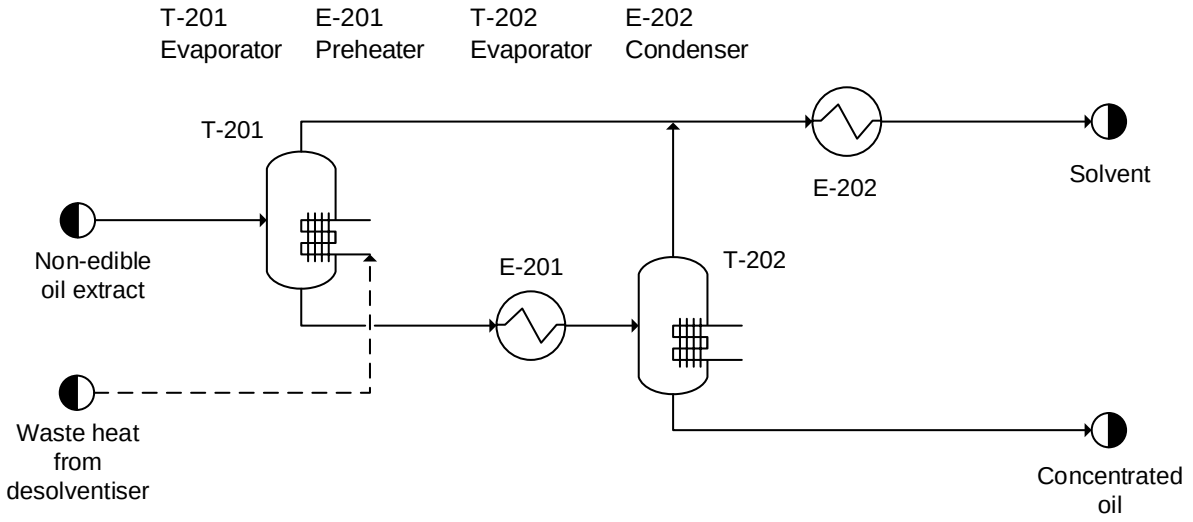

Figure 2.4: Heat integration by recovering waste heat from the desolventiser downstream to the solvent recovery unit for the refining of non-edible oil.

Through heat integration, the portion of waste heat from the desolventiser is enough for the first evaporator and no additional heat generation was necessary. Werth et al. (2017b) observed a 45% reduction in total steam consumption upon heat integration. This leads to a 32% decrease in operating cost which includes the cost of steam and cooling water.

The energy consumption, operating cost and capital cost of the atmospheric distillation unit in Figure 2.3c was also estimated but did not take the effect of heat integration into account. Micovic et al. (2014) provided the total annualised cost but did not provide a breakdown of the cost distribution. For the single-stage evaporator in Figure 2.3.b, only energy consumption was estimated (Peshev & Livingston, 2013).

Table 2.1 provides the cost and energy consumption of the process configurations in Figure 2.3 and Figure 2.4.

Table 2.1: Cost and energy consumption of the classical process configurations in Figure 2.3 and Figure 2.4.

	Two-stage evaporation; no heat integration (Figure 2.3a)	**Two-stage evaporation; with heat integration (Figure 2.4)**	**Single-stage evaporation (Figure 2.3b)**	**Distillation (Figure 2.3c)**
Feed capacity (m^3/h):	11	11	0.6	6
Overall solvent recovery:	79%	79%	64%	99%
Annualised capital cost (ZAR/m^3 solvent recovered):	14*+	14*+	-	-
Operating cost (ZAR/m^3 solvent recovered):	37*	21*	-	-
Total annual cost (ZAR/m^3 solvent recovered):	51*	35*	-	71*
Energy consumption (kWh/m^3 solvent recovered):	156	107	195	89**
Reference:	Werth et al. (2017b)	Werth et al. (2017b)	Peshev & Livingston (2013)	Micovic et al. (2014)

* 16 ZAR/EUR exchange rate

** Energy demand for the reboiler

+ Depreciation period and interest rate was 5 years and 7%

Table 2.1 shows that the distillation unit has a larger total annualised cost than evaporation. The lower cost for the evaporation unit. However, the economy of scale is more appropriate for comparing capital investment costs, but this was not possible as the capital of the distillation unit was not disclosed in Micovic et al. (2014).

Werth et al. (2017b) demonstrated that through the integration of heat, the energy consumption of the two-stage evaporation unit could be reduced by 31%. Table 2.1 shows that the corresponding savings in operating cost was 32%. However, what Werth et al. (2017b) did not take into consideration is the effect on capital cost. Chen et al. (2013) showed that including heat integration networks would

affect not only the operating cost but the investment capital of separation processes as well. They demonstrated that recovering heat downstream to a distillation column requires a lower capital investment than recovering heat within the column, although the latter reduced the operating cost.

Werth et al. (2017b) and Micovic et al. (2014) compared the cost and energy consumption of the classical separation process configurations in Figure 2.3 and Table 2.1 with OSN separation units. Peshev and Livingston (2013) only compared the energy demand between OSN and evaporation. Details of the process configurations, cost and energy consumption are provided in the following section.

2.1.2 Process configurations of OSN solvent recovery units

Process configurations are presented in Figure 2.5 for solvent recovery units that include OSN separation units. The process configurations include:

(a) Hybrid-OSN and evaporation for the recovery of solvent from non-edible oil, shown in Figure 2.5a (Werth et al., 2017b).
(b) Single-stage OSN for the recovery of ethanol from an antioxidant rosemary extract, shown in Figure 2.5b (Peshev & Livingston, 2013).
(c) Hybrid-OSN and distillation for the purification of a hydroformylation product stream, shown in Figure 2.5c (Micovic et al., 2014).

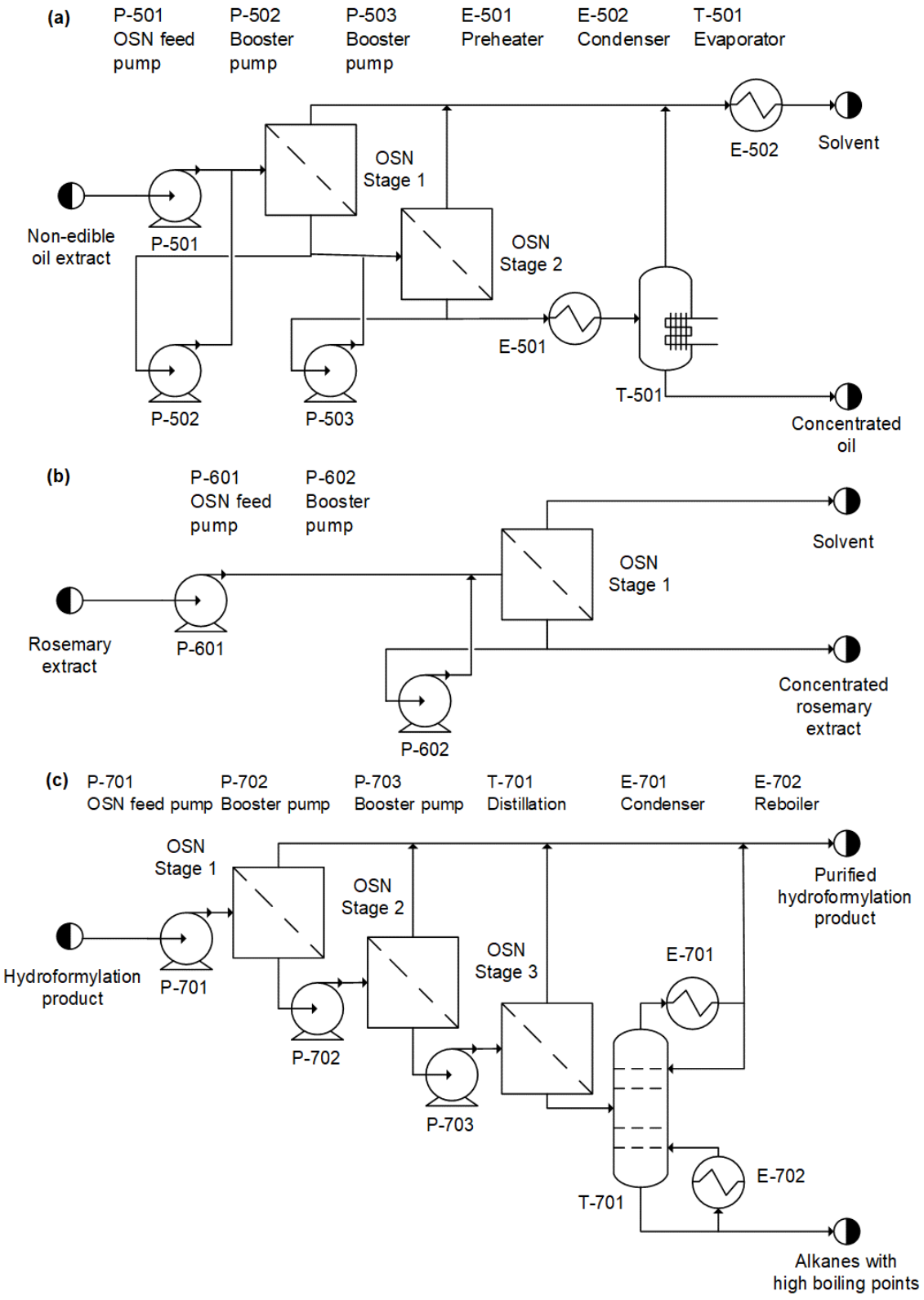

Figure 2.5: Process configurations including OSN solvent recovery units to recover (a) hexane from non-edible oil (Werth et al., 2017b), (b) ethanol from rosemary extracts (Peshev & Livingston, 2013), and to (c) purify hydroformylation streams from alkanes with high boiling points (i.e. heavy boilers) (Micovic et al., 2014).

Figure 2.5b is a stand-alone, single-stage OSN unit and recovers ethanol from an antioxidant rosemary extract. The OSN process configuration by Peshev & Livingston (2013) could recover 64% solvent at a purity of 99%.

Figure 2.5a is a process configuration of a two-stage OSN solvent recovery unit followed by a single-stage evaporation unit to recover n-hexane from non-edible oil. In the OSN process configuration a portion of the retentate is recycled back to the feed. The purpose of the retentate recycle is to control the flowrate to membrane modules when fluctuations in the feed arise. Membrane manufacturers often provide a recommended flowrate at which membrane damage and pressure-reducing effects are minimised (Evonik, 2017; Solsep BV, 2018). The hybridized OSN process configuration by Werth et al. (2017b) could recover 78% solvent at 99% purity. The recovery and purity corresponded to that of the classical solvent recovery unit in Figure 2.3a.

In Figure 2.5c, a process configuration of a three-stage OSN unit followed by distillation is presented. Micovic et al. (2014) observed by means of a multi-objective optimization routine that a retentate recycle loop was not necessary for the OSN unit. The hybridized OSN unit could recover 99% solvent at a 99% purity which is like the classical process configuration in Figure 2.3c.

The cost and energy consumption of the process configurations in Figure 2.5 including OSN separation were compared to the classical process configurations in Figure 2.3 and Figure 2.4. The results from these comparisons are presented in Table 2.2 with respect to the volume of solvent recovered per year. Both Micovic et al. (2014) and Werth et al. (2017b) based the cost of the membrane equipment 200 EUR/m^2 effective membrane area and a membrane replacement of 2 years.

Table 2.2: Cost and energy consumption of the classical process configurations in Figure 2.3 and OSN process configurations in Figure 2.5.

	Evaporation; no heat integration (Figure 2.3a)	**Evaporation; with heat integration (Figure 2.4)**	**Hybrid OSN-evaporation; no heat integration (Figure 2.5a)**	**Evaporation (Figure 2.3b)**	**OSN (Figure 2.5b)**	**Distillation (Figure 2.3c)**	**Hybrid OSN-distillation (Figure 2.5c)**
Feed capacity (m^3/h):	11	11	11	0.6	0.6	6	6
Overall solvent recovery:	79%	79%	79%	64%	64%	99%	99%
Annualised capital cost (ZAR/m^3 solvent recovered):	14*+	14*+	23*+	-	-	-	-

Table 2.2 (continued): Cost and energy consumption of the classical process configurations in Figure 2.3 and OSN process configurations in Figure 2.5.

	Evaporation; no heat integration (Figure 2.3a)	**Evaporation; with heat integration (Figure 2.4)**	**Hybrid OSN-evaporation; no heat integration (Figure 2.5a)**		**Evaporation (Figure 2.3b)**	**OSN (Figure 2.5b)**	**Distillation (Figure 2.3c)**	**Hybrid OSN-distillation (Figure 2.5c)**
Operating cost (ZAR/m^3 solvent recovered):	36*		21*	18*	-	-	-	-
Total annualised cost (ZAR/m^3 solvent recovered):	50*		35*	42*	-	-	71*	72*
Energy consumption (kWh/m^3 solvent recovered):	160		123	43	195	2.4	89**	74**
Reference:	Werth et al. (2017b)				Peshev & Livingston (2013)		Micovic et al. (2014)	

* 16 ZAR/EUR exchange rate

** Energy demand for the reboiler

+ Depreciation period and interest rate of 5 years and 7%

Table 2.2 shows that for all the process configurations described in Figure 2.3 and Figure 2.4, including an OSN unit reduces overall energy consumption. The most significant reduction is observed for the 64% recovery of ethanol from a rosemary extract. On the other hand, the least significant reduction is seen for the purification of a hydroformylation product through recovering 99%.

It seems that as the extent of solvent recovery increases from 64% to 99%, the energy savings associated with OSN reduces. A possible explanation is that as more solvent is recovered, the feed becomes more concentrated in the solute. This buildup of solute causes an increase in osmotic pressure on the feed-side of the membrane. For solvent to carry-on passing through the membrane to the permeate-side, the osmotic pressure must be overcome. A higher operating pressure must be applied to compensate for the increased osmotic pressure, thereby increasing pump power leading to reduced energy savings.

The total annualised cost of the process configurations including an OSN unit is more expensive than the classical process configuration – except where heat integration was neglected for the evaporation process. Table 2.2 shows that the operating cost of the hybrid OSN-evaporation process is lower than evaporation with heat integration and it is believed that the reduction in energy consumption might

be a possible reason. However, the hybrid OSN-evaporation process requires a larger capital investment.

Micovic et al. (2014) found that if the initial membrane cost coefficient of 200 EUR/m^2 reduced to 150 EUR/m^2, the hybrid OSN-distillation process would have the same total annualised cost as the classical unit. However, it is unclear what the effect of prolonging membrane life would have on cost.

The investigations in Werth et al. (2017b), Micovic et al. (2014) and Peshev & Livingston (2013) present the potential benefits of OSN units, but there are aspects of OSN membranes with regards to cost and membrane life have not yet been addressed. The next step is therefore to discuss characteristics that could affect the performance of OSN membranes. Such knowledge would be valuable for a more in-depth comparison between OSN and classical separations for the recovery of solvent.

2.2 Organic solvent nanofiltration (OSN)

OSN is the membrane-based size-exclusion of species based on their molecular weights. OSN can separate species with molecular weights ranging from 50 to 2000 g/mol (Szekely et al., 2014). Permeable species are transported through the membrane due to a positive pressure difference or concentration gradient between the feed-side and permeate-side of the membrane. Porous membranes allow for a more convective mode of transport, driven by the positive pressure difference between the feed- and permeate-side (Marchetti et al., 2014). Dense membranes favour a more diffusive transport for which the driving force would be a concentration gradient over the membrane (Marchetti and Livingston, 2015).

The size-exclusion of an OSN membrane is based on the molecular weight cut-off (MWCO). The MWCO is the molecular weight of species which will be 90% rejected by the membrane (Vandezande et al., 2008). The total flow of material through the membrane per effective membrane area is referred to as permeate flux. Rejection describes how well a membrane prevents species with molecular weights larger than the MWCO from permeating through the membrane.

For the purpose of recovering solvent by OSN, the separation performance is measured by solvent recovery and solute rejection. Since flux is expressed as volumetric flow per effective membrane area, increasing the overall membrane area will result in a higher recovery. To elaborate further, multiplying permeate flux with effective membrane area yields the flowrate of the permeate which is 99% solvent for a 97% lube-oil rejection. If more membrane modules are added to a membrane skid, the overall effective area will increase which will thus increase the permeate flowrate. However, adding more modules will increase the pressure drop across the pressure vessel and increase osmotic pressure

since the feed becomes more concentrated in solute. The operating pressure could be increased but only up to the maximum allowable pressure. Above this irreversible membrane damage will occur.

Hence, separation performance is limited by osmotic pressure, maximum allowable operating pressure, flux decline, recommended feed flowrate and permeate purity. An understanding of the membrane characteristics that would affect separation performance will assist with optimising OSN unit operations to maximise solvent recovery.

The first aspect of this section is to discuss various materials used to manufacture OSN membranes and their performance with regards to permeate flux and solute rejection. The second subsection provides information regarding transport equations that may be used to estimate the permeate flux and solute rejection over the OSN membrane. Thirdly, the long-term stability of OSN membranes are discussed based on the Max-Dewax unit. The fourth subsection will address the design of a membrane module, focusing on a spiral-wound membrane module. Thereafter, the process configuration of an OSN unit for the recovery of solvent is addressed. The final subsection explains the input variables, parameters and output variables for an OSN unit simulation.

2.2.1 Permeability through a flat sheet OSN membrane

OSN membranes are manufactured from either ceramic or polymeric material. Most commercial membranes are polymer-based due to their versatility and reduced manufacturing cost (White et al., 1993).

Membrane permeate rate is a property of the system and is unique for a certain combination of membrane, solvent and solute. It is determined by measuring the volumetric flowrate of pure solvent species moving through a membrane for a range of applied feed-side pressures. Since the feed is pure solvent, concentration polarisation will be negligible and a linear relationship between flowrate and applied pressure will develop. A linear trendline is fitted to data arranged as volumetric flowrate on the y-axis and operating pressure on the x-axis. The gradient from fitting a linear trendline can be divided by the effective membrane area to yield the membrane permeate rate of the specie in $L/h/m^2$ or mm/h. These experiments can be performed on a bench scale using a single membrane sheet and since permeate rate is independent of area, the process can be scaled up. The parameters that should remain constant includes temperature since it affects viscosity and solvent purity as it might otherwise lead to concentration polarisation.

Silva et al. (2010) found that the transport across a single flat-sheet OSN membrane can be used to make accurate transport predictions for a large-scale OSN unit. This assumes that each specie has a constant membrane permeate rate under constant temperature. The fact that the performance of an

OSN unit can be related to the separation across a flat-sheet membrane demonstrated the ease of scale-up.

Size-exclusion is facilitated by free-volume positions forming in the membrane due to statistical fluctuations of polymer segments (Tsarkov et al., 2013). If the size of a molecule is comparable with the free volume, it will permeate through the membrane, otherwise it is rejected. The preferential permeation of one specie over another is referred to as permselectivity (Micovic et al., 2014). In the present investigation, permselectivity represents the membrane permeate rate, b_i, of solvent over the solute as is shown in Equation 2.1.

$$\alpha = \frac{b_{solvent}}{b_{solute}} \quad [2.1]$$

Membrane permeate rates can be determined by measuring the permeate flux and composition across a flat sheet membrane. Membrane permeate rates across a polyimide (PI), polyetherimide (PEI) and a poly(dimethylsiloxane) (PDMS) membrane were taken from literature and presented in Table 2.3. The membrane permeate rates were determined for OSN membranes for the recovery of solvent (Case no. 2, no. 3 and no. 5), the enrichment of aromatic streams (Case no. 1) or for the purification of hydroformylation product streams (Case no. 4).

Table 2.3: Solute rejection and permeate flux of OSN membranes in different solvent-solute-membrane systems.

Case	Components and their molecular weight (g/mol)	Membrane material	Solute rejection	Specific permeate flux (L/m²/h/bar)*	References
1	Aromatics (102 g/mol) and non-aromatic (125 g/mol)	PI	83% of non-aromatics	0.30	White and Wildemuth (2006)
2	MEK (72 g/mol), toluene (92 g/mol) and lube-oil (>350 g/mol)	PEI	95% of lube-oil	0.67	Namvar-Mahboub and Pakizeh (2013)
3	MEK, toluene and lube-oil (>350 g/mol)	PI	96% of lube-oil	0.30	White and Nitsch (2000)
4	n-Decane (142 g/mol), dodecanal (184 g/mol) and hexacosane (367 g/mol)	PDMS	68% of hexacosane	1.49	Micovic et al. (2014)
5	n-Hexane (86 g/mol), triolein (885 g/mol) and oleic acid (282 g/mol)	PDMS	60% of oleic acid	0.97	Werth et al. (2017a)

* With respect to operating pressure

Namvar-Mahboub and Pakizeh (2013) showed through Case no. 2 that higher fluxes can be achieved for the recovery of dewaxing solvent from lube-oil after membrane treatment. The membrane was

equipped with a support layer made from silicon dioxide to minimise membrane swelling, which is the sorption of solvent into the polymer membrane, causing an increase in the pore size of the membrane (Robinson et al., 2003).

In Cases no.4 and no.5, higher permeate flux but lower rejections were observed with PDMS compared to the PI and PEI membranes. Both cases have a solute rejection between 60 and 70% but No.5 has a 35% lower flux than No.4. The goal of case No.5 was for the recovery of n-hexane and the reduction of oleic acid in the oil (Werth et al., 2017a). The molecular weight of oleic acid is 196 g/mol more than n-hexane. The large difference in molecular weight between the two species that should be permeated means that the larger specie, oleic acid, will have a slower membrane permeate rate through the membrane.

The buildup of rejected species on the feed-side of the membrane increases the osmotic pressure, which is the minimum pressure required to prevent the backflow of pure solvent across the semi-permeable membrane (Silberberg, 2013). The applied operating pressure must be higher than the osmotic pressure to ensure that the permeated solvent does not flow back to the feed-side of the membrane. Osmotic pressure of a species is the difference in its concentration on the feed-side, c_F, and the permeate-side, c_P, at a certain temperature, T. An equation to determine osmotic pressure, is presented in Equation 2.2.

$$\Delta\pi = R_c T(c_F - c_P) \qquad [2.2]$$

Equation 2.2 shows how an increase of solute concentration on the feed-side (c_F) can increase the osmotic pressure.

The membranes used in Cases no. 1 and no. 3 exhibit a high solute rejection which assists with the recovery of solvent at a high purity but a low permeate flux compared to Cases no. 4 and no. 5. The feed in Case no. 1 and no. 3 contains approximately 20% solute whereas the hexacosane mass content in Case no. 4 is 5%. The lower solute concentration in the feed of no. 4 resulted in a lower osmotic pressure, higher driving force and thus a higher permeate flux.

The experimental data gathered through membrane permeability tests can be used to determine the membrane permeate rate of species through an OSN membrane. This membrane permeate rates are applied to transport equations to predict the permeate flux and membrane rejection. Details regarding transport equations and their applicability is presented in the following subsection.

2.2.2 Transport equations to characterise OSN membrane separation

There are three main groups of transport equations that have been used to characterise the transport of species through an OSN membrane (Marchetti et al., 2014):

(1) solution-diffusion, for which the driving force is a concentration gradient,

(2) pore-flow, where the driving force for separation is a positive pressure difference across the membrane, and

(3) solution-diffusion with imperfections, which is a combination of (1) and (2).

The combination of membrane, solvent and solute has an influence on the appropriateness of a specific transport model. For example, pore-flow transport will be more applicable for a swollen membrane with an increased pore size. Similarly, solution-diffusion would be more appropriate for dense membranes where diffusive transport is more common. Table 2.4 presents some literature on the transport modelling across OSN membranes.

Table 2.4: Transport models which were the most appropriate for certain membrane, solvent and solute combinations.

Case	System	Membrane material	Transport model	Reference
1	MEK, toluene and lube oil	PI	Classic solution-diffusion	White and Nitsch (2000)
2	Sarafin-O dye dissolved in ethanol	PI	Classic solution-diffusion	Marchetti and Livingston (2015)
3	Sarafin-O dye dissolved in ethanol	PTSP	Poreflow	Marchetti and Livingston (2015)
4	n-Decane, dodecanal and hexacosane	PDMS	Solution-diffusion with imperfections	Micovic et al. (2014)
5	n-Hexane, triolein and oleic acid	PDMS	Solution-diffusion with imperfections	Werth et al. (2017a)

PI: Polyimide PTSP: poly[1-(trimethylsilyl)-1-propyne] PDMS: Poly(dimethylsiloxane)

It seems through Table 2.4 that the pore-flow equation to predict the permeate flux across a poly[1-(trimethylsilyl)-1-propyne] (PTSP) membrane was preferred by Marchetti and Livingston (2015). PTSP is a rigid, highly permeable membrane with a high concentration of free volume elements which are formed during membrane treatment (Marchetti et al., 2014). The result is a microporous layer that allows molecules with a comparable size to permeate through the free volumes with ease.

Unlike the rigid PTSP membranes, PI membranes have a flexible polymer backbone (Marchetti and Livingston, 2015). The flexibility of the polymer backbone leads to the formation of irregular voids. The solution-diffusion model simulates the transport of a molecule from one void to another and thus works well for dense, PI membranes.

Robinson et al. (2004) observed that the permeation mechanism is hydraulic through a PDMS membrane at pressures above 300 kPa, but diffusive at lower pressures. The hydraulic mechanism is caused by membrane swelling which is a common occurrence in PDMS membranes (Leitner et al., 2014; Tarleton et al., 2009; Marchetti and Livingston, 2015). Micovic et al. (2014) and Werth et al. (2017a) accounted for both transport mechanisms by applying the solution-diffusion with imperfections model. The model permeability parameters are diffusive coefficients and hydraulic coefficients and could predict the transport through a PDMS membrane well.

Table 2.4 shows that the classical solution-diffusion model was the preferred choice to predict the permeate flux of MEK, toluene and lube-oil across a PI membrane. In Table 2.3 it was shown that PI membranes achieve a high lube-oil rejection which will lead to the recovery of a high-purity solvent. The present investigation will therefore focus on applying the classical solution-diffusion model to the PI membrane used in the White & Nitsch (2000) study.

The **classical solution-diffusion** model treats every component as the solute and does not require distinguishing between species making up the solvent and those making up the solute (Marchetti et al., 2014). The advantage is that the model can easily be extended for a feed mixture involving many components.

The solution-diffusion transport equation is presented in Equation 2.3 to predict the specific flux, J, of each component, k, for a known molar feed composition, x_F, constant temperature, T, feed-side pressure, P_F, permeate-side pressure, P_P, and osmotic pressure, $\Delta\pi$ (Marchetti et al., 2014). The universal gas constant, R_c, membrane permeate rate, b, and pure species molar volume, v, remains fixed for constant T.

$$J_k = b_k \left(x_{F_k} - x_{P_k} \exp\left(-\frac{v_{F_k}((P_F - P_P) - \Delta\pi_k)}{R_c T} \right) \right) \qquad [2.3]$$

Total permeate flux, J, is the sum of J_k so that the permeate composition, x_{P_k}, becomes the ratio of J_k over J (Peeva et al., 2004). Recall that the values of the membrane permeate rates are based on pure-species flux tests - one for each permeable component present in the feed. The only source for b_k with regards to MEK, toluene and dewaxed lube-oil could be found in White and Nitsch (2000) who used a PI OSN membrane.

Multiple membrane sheets are packaged in a single unit for an increased effective membrane area per membrane module volume (Buonomenna, 2013). The following section will discuss aspects of an OSN membrane module.

2.2.3 Membrane module

There are four types of membrane modules for OSN (Szekely et al., 2014).:

- Hollow fiber,
- plate-and-frame,
- spiral-wound and
- tubular modules.

The most popular type for commercial operations is spiral-wound modules (SWM) due to their robustness, modular design and large effective membrane area relative to the size of the module (White and Wildemuth, 2006). SWM are typically chosen for the water and wastewater treatment industry (Owen et al., 1995), pharmaceutical (Darvishmanesh et al., 2011; Vanneste et al., 2013; Vanndezande et al., 2013; Peshev & Livingston, 2013), petrochemical (Gould and Wildemuth, 2001; Micovic et al., 2014) and oleochemical industry (Werth et al., 2017b). A schematic representation of a SWM is presented in Figure 2.6.

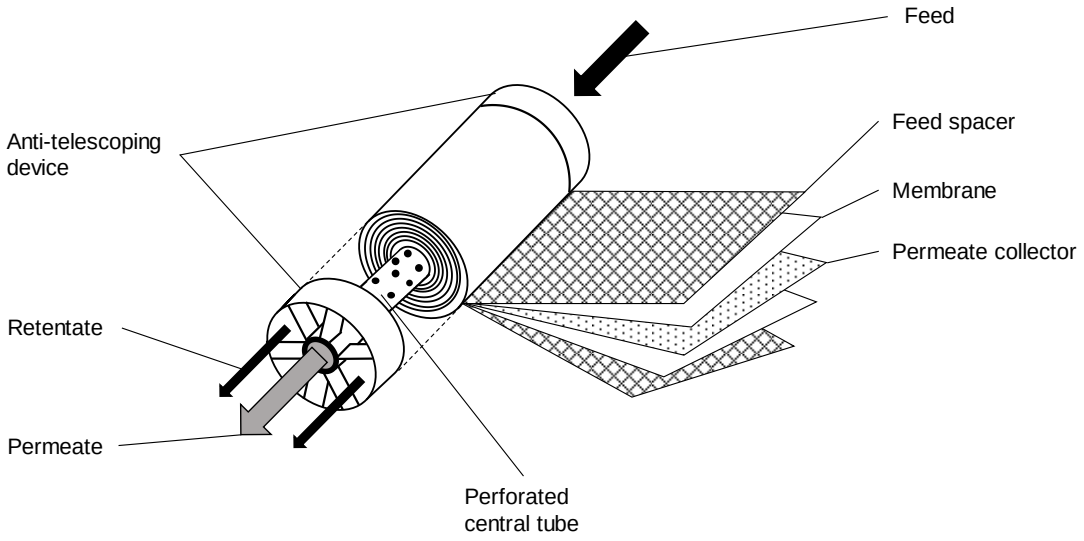

Figure 2.6: Schematic of a spiral-wound module.

The feed passes through an anti-telescoping device to prevent membrane damage at high flowrates (Schwinge et al., 2004). Multiple membrane sheets are spirally wound around a central perforated tube. A mesh-like spacer is positioned on top of each membrane to distribute the material across the membrane sheet. The volume between the membrane sheet and feed spacer is referred to as the feed channel. Below the membrane sheet lies a permeate collector mesh to guide permeate to the perforated central tube. The stacking procedure is repeated for every membrane sheet.

The interior design has an influence on the hydrodynamic flow through the module. The spacer design for the feed channel effects the **pressure drop** along the flow path. The presence of a pressure drop would decrease the driving force for permeation thereby lowering the permeate flux. According to Evonik, the pressure-drop for any OSN SWM will not exceed 1 bar if operated within +/- 10% of the suggested feed flowrate (Evonik, 2018). Shi et al. (2016) observed a pressure-drop of 0.01 to 0.75 bar for a 102 mm diameter by 1016 mm length SWM. Peshev and Livingston (2013) found that by assuming a maximum pressure drop of 1 bar, flux and rejection predictions correlate well with experimental observations.

Another factor to consider is the buildup of solute species near the membrane surface, which increases osmotic pressure. The phenomenon is referred to as **concentration polarisation** and is the formation of a concentration gradient between the feed entrance and membrane surface. The occurrence is often found in organic systems where the viscosity of a mixture changes significantly with solute concentration (Stamatialis et al., 2006).

The overall result of concentration polarisation and pressure drop is a decrease in the driving force for membrane separation (Peeva et al., 2004). Peshev and Livingston (2013) showed that for OSN unit process simulation, the hydrodynamic phenomena could be ignored and still generate accurate predictions within a +/- 5% deviation from predictions made with models that included pressure drop in the feed channel and concentration polarisation.

The **long-term stability** of OSN membrane modules is important to take into consideration when simulating an OSN unit. The replacement frequency of OSN membranes have been assumed by many between 1.5 and 2 years (Bhore et al., 1999; Micovic et al., 2014; Werth et al., 2017b). However, the actual replacement frequency and long-term stability (i.e. flux decline) are two very uncertain variables, along with the cost of membrane modules. Nonetheless, the long-term stability tests of polymer OSN membranes used for the Max-Dewax unit were performed. Results and details from the long-term stability tests are discussed in the following subsection.

2.2.4 Long-term membrane stability

The membrane modules used for the Max-Dewax unit underwent long-term stability tests spanning over 14 months. The overall permeate flowrate and oil content in the permeate from the unit was documented every few days.

Upon plotting permeate flowrate and purity over time, Bhore et al. (1999) observed a nonlinear decrease in permeate flow while the oil content in the permeate remained consistently below 1%. Figure 2.7 is adapted from Bhore et al. (1999) to illustrate flux decline after long-term operation.

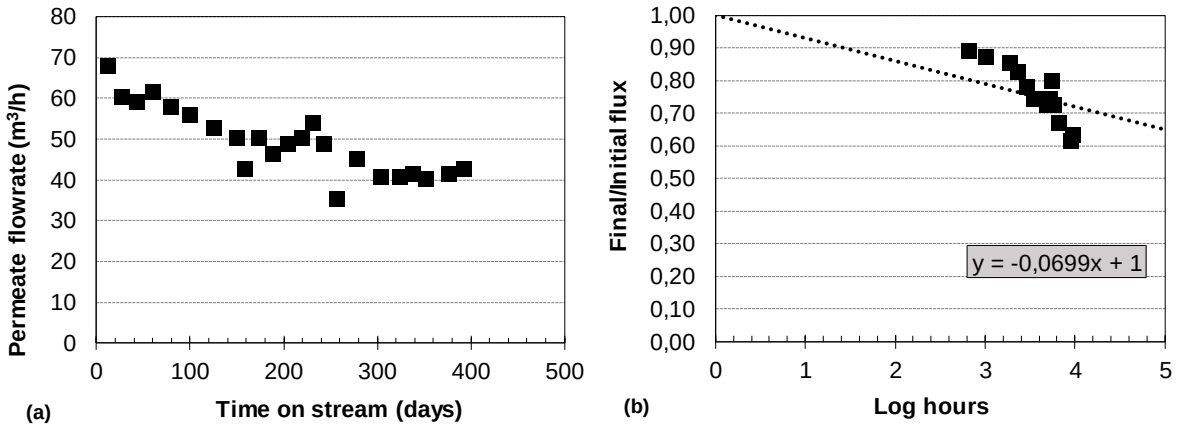

Figure 2.7: Long-term membrane performance of the Max-Dewax process over (a) membrane life in days and (b) logarithmic hours (adapted from Bhore et al. (1999)).

It was observed that after 400 hours membrane life, the flux declined by almost 30%. From Figure 2.7b, plotting flux decline over log hours and setting the y-intercept to 1 after 1 hour was based on the approach by White and Nitsch (2000) from which the membrane permeate rates were taken. The data was based on long-term experiments with the Max-Dewax unit. The trendline with the squared residual closest to 1 fitting flux decline over time (see Figure 2.7a) between exponential, linear, logarithmic and the power function was found to be a logarithmic. Plotting flux against log hours followed by fitting a trendline allows for extrapolation beyond 400 hours (White and Nitsch, 2000):

$$\frac{Final\ flux}{Initial\ flux} = (-0.0699 \times \log(hours)) + 1 \qquad [2.4]$$

The trendline shown as Equation 2.4 was based on an initial permeate rate of 72 m^3/h after 20 days membrane life. The gradient of the trendline corresponds to that obtained by White and Nitsch (2000). By extrapolating to 1.5 years (11 952 hours), the final flux remains within 73% of the flux initially observed at 20 days (480 hours) membrane life. The trendline would be used to account for flux decline over membrane life so that long-term membrane stability can be included for process simulations.

2.2.5 Process configuration of an OSN unit

As previously mentioned, a major benefit of OSN technology is that the scale-up from a single membrane module to a large-scale unit is easy (Buonomenna, 2013; Szekely et al., 2014; Gould et al., 2001; Werth et al., 2017). The main processing steps for any membrane unit includes the following (Micovic et al., 2014; Werth et al., 2017b; Peshev and Livingston, 2013; Bhore et al., 1999; Accepta water treatment, 1997):

(1) feed-intake,

(2) pretreatment,

(3) pressure increase, and

(4) membrane separation.

The equipment groupings are shown in Figure 2.8.

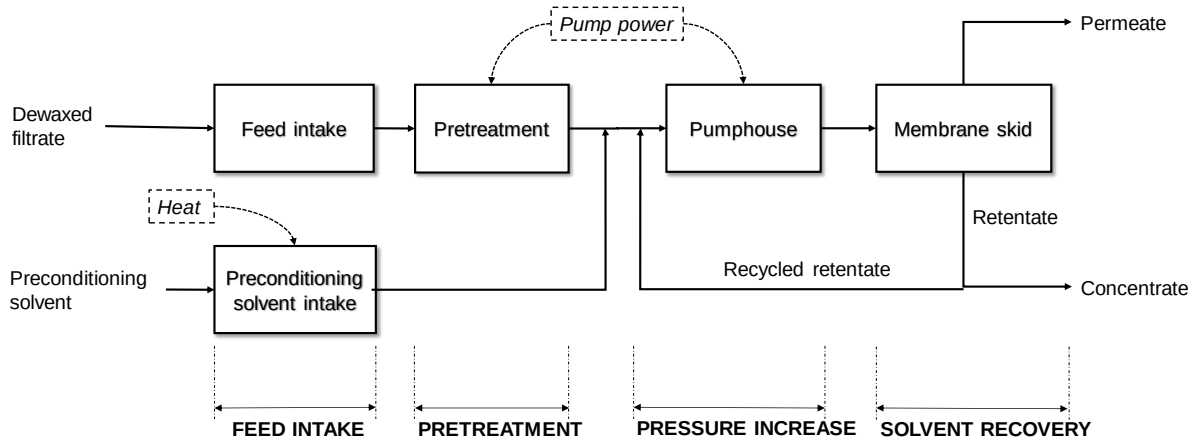

Figure 2.8: Simplified schematic illustrating the processing steps in an OSN membrane system to recover solvent from dewaxed filtrate.

The feed to the OSN unit will receive either:

(1) Preconditioning solvent - clean solvent, or

(2) Dewaxed filtrate - a mixture of solvent and dewaxed lube-oil.

Preconditioning is performed when a new membrane module has been installed. Polymer membrane modules are typically stored in a preservative solution to prevent membrane sheets from drying while being transported. After installation, the preservative is removed from the module by washing with clean dewaxing solvent (i.e. no lube-oil). It is recommended that at least 20 L/m^2 effective membrane area is necessary to wash out all the preservative. The preconditioning solvent is preheated to 50^{o}C to ensure complete dissolution of the preservative (Evonik Resource Efficiency GmbH, 2017). The feed pressure is initially set at 3 to 5 bar and the mixture of solvent and preservative is collected in a permeate collection tank. The retentate is recycled to the stage inlet. The pressure is slowly increased to the system pressure of the OSN unit. Once the permeate discharge is colourless it is recycled back to the feed tank and the membrane module is ready for use. However, the permeate containing the preservative cannot be reused as is and should be discarded or purified. (Evonik Resource Efficiency GmbH, 2017)

The feed intake receiving **dewaxed filtrate** involves a buffer tank. The dewaxed filtrate does not require heating since solvent recovery by an OSN membrane is a non-thermal separation (Gould et al., 1994).

After agitation, the dewaxed filtrate is sent through **pretreatment filters** to remove any scaling particulates and wax crystals. Multiple filters can be placed in parallel to maintain the feed flow near the recommended rate provided by the manufacturer, and to act as backup filters to minimise plant downtime (Bhore et al., 1999).

Pumps are arranged in the **pumphouse** and their function is to either (Peshev and Livingston, 2013; Werth et al., 2017b):

(1) Maintain the high operating pressure for the OSN feed,
(2) Provide low-pressure for pretreatment and preconditioning, or
(3) Boost feed streams after the retentate recycle loop to compensate for pressure drop.

Figure 2.9 provides a schematic representation of how membrane modules and pressure vessels are arranged in a stage and skid.

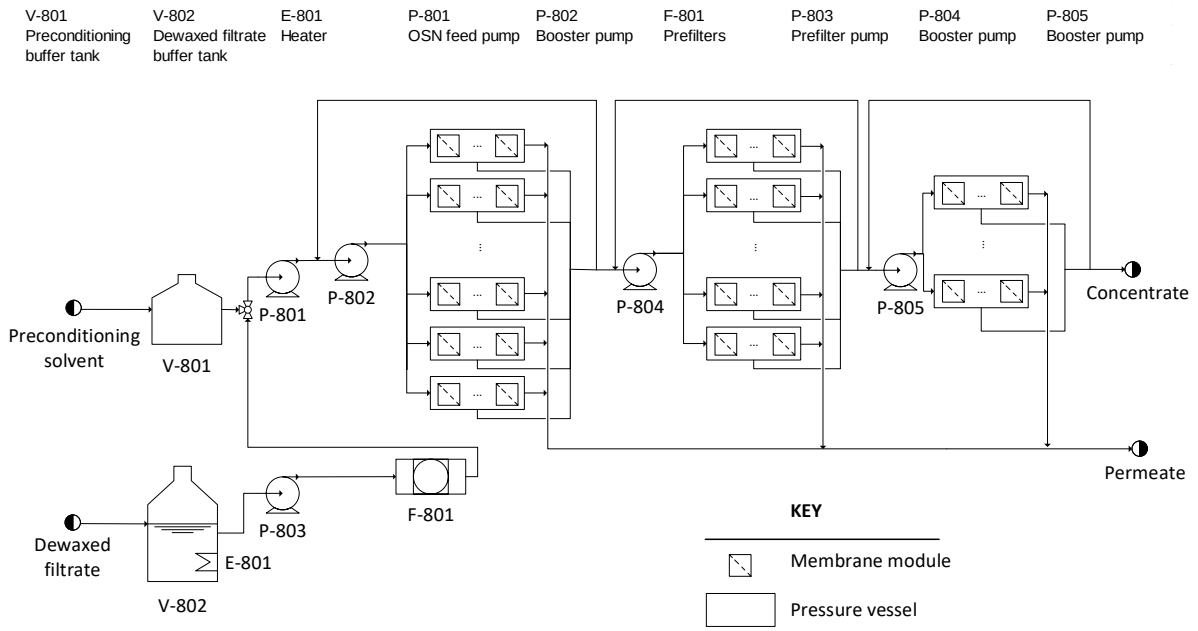

Figure 2.9: Illustration of a membrane skid including stages, pressure vessels, membrane modules and traditional process equipment such as pumps, heat exchangers, prefilters and tanks.

Membrane modules are connected in series and contained in a **pressure vessel**. Typically, 2 to 8 modules can be connected (Werth et al., 2017b; Micovic et al., 2014), however 7 is generally preferred, since the pressure-drop increases with pressure vessel length (Peck, 2017). Schäfer et al. (2005)

observed that the pressure-drop in a pressure vessel involving 7 membrane modules does not exceed 3.5 bar. As is shown in Figure 2.9, if the function of OSN is to recover solvent, the concentrated product from a stage will feed the following stage (Schwinge et al., 2004). The drop in feed pressure between stages is nullified by the interstage booster pumps.

For a large-scale OSN unit, pressure vessels are often arranged in a parallel configuration to distribute the feed over pressure vessels. A group of pressure vessels is referred to as a **stage.** The number of stacked vessels is limited by plant design specifications such as plant ceiling height, maintenance requirements and possibly crane design (Sinnott, 2005). For fluctuations in the feed, the flowrate through a vessel is maintained by adjusting the retentate recycle.

Pressure vessels are mounted on a metal framework referred to as a **skid**. For the present investigation, a **membrane unit** involves multiple membrane skids in addition to a feed intake, pretreatment, a permeate tank, feed pumps, low-pressure pumps and high-pressure booster pumps.

The solvent recovery and solute rejection achieved by the OSN unit can be estimated through simulating the process configuration. The flow of information throughout the simulation is discussed in the following subsection.

2.2.6 Flow of information for an OSN unit simulation

Process simulation environments (PSEs) are equipped with built-in mass and energy balances for traditional process equipment such as pumps, heat exchangers, columns and evaporators. In addition, a PSE such as Aspen Plus can predict the size of equipment and calculate the energy consumed.

Commercial PSEs cannot estimate the size and energy demand of membrane-based separation equipment such as an OSN unit. However, the size and energy consumption of an OSN unit can be simulated using numerical modellers such as Excel and MATLAB. Thereafter, interoperability techniques can be applied to transfer information between the numerical modellers and PSE. This would be very useful for hybrid-OSN process configurations.

Figure 2.10 shows how information would flow between a PSE and numerical modeller.

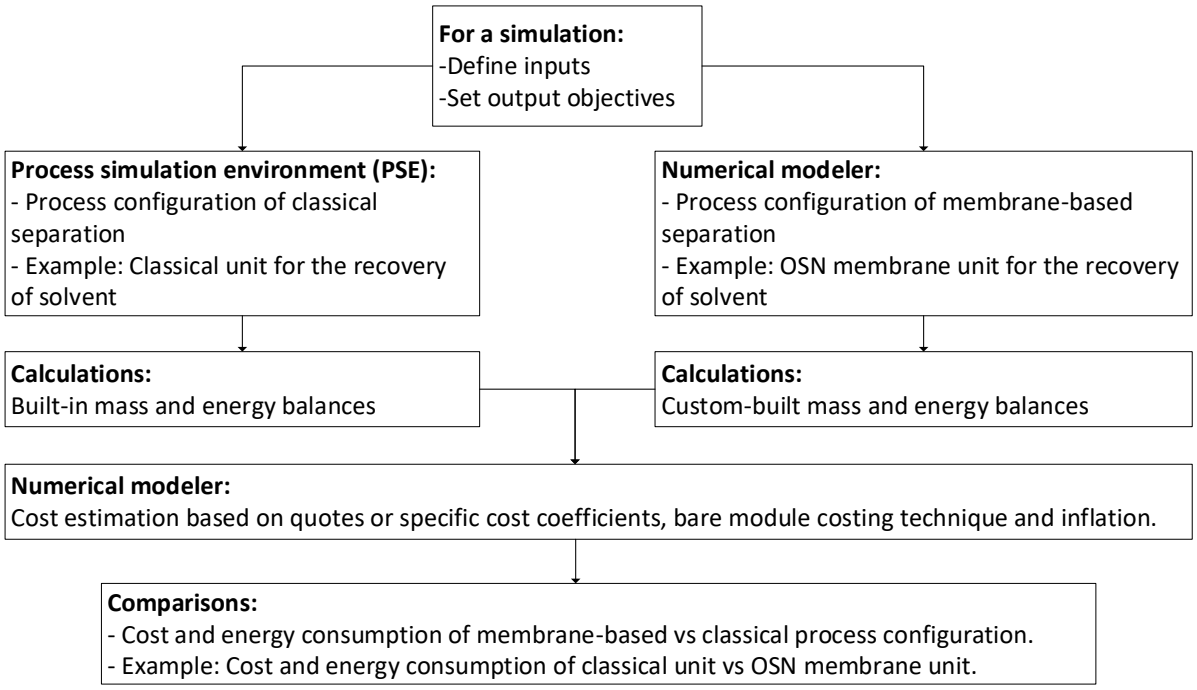

Figure 2.10: Flow of information between a process simulation environment (PSE) and numerical modeller.

Peshev and Livingston (2013) combined Aspen Plus and MATLAB to simulate the solvent recovery and energy consumption for an OSN membrane. The transport across the OSN membrane was calculated through a set of equations solved in MATLAB (the numerical modeller). The modelled results were transferred to Aspen Plus (the PSE). Peshev and Livingston (2013) used a CAPE OPEN Unit Operation to establish the interoperability between MATLAB and Aspen Plus (CoLan, 2010). However, incorporating the CAPE-OPEN set of compliance standards is not freely available.

Following the demonstration of using CAPE OPEN, Peshev and Livingston (2013) also recommended the use of component object modellers (COM) to create re-usable software components. The first advantage of this approach is that the COM add-ins are freely available in Excel. The second advantage is that setting up the COM add-in requires a basic knowledge of well-known programming languages such as FORTRAN, C++ or Visual Basic.

Fontalvo (2014) followed a similar method as Peshev and Livingston (2013) to incorporate a MATLAB subroutine with a user model in Aspen Plus using Excel as the link. The mass and energy balance around the OSN unit was performed in MATLAB. In Aspen Plus, the OSN unit was represented by a "User2" block. The block allows the user to define the stream flows, energy consumption and cost of the OSN unit using a FORTRAN wizard. The FORTRAN wizard connects the User2 block with an Excel workbook which in turn is connected to MATLAB. The advantages of using Excel as the link is that:

- It is a familiar interface for many in industry,
- It is well known for data trending, graph generation and presentation capabilities, and
- Process simulations are performed in Excel without having to physically open either MATLAB or Aspen Plus since they run as background operations.

Micovic et al. (2014) and Werth et al. (2017b) included an OSN unit with a classical process configuration to represent a hybrid-OSN unit in Aspen Plus using the Aspen Plus Custom Modeller (ACM). The technique requires thorough knowledge of the ACM programming language and the Aspen Plus interface. In addition, this method is exclusive to Aspen Plus.

Two useful COM add-ins that can be used to connect MATLAB with Excel and Excel with Aspen Plus is the Spreadsheet Link and the Aspen Simulation Workbook (ASW). The Spreadsheet Link uses Visual Basic to call MATLAB functions (MathWorks, 1997). The ASW add-in assigns input values to an Aspen Plus process configuration, initiates the simulation and extracts results from the simulation.

In Section 2.1, the process configuration, cost and energy consumption of OSN and classical solvent recovery units were described and compared. In Section 2.2, OSN membrane characteristics, scale-up from membrane module to process unit and the process simulation approach was discussed. The following section will provide further details on how other studies in literature estimated the cost and energy consumption of an OSN unit.

2.3 Cost and energy of OSN units

This section provides details on the main cost and energy contributors of an OSN unit. The process configurations taken into consideration were discussed in Section 2.1.2.

2.3.1 Energy consumption

The literature suggests that OSN separation reduces the energy demand for solvent recovery units by 20 to 90% in comparison to classical separations (Bhore et al., 1999; Werth et al., 2017b; Peshev & Livingston, 2013). The main reason for a reduction in energy is that OSN is a non-thermal separation, whereas evaporation and distillation are more energy intensive since they are thermal separations (Sholl & Lively, 2016).

An important aspect that requires clear clarification when comparing the energy or cost of different process configurations is the scope of each process. A breakdown of the energy consumers for the OSN units in Section 2.1.2 are presented in Table 2.5.

Table 2.5: Energy consumers of the classical process configurations in Figure 2.3 and OSN process configurations in Figure 2.5. The percentage contribution of each towards overall energy consumption is provided in brackets.

	Evaporation; no heat integration (Figure 2.3a)	**Evaporation; with heat integration (Figure 2.4)**	**Hybrid OSN-evaporation; no heat integration (Figure 2.5a)**	**Evaporation (Figure 2.3b)**	**OSN (Figure 2.5b)**	**Distillation (Figure 2.3c)**	**Hybrid OSN-distillation (Figure 2.5c)**
Feed capacity (m^3/h):	11	11	11	0.6	0.6	6	6
Overall solvent recovery:	79%	79%	79%	64%	64%	99%	99%
OSN pressure pump(s) (kW):	-	-	17 (5%) at 34 bar**	-	1 at 39 bar**	-	-
Evaporators (kW):	541 (39%)	215 (20%)	91 (23%)	75	-	-	-
Heater (kW):	178 (13%)	178 (17%)	122 (32%)	-	-	-	-
Reboiler (kW):	-	-	-	-	-	529	440
Condenser (kW):	672 (48%)	672 (63%)	144 (39%)	-	-	-	-
Energy consumption (kWh/m^3 solvent recovered) ***:	160	123	43	195	2.4	89*	74*
Reference:	Werth et al. (2017b)			Peshev & Livingston (2013)		Micovic et al. (2014)	

* Energy demand of reboiler ** Permeate-side pressure is 1 bar *** Specific energy consumption (SEC)

Table 2.5 shows that the energy demand to condense the vapour product from the evaporator is the largest contributor towards total energy consumption (Werth et al., 2017b). Since OSN is a non-thermal separation, the condenser energy demand is reduced by 78% for the hybrid-OSN process configuration.

The energy consumed by the OSN pressure pumps is the smallest consumer compared to two-stage evaporation with and without heat integration, and single stage evaporation (Werth et al., 2017b; Peshev & Livingston, 2011). This demonstrates that OSN membrane separation is not as energy intensive as classical separations.

The energy consumption of the OSN units studied by Werth et al. (2017b) and Peshev & Livingston (2013) only took the pump work into account. The energy consumption for pump work may be determined with Equation 2.5 (Szekely et al., 2014).

$$W_{OSN} = \frac{\dot{V}_F(P_F - P_P)}{\eta} + \frac{\dot{V}_{RR}(P_F - P_{RR})}{\eta} \quad [2.5]$$

The first term describes the work for the feed pressure pump based on volumetric feed flowrate, $\dot{V}_F$, feed-side pressure, P_F, and permeate pressure, P_P. The second term accounts for the pressure drop across the membrane module or pressure vessel. A booster pump increases the pressure of the recycled retentate stream, P_{RR}, to the feed-side pressure. The difference between P_F and P_P is referred to as the transmembrane pressure. Finally, pump efficiency is included through η. The pump efficiencies assumed in Werth et al. (2017b) was 60% and Peshev & Livingston (2013) was 70%.

Comparing the W_{OSN} determined by Werth et al. (2017b) with that estimated by Peshev & Livingston (2013), the former has a higher value. The reason is that the capacity for the Werth et al. (2017b) process is 18 times larger. However, if W_{OSN} was divided by the amount of solvent recovered, the values would be 2.0 for Werth et al. (2017b) and 2.4 kWh/m^3 for Peshev & Livingston (2013).

The comparisons in Table 2.5 demonstrates the energy savings of OSN separations compared to evaporation and distillation. However, the overall cost should also be taken into consideration and is thus discussed in the following section.

2.3.2 Plant cost

The plant cost of a unit refers to the operating costs per year and annualised capital investment. The annualised capital cost, also referred to as the equivalent annual cost (EAC), represents the annual cost of owning, operating and maintaining an asset over its entire life (Owen et al., 1995). The sum of the EAC and operating cost is referred to the total annual cost (TAC). The EAC can be estimated using Equation 2.6.

$$EAC = \frac{CI \times i}{1 - (1+i)^{-n}} \quad [2.6]$$

The EAC in Equation 2.6 includes the capital invested to purchase an asset, CI, an interest rate, i, and a write-off or period or useful life, n. Werth et al. (2017b) assumed an interest rate of 7% and a write-off period of 5 years for all equipment in the classical and hybrid OSN solvent recovery unit.

Werth et al. (2017b) based the capital investment for the heaters, condensers and evaporators on cost correlations in literature. The equipment size was estimated using Aspen Plus. The investment cost for pumps are taken from Hirschberg (1999), the costs for heaters and condensers from Matley (1984) and evaporators from Woods (2007). Additional expenses for periphery equipment such as piping,

instrumentation and control are based on the factors in Hirschberg (1999). The equipment costs were updated using the Chemical Engineering Plant Cost Index (CEPCI) to the year 2014. Utility consumption such as steam for evaporators, cooling water for the condenser and electricity for pumps were simulated in Aspen Plus. The cost of utilities was taken from Luyben (2011) for cooling water and steam and Baerns (2009) for electricity.

Werth et al. (2017b) based the cost for both membranes and membrane modules on a specific cost of 200 EUR/m^2. The difference in total membrane area and total module area was considered through Equations 2.7 and 2.8.

$$CI_{membranes} = C_{membrane} \times A_{membrane,total} \quad [2.7]$$

$$CI_{modules} = C_{module} \times A^{0.7}_{membrane,total} \quad [2.8]$$

The distribution in operating costs, capital costs and TAC of the classical and hybrid OSN unit developed by Werth et al. (2017b) are presented in Table 2.6. The cost of membrane replacement was based on a membrane life of 2 years.

Table 2.6: Distribution of the total annual cost (TAC) of classical and OSN units for the recovery of solvent. Costs are presented in ZAR/m^3 solvent recovered. Values are adopted from Werth et al. (2017b).

	Evaporation; no heat integration (Figure 2.3a)	Evaporation; with heat integration (Figure 2.4)	Hybrid OSN-evaporation; no heat integration (Figure 2.5a)
Feed capacity (m^3/h)	11	11	11
Overall solvent recovery	79%	79%	79%
Equivalent annual cost (EAC)*	14	14	23
Steam*	33	18	10
Cooling water*	3	3	1
Membrane replacement*	-	-	6
Electricity*	-	-	2
Total annual cost (TAC)*	50	35	42

* 16 ZAR/EUR exchange rate

The cost of steam makes the largest contribution towards the TAC of the classical unit with and without heat integration. However, through heat integration the steam consumption reduced by 45% which equates to savings of 15 ZAR/m^3 of solvent recovered.

The largest contribution toward the TAC of the hybrid OSN process is the EAC. However, Table 2.6 shows that the hybrid OSN process configuration has a lower TAC than evaporation without heat integration, but a higher TAC when heat integration is taken into consideration. The addition of an OSN unit reduces the steam and cooling water demand which leads to an overall reduction in total operating cost. However, the higher EAC of the hybrid-OSN unit suggests that the capital investment for the OSN unit is more than for an evaporation unit. The increased investment capital contradicts the findings for the Max-Dewax OSN unit which was apparently a third of the capital of a classical unit (Bhore et al., 1999). It is possible that the increase in capital was due to the improvement of the stability of OSN membranes from 1999 to 2014 and hence membrane costs have increased since 1999.

2.4 Conclusions drawn from literature review

Comparisons in the cost and energy consumption of classical, OSN and hybrid-OSN solvent recovery units were presented in the literature review. The main findings were as follows:

- The addition of an OSN unit lowers the overall energy consumption of a solvent recovery process.
- Werth et al. (2017b) observed that the capital cost of a hybrid OSN unit is more than evaporation. This contradicts the cost comparisons in Bhore et al. (1999) who reported that the cost of an OSN unit is a third of the capital of a classical separation unit.

The literature review also addressed the aspects of OSN separation on a single membrane to a membrane unit scale. These aspects included membrane characteristics such as membrane permeability and long-term stability, and design specifications such as membrane and module type and process flow configuration of OSN units.

The comparisons in cost and energy consumption between classical and OSN units by Werth et al. (2017b), Micovic et al. (2014) and Peshev & Livingston (2013) included a single set of model assumptions and inputs. Thus, one of the aims of this investigation is to evaluate how changes in membrane cost, long-term stability and membrane permeate rates would affect the conclusions drawn from the comparisons. To achieve this, Chapter 3 focusses on the development of a model to predict OSN separation. A conceptual OSN unit is developed in Chapter 4, which includes both membrane equipment and non-membrane equipment. The cost and energy consumption of the conceptual OSN unit is estimated and discussed in Chapter 5. In Chapter 6 comparisons of the TAC and SEC will be made for a classical solvent recovery unit and a hybrid-OSN unit. The techno-economic evaluation demonstrates if and how the estimated cost and energy of an OSN unit are affected by changes in model assumptions and inputs. These inputs include:

- Long-term membrane stability (i.e. average decline in membrane flux over membrane life) and membrane life,
- Membrane module cost,
- Solvent permeability,
- Pressure vessel cost, and
- Operating pressure.

CHAPTER 3: SIMULATING THE OSN MEMBRANE SYSTEM

Process simulation provides practical feedback when real-world applications are to be designed. A simulation can be used to assess the effectiveness of a process before it is installed.

To perform a process simulation, the following needs to be addressed:

- **The scope** – the boundaries of the simulation is clearly defined by making process assumptions, stating the objectives and providing the limitations of the simulation.
- **The methodology** – the solution approach is logically described with regards to inputs, equations, calculations and outputs.
- **Application and validation** – the output values of the objectives are simulated and validated with actual data from literature to assess the accuracy of the simulation.

Chapter 3 will provide the necessary insight behind the simulation of an OSN membrane system.

3.1 Scope of the OSN membrane simulation

A membrane system includes membrane stages of which a single stage is shown in Figure 3.1. The stages are placed in series and tapered (see Figure 2.9). Tapering compensates for the reduction of feed flow along the membrane housing due to permeation (Schwinge et al., 2004). Tapering allows a reduction in cross-sectional area along consecutive stages in a membrane system proportional to the reduction in flowrate. The degree of tapering depends on the following:

- Maximum applied pressure to avoid membrane damage due to telescoping and tensile stressing,
- Maximum allowable feed flowrate for the determination of the number of parallel pressure vessels, and
- Minimum allowable feed flowrate below which excessive concentration polarisation would lead to flux decline and membrane fouling.

A stage involves pressure vessels arranged in parallel so that the feed is distributed evenly amongst each vessel. The number of pressure vessels placed in parallel was based on the maximum allowable feed flowrate. Each pressure vessel contains multiple membrane modules arranged in series. Figure 3.1 provides a visual explanation of a stage involving three parallel pressure vessels – each containing three spiral wound membrane modules to serve as an example.

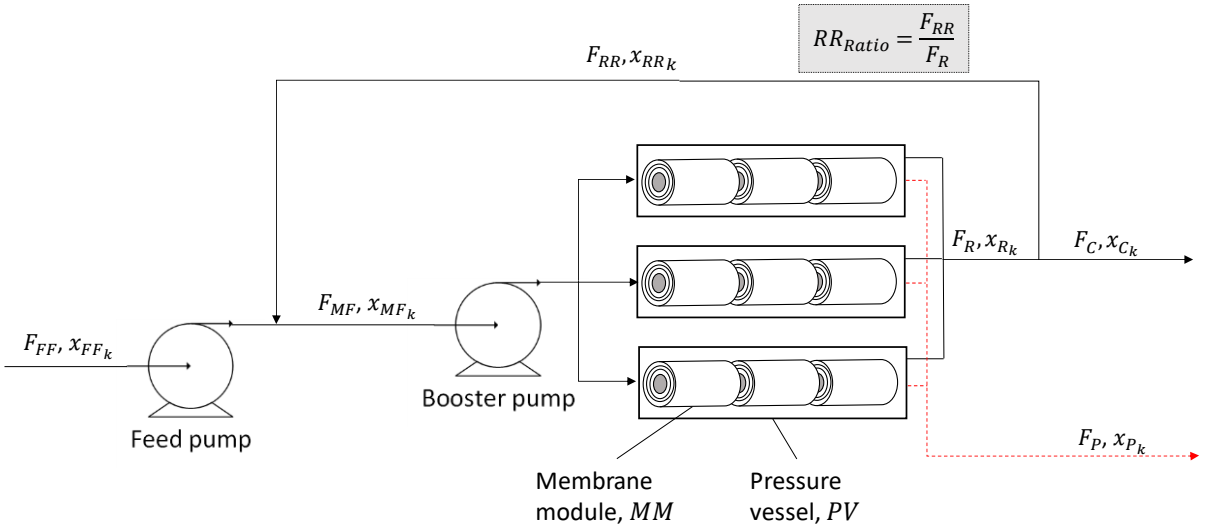

Figure 3.1: Schematic of a single membrane stage of an OSN membrane system.

The two product streams leaving the stage in Figure 3.1 are referred to as the permeate (F_P, x_{P_k}) and concentrate stream (F_C, x_{C_k}). The permeate stream is rich in species with a high membrane permeate rate relative to the rejected solute. On the other hand, the concentrate stream becomes richer in the rejected solute.

A portion of the retentate (F_R, x_{R_k}) is recycled back to the stage feed and is referred to as the retentate recycle (F_{RR}, x_{RR_k}). The purpose of a retentate recycle was to maintain the desired permeate rate at which concentration polarisation and pressure drop are at a minimum. Although it is not shown in Figure 3.1, a drop in pressure might appear along the length of the pressure vessel. This is due to pressure drops along the feed channels in a membrane module and from fittings used to connect membrane modules in a pressure vessel.

The objective for simulating a membrane system was to predict the flowrate and composition of the permeate streams and concentrate stream leaving each stage. Referring to Figure 2.9, the overall permeate was the sum of each permeate stream leaving a stage. The concentrate is the retained feed which becomes more concentrated in the rejected solute after each stage.

As part of defining the scope, certain simulation assumptions were necessary. The following assumptions were made for a filtrate feed containing dewaxed lube-oil dissolved in a solvent mixture of MEK and toluene:

- Initial membrane permeate rates for MEK, toluene and lube-oil are 214, 54 and 1 mm/h (White & Nitsch, 2000),
- Pentacosane ($C_{25}H_{52}$) was selected to represent lube-oil (White & Nitsch, 2000),

- The temperature across the membrane system remains constant at -5°C (White & Nitsch, 2000),
- The effective membrane area of a single module was 24 m^2 (Evonik, 2017),
- The pressure drop across a pressure vessel was 3.5 bar (Werth et al., 2017b),
- The operating pressure was 41.5 bar (White & Nitsch, 2000),
- The maximum feed pressure was 60 bar (Evonik, 2017),
- The maximum feed flowrate is 7.5 m^3/h (Evonik, 2017),
- Each pressure vessel contains 7 spiral wound membrane modules (Werth et al., 2017b),
- Membrane life is 2 years (Werth et al., 2017b; Micovic et al., 2014), and
- Long-term membrane stability is related to the 27% decline in membrane flux observed over time for the Max-Dewax unit after 12 500 hours membrane life.

The scope of the simulation was specifically defined to achieve the desired objectives. The limitations of the definitive scope, i.e. what could not be simulated, is discussed in the following section.

3.2 Limitations of the simulation

Simulating the membrane system did not take fluid dynamics and mass transfer characteristics into consideration. These aspects may be used to describe concentration polarisation and pressure drop in the feed channel of a membrane module. To apply fluid dynamics and mass transfer equations requires knowledge of the internal design of a membrane module such as the channel dimensions along with the fluid properties such as viscosity.

Concentration polarisation is measured in terms of a mass transfer coefficient, k_k. It can be estimated through the Sherwood correlation which in turn is a function of a species' diffusion coefficient. Since lube-oil is a mixture of alkanes, the task of assigning a single diffusion coefficient is troublesome. One approach is to perform parameter regression for semi-empirical mass transfer correlations and experimental data at various operating pressures (Shi et al., 2015). Since the present investigation involves a conceptual OSN unit, experimental work was not performed, and thus concentration polarisation was not taken into consideration.

3.3 Simulation methodology

A basic description of the separation across the entire membrane system can be done by assuming an average permeate flux and rejection. However, this simplified approach does not take into consideration the reduction in the driving force due to an increased osmotic pressure per stage. A common behavior observed in OSN membrane separation is a flux decrease with increasing solute concentration in the feed (Silva et al., 2014; Shi et al., 2015; Micovic et al., 2014). The osmotic pressure

would increase along the OSN membrane system as the solute content in the concentrate stream increases after each stage. Therefore, the simulation methodology for the membrane system estimates the separation for each stage. The set of equations provided in Figure 3.2 was used to estimate the separation through a single OSN stage.

Permeate flux:

$$J_k^V = b_k(x_{MF_k}^V - x_{P_k}^V \exp\left(\frac{-v_k((P_{MF}-P_P)-\Delta\pi_k)}{R_cT}\right) \quad [3.1]$$

$$\Delta\pi_k = v_k R_c T\left(c_{MF_k} - c_{P_k}\right) \quad [3.2]$$

$$x_{P_k}^V = \frac{J_k}{J_T} \quad [3.3]$$

$$J_T^V = \sum_{k=1}^{n} J_k^V \quad [3.4]$$

$$J_T^M = \sum_{k=1}^{n}(J_k^V \times \rho_k) \quad [3.5]$$

Total effective membrane area:

$$A_S = A_{MM} \times N_{MM} \times N_{PV} \quad [3.6]$$

Mass balance around stage:

$$F_P = J_T^M \times A_S \quad [3.7]$$

$$F_C = F_{FF} - F_P \quad [3.8]$$

$$x_{C_k}^M = \frac{x_{FF_k}^M F_{FF} - x_{P_k}^M F_P}{F_C} \quad [3.9]$$

$$F_{MF} = \frac{F_{FF} - F_P RR_{Ratio}}{1 - RR_{Ratio}} \quad [3.10]$$

$$x_{MF_k}^M = \frac{\left(x_{FF_k}^M F_{FF} - x_{P_k}^M F_P RR_{Ratio}\right)}{F_{MF}(1 - RR_{ratio})} \quad [3.11]$$

Solvent recovery and solute rejection:

$$R^M = 1 - \left(\frac{x_{P_{lube}}^M}{x_{MF_{lube}}^M}\right) \quad [3.12]$$

$$SR^M = \frac{F_P\left(1 - x_{P_{lube}}^M\right)}{F_{FF}\left(1 - x_{FF_{lube}}^M\right)} \quad [3.13]$$

Membrane flux decline over time onstream:

$$J_{Final}^V = J_{Initial}^V m_{FD}(\log(hours)) - 1 \quad [3.14]$$

Figure 3.2: List of equations to describe the solvent recovery over an OSN stage.

Volumetric permeate flux is described by the solution-diffusion transport model in Equation 3.1 for which osmotic pressure was determined through Equation 3.2. Since the sum of the mass fractions must equate to 1, the composition, x_{P_k}, for each k species was determined with Equation 3.3. The collected permeate from each pressure vessel was combined to provide the total permeate flux, J_T, as is shown in Equation 3.4 and 3.5. The permeate flowrate was then calculated with Equation 3.7 as the total permeate flux multiplied by the overall effective membrane area of a stage, A_S. The overall stage area was the product of the effective membrane area in a membrane model, A_{MM}, the number of serial modules in a pressure vessel, N_{MM}, and the number of pressure vessels, N_{PV}, per stage. Equations 3.8 to 3.11 represent the remaining mass balances to estimate the mass flowrate and composition of the concentrate stream, F_C and $x_{C_k}^M$, and the mixed feed, F_{MF} and $x_{MF_k}^M$. The overall solvent recovered in a stage, SR, was calculated with Equation 3.13 and membrane rejection of the lube-oil, R, with Equation 3.12. The long-term membrane stability with regards to flux decline over membrane life was accounted for through Equation 3.14. The final permeate flux, J_{Final}^V, was based on initial flux, $J_{Initial}^V$, and the rate of flux decline, m_{FD}, over the time the membrane was kept on stream in log-hours.

The fully specified system of equations in Figure 3.2 was solved by means of approximation. A solution was obtained when the result from Equation 3.15 is less than or equal to an accepted error for convergence, E. The approximation was an iterative approach to find a solution that would result in the convergence between an initial estimate for permeate flux, J_k, and secondary estimate, J_k^{+1}. For the membrane simulation, an accepted error of 1% was arbitrary chosen. All possible solutions, their error and additional results were arranged in a matrix. The least squares method was applied to find an approximate solution for the system with the smallest error.

$$J^{dif} = \frac{\sum_{k=1}^{n}(J_k^{+1} - J_k)}{\sum_{k=1}^{n} J_k} \quad [3.15]$$

$$J^{dif} \leq E \rightarrow convergence \quad [3.16]$$

Numerical modelers were used in combination to simulate the permeate flux and lube-oil rejection across a membrane system including multiple membrane stages. Aspen Plus will be used in Chapter 6 to estimate the size and energy consumption of traditional process equipment (i.e. pumps, heat exchangers, vessels, evaporators and distillation columns) in order to calculate the overall cost. Following the work by Fontalvo et al. (2014), the following three programs were chosen:

- **Microsoft Excel:** Well-known user interface to organize, link programs and present data,
- **MATLAB:** Strong numerical solver for user models and special units, and

- **Aspen Plus:** Commercial software for process design with integrated tools for energy analysis and economic evaluation.

The flow of information between Excel, MATLAB and Aspen Plus is described in the form of an illustration in Figure 3.3. The reader is referred to the "List of symbols" on Page vii for a description of each variable.

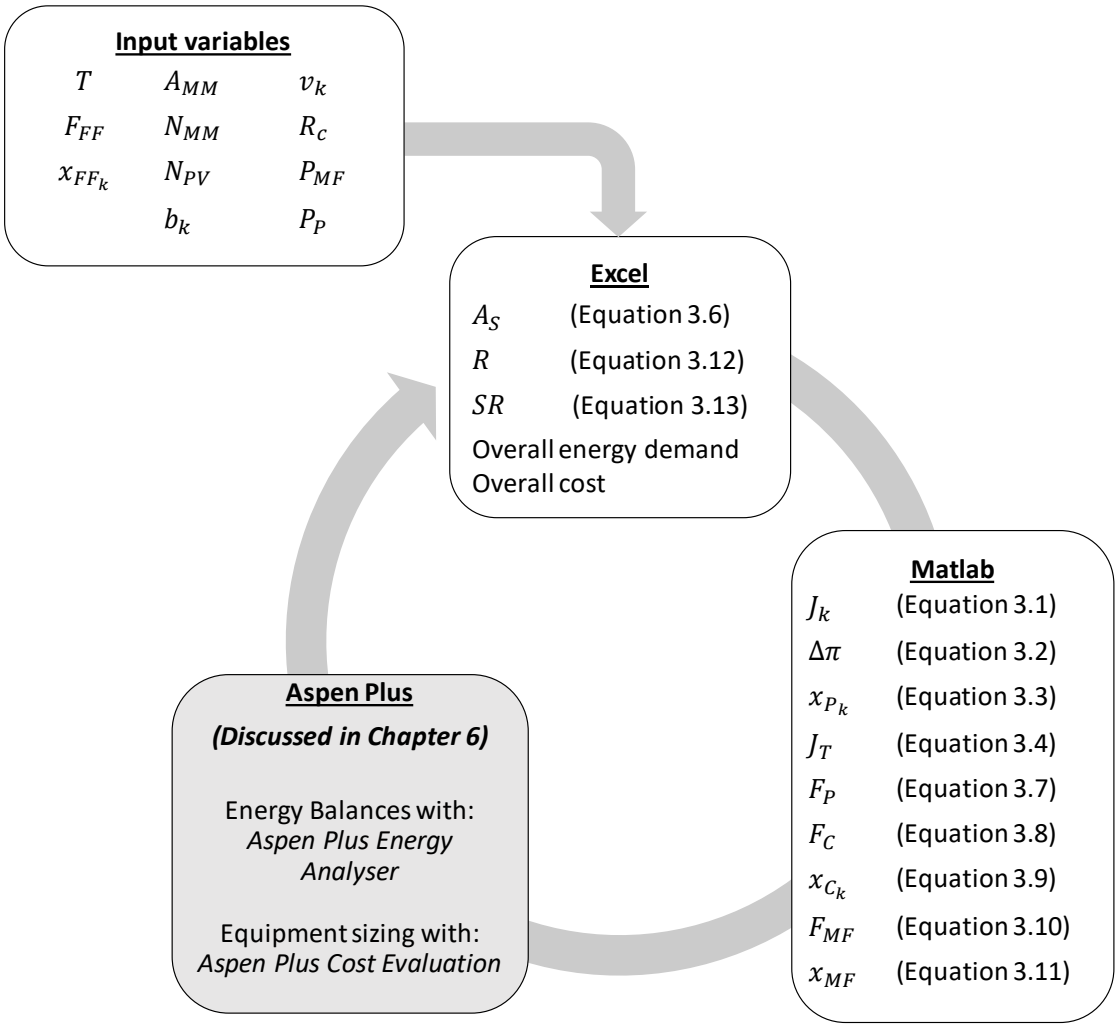

Figure 3.3: Flow of information in membrane system simulation.

The variables in Figure 3.3 are transferred by means of command (COM) add-ins freely available in Excel. These include Spreadsheet Link, Aspen Simulation Workbook and Macros in Visual Basic. In addition, all commands are performed in Excel while MATLAB and Aspen Plus run as background applications.

The simulation methodology can predict the solvent recovery and solute rejection per stage along a membrane system. To validate the simulation, the membrane permeate rates by White & Nitsch (2000) for the recovery of solvent from lube-oil was used to simulate permeate flux and composition

over an OSN membrane. The simulated results were compared to the experimental values measured by White & Nitsch (2000).

3.4 Validation and application

To serve as a validation, the simulation methodology was applied to estimate the permeate flux and composition for the recovery of solvent from dewaxed lube-oil by means of OSN membrane separation. The membrane permeate rates estimated in White & Nitsch (2000) were used since this study was the only literature source for the membrane permeate rates for a MEK, toluene and lube-oil system. The membrane system is described in Table 3.1.

Table 3.1: The membrane system configuration in White & Nitsch (2000).

Feed conditions:		
Temperature	-5°C	
Operating pressure	41 atm	
Composition by mass	MEK: 46.5%	
	Toluene: 34.7%	
	Lube-oil: 18.8%	
Feed flowrate	2.34 kg/h	
	2.76 L/h	
Membrane permeate rates	MEK: 214 L/m^2/h	
	Toluene: 54.3 L/m^2/h	
	Lube-oil: 1 L/m^2/h	
Membrane system configuration		
Number of pressure vessels	1	
Number of membrane modules per pressure vessel	4	
Retentate recycle by mass	-	
Effective membrane module area	3.55 cm^2	
Results	**White & Nitsch (2000)**	**Simulation**
MEK content in permeate	61%	60%
Toluene content in permeate	39%	38%
Lube-oil content in permeate	0.4%	2%
Permeate flowrate	16.1 ml/h	10.2 ml/h
Lube-oil rejection	98%	88%

A comparison between the simulated results and that in White & Nitsch (2000) is shown in Table 3.1. The mean absolute error in simulated permeate composition is 1.4%. The simulated permeate

flowrate was 2.3 mL/h less than what was experimentally observed by White and Nitsch (2000). In addition, the simulated rejection was 10% less than the experimental measurement.

One possible reason for the deviation could be that for the simulation, pure pentacosane was chosen as the reference for lube-oil. White & Nitsch (2000) carried out the experiments using real lubricant oil which is a mixture of alkanes. Since OSN is the size exclusion of species across a membrane, physical properties such as molecular weight and density would affect the separation.

Another reason could be related to the membrane permeate rates. White & Nitsch (2000) estimated the membrane permeate rates for MEK, toluene and lube-oil using the classical solution-diffusion model. However, no simulations were performed by White & Nitsch (2000) to demonstrate the validity of the regressed membrane permeate rates. Therefore, a secondary simulation was performed with adjusted membrane permeate rates for which the simulated results are shown in Table 3.2.

Table 3.2: The adjusted membrane system configuration based on White & Nitsch (2000).

Property	**White & Nitsch (2000)**	**Simulation with adjusted permeabilities***
Membrane permeate rates	MEK: 214 L/m^2/h	MEK: 360 L/m^2/h
	Toluene: 54 L/m^2/h	Toluene: 91 L/m^2/h
	Lube-oil: 1 L/m^2/h	Lube-oil: 1 L/m^2/h
MEK content in permeate	61%	61%
Toluene content in permeate	39%	38%
Lube-oil content in permeate	0.4%	1%
Permeate flowrate	16.1 ml/h	16.1 ml/h
Lube-oil rejection	98%	92%

* Toluene and MEK membrane permeate rates were adjusted by 168%.

The simulated results shown in Table 3.2 are closer to the experimental measurements after membrane permeate rates have been adjusted. The most significant improvements are seen for permeate flowrate and MEK content. However, the toluene and lube-oil composition and lube-oil rejection remain below that found by White & Nitsch (2000).

In Section 3.2 it was mentioned that one limitation for the simulation is that concentration polarisation was not taken into consideration. By neglecting solute buildup near the membrane surface on the feed-side, the simulated permeation rate of species would be higher than in experimental measurements. Silva et al. (2010) found that for highly rejected systems, the inclusion of fluid mechanics and concentration polarisation will produce more accurate predictions, especially when multiple membrane modules are connected in series.

To demonstrate how permeate flux and lube-oil rejection was estimated for a membrane system involving multiple stages, a system as described in Table 3.3 was simulated. The membrane system had a feed capacity of 480 m^3/h which is like the feed capacity of the Max-Dewax unit (Bhore et al., 1999). Membrane characteristics, feed conditions and composition were based on the adjusted membrane permeate rates in Table 3.2. Tapering and retentate recycle were based on the optimal feed conditions to each membrane module as per the manufacturer's recommendations (Evonik, 2018). The first three stages were to concentrate the residual feed by transporting solvent through the membranes. An additional polishing stage was included to increase the solvent purity of the permeate recovered from stages 1, 2 and 3.

Table 3.3: Inputs for the simulation of an OSN membrane system.

Feed conditions*				
Temperature	-5°C			
Operating pressure	41 atm			
Composition by mass	MEK: 46.5%			
	Toluene: 34.7%			
	Lube-oil: 18.8%			
Flowrate	406 t/h			
	480 m^3/h			
Membrane permeate rates	MEK: 360 L/m^2/h			
	Toluene: 91 L/m^2/h			
	Lube-oil: 1 L/m^2/h			
Membrane module design				
Effective membrane module area[+]	24 m^2			
Recommended feed flowrate[+]	7.5 m^3/h			
Membrane life [x]	2 years			
Average decline in membrane flux over membrane life*	28% after 15 936 hours (2 years)			
Membrane system configuration	**Stage 1**	**Stage 2**	**Stage 3**	**Polishing stage**
Number of pressure vessels	64	62	50	28
Number of membrane modules per pressure vessel	7	7	7	7
Retentate recycle by mass	-	0.255	0.195	0.155
* Bhore et al. (1999) and White & Nitsch (2000)	[+] Evonik: Puramem 4080 spiral wound polyimide membrane		[x] Werth et al. (2017b) and Micovic et al. (2014)	

The permeate flux, lube-oil rejection and accumulated solvent recovery per stage is presented in Figure 3.4.

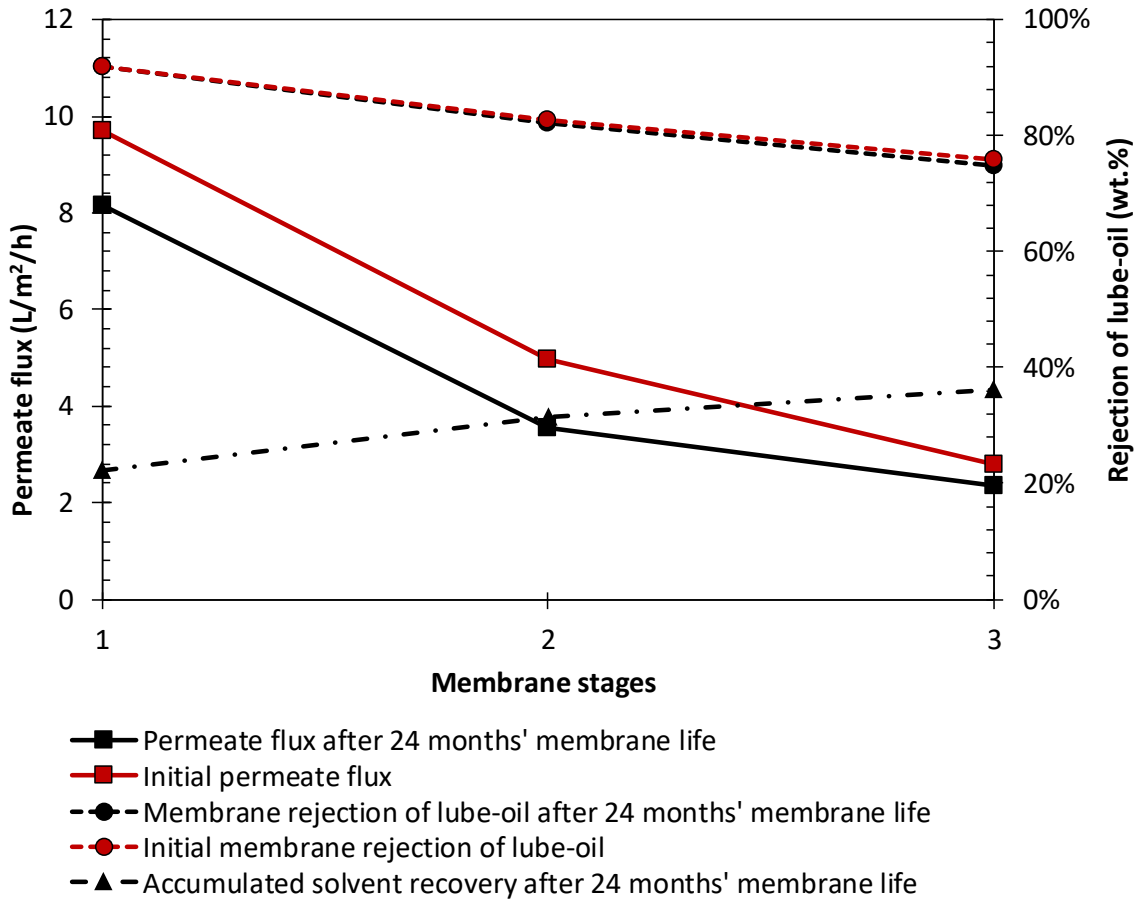

Figure 3.4: Accumulated solvent recovery, initial and final permeate flux and lube-oil rejection across the 3 concentrating stages. The feed capacity is 480 m^3/h and each stage include 7 membrane modules per pressure vessel.

In Figure 3.4 it is shown that both permeate flux and lube-oil rejection decreases along the membrane system. The greater amount of solvent passing through the membranes concentrates the residual feed. Since the driving force for membrane transport is the operating pressure minus osmotic pressure, permeate backpressure and pressure drop across a vessel, increased osmotic pressure will reduce permeate flux. Since the relative amount of solvent passing through the membrane compared to oil reduces, so too will the lube-oil rejection be reduced.

Figure 3.4 also shows that the accumulated solvent recovery increases as the number of stages increases. However, if the oil concentration in the residual feed goes beyond its solubility limit in the solvent, it will precipitate out of the solution and cause damage to the membrane.

In addition, any extent of solvent recovery is possible through including a retentate recycle loop over the concentrating stage. However, the operating pressure limits of the membrane will determine the

limits of solvent recovery. For OSN membrane modules, the maximum operating pressure is typically 60 bar.

The influence of using OSN membranes for a long duration compared to its initial performance is also shown in Figure 3.4. The stability of the membranes in the membrane system was based on the long-term demonstrations with the Max-Dewax unit. It was estimated that the initial permeate flux will reduce by 28% after keeping the membranes on stream for 2 years. It is clear in Figure 3.4 that lube-oil rejection is hardly affected by the decline in flux after 2 years. A similar trend was observed for the Max-Dewax unit where the lube-oil content in the recovered permeate remained below 1% from the start to after 560 days' operation (Bhore et al., 1999).

Figure 3.4 shows that after the first three stages, the lube-oil content in the overall permeate is 3%. Solvent recovery units at lube-oil refineries typically recover 99%-pure solvent (Sequiera, 1991). A polishing stage was therefore included to increase the purity of the final recovered solvent from 97% 99% resulting in an overall solvent recovery of 51%. Abejón et al. (2014) investigated how the overall solvent recovery and purity in OSN membrane systems are affected when the number of stages is varied. They showed that as the amount of solvent recovered increases, the purity of the solvent will decrease. Abejón et al. (2014) also demonstrated that increasing the number of stages will increase the amount of solvent recovered. The study also showed that purifying the permeate further through additional OSN membranes produces the highest purity and solvent recovery.

3.5 Conclusions drawn from the OSN process model

The aim of Chapter 3 was to describe a method for the simulation of an OSN membrane system. The methodology to simulate the separation across the membrane system involved combining two numerical modelers namely Excel and MATLAB. Aspen Plus will be used for its built-in energy balances and equipment sizing of classical process equipment in Chapter 6. The accuracy of the simulated OSN membrane stage performance was within 1% of the OSN experiments performed by White & Nitsch (2000) to recover solvent from dewaxed lube-oil.

The solution methodology was applied to predict flux, rejection, osmotic pressure and solvent recovery across a membrane system involving 3 concentrating stages and a polishing stage. The main findings from the simulation were

- Osmotic pressure increases as residual feed becomes more concentrated.
- An increase in osmotic pressure leads to a decrease in driving force.
- A decrease in driving force reduces permeate flux and lube-oil rejection since the relative amount of solvent passing through the membrane compared to lube-oil decreases.

- Accumulated solvent recovery increases along the membrane system.
- Solvent purity decreases as residual feed becomes more concentrated.
- The overall solvent recovery and purity for a 2-year membrane life is 51% and 99.9%.

The following Chapter will focus on developing a conceptual solvent recovery unit involving an OSN membrane system and the periphery equipment such as pumps, heaters, instruments, etc.

CHAPTER 4: CONCEPTUAL OSN PLANT TO RECOVER SOLVENT

Details of a conceptual design of an OSN plant to recover solvent from dewaxed lube-oil is provided in the present text. An overview of the plant design is given with regards to the feed intake, membrane skids and plant instrumentation.

Design assumptions are provided based on literature and through correspondence with suppliers such as Evonik, Germ Africa, Endress and Hauser, Proxa and Thermon South Africa. Sample calculations regarding equipment sizing is provided in Appendix B.

4.1 Scope of the conceptual OSN plant

A dewaxed lube-oil feed to a solvent recovery unit typically contains 20% lube-oil dissolved in an organic solvent or solvent mixture (Pitman and Harrison, 1982; Sequiera, 1991; Bhore et al., 1999; Khan et al., 2006). White & Nitsch (2000), Kong et al. (2006) and Yuan et al. (2013) performed OSN membrane experiments to recover dewaxing solvent from lube-oil. White & Nitsch (2000) is the only study that performed parameter regression to estimate the membrane permeate rates through a polyimide membrane. For the purpose this investigation, it was decided that the feed to the conceptual OSN plant will resemble that used by White & Nitsch (2000). In addition, the feed capacity was the same as the Max-Dewax unit since it was the largest and the first commercial implementation of OSN membrane separation for the lube-oil industry. The conditions of the feed to the conceptual OSN plant is shown in Table 4.1.

Table 4.1: Filtrate composition and feed conditions for conceptual OSN plant solvent recovery plant.

Property	Value
Temperature*	-5 ^{o}C
Feed flowrate**	480 m^3/h
MEK content*	46.5 wt.%
Toluene content*	34.7 wt.%
Lube-oil content*	18.8 wt.%

* White & Nitsch (2000) ** The Max-Dewax unit (Bhore et al., 1999)

In Chapter 3 it was shown that a membrane system operating at 41.5 bar and -5^{o}C can recover 51% solvent at a purity of 99.9% and average permeate flux of 11 L/m^2/h. The tapering per concentrating stage was 64, 62 and 50 pressure vessels. The polishing stage included 28 pressure vessels in parallel. Each pressure vessels contained 7 serial membrane modules. The tapering was based on a feed flowrate of 7.5 m^3/h which is recommended by the manufacturer, Evonik, for a Puramem 8040-type spiral wound OSN module. A process flow diagram of the conceptual OSN plant is shown in Figure 4.1.

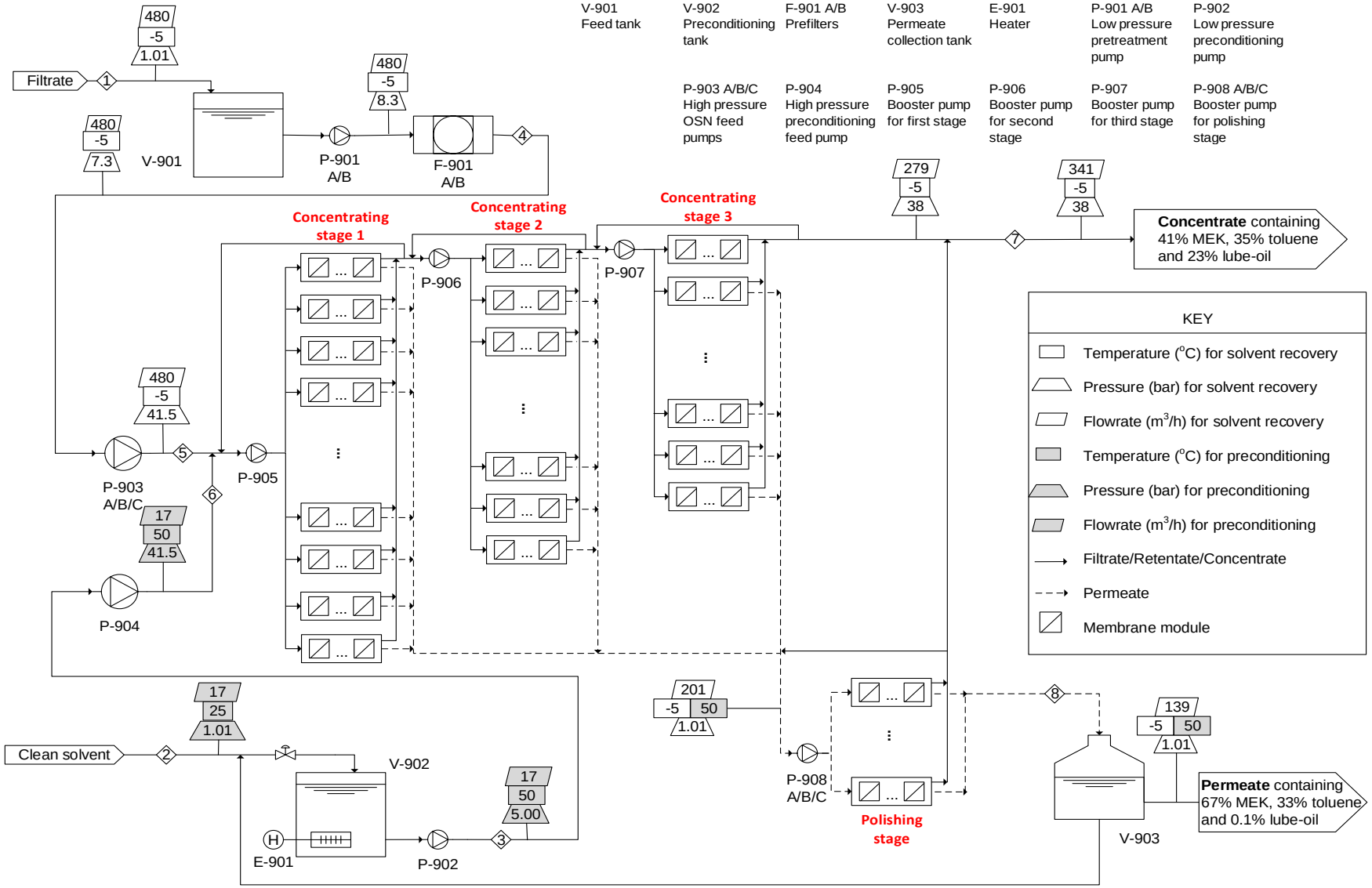

Figure 4.1: Process flow diagram of conceptual OSN plant for the recovery of solvent from dewaxed lube-oil.

4.2 Feed intake

Preconditioning is performed when a new membrane module is installed. Membrane modules are transported in a preservative solution to prevent them from drying. If a module becomes dry, the membrane sheets will start to pull apart causing irreversible damage (Evonik Resource Efficiency GmbH, 2017). Before the module can be used, the preservative is washed out with clean solvent. The preparation process is also referred to as preconditioning.

The present text involves PuraMem 8040-type spiral wound module manufactured by Evonik (Evonik Resource Efficiency GmbH, 2017). For preconditioning, at least 20 litres of clean solvent per m^2 of effective membrane area is required. The solvent was heated to 50°C and fed to each membrane element at an initial pressure of 3 to 5 bar. Heating the solvent is necessary to ensure that the preservative remains in solution during preconditioning. The permeate is collected in a permeate collection tank while the retentate is recycled back to the feed tank and fed to the membrane system. The system pressure was slowly increased to the operating pressure ranging from 20 to 50 bar. Once the recommended amount of clean solvent has been delivered, or the collected permeate is colourless, the permeate may be recycled to the feed tank and module is ready for use.

Referring to Figure 4.1, during preconditioning, clean solvent enters V-902 thereby bypassing V-901. The solvent is heated to the recommended preconditioning temperature of 50°C with heat exchanger E-901. Low-pressure pump, P-902, increases the pressure to the initial recommended pressure rage of 3 to 5 bar (Evonik Resource Efficiency GmbH, 2017).

Solvent recovery is the most frequent operation per annum, whereas preconditioning is only carried out when new membranes are installed which is every 1.5 to 5 years for polymeric membranes (Werth et al., 2017b; Micovic et al., 2014; Owen et al., 1995). During solvent recovery, filtrate is fed to a vessel, V-901. The pressure is increased with the low-pressure pump, P-901, to the recommended forward differential pressure to prefilter F-901. The prefilter offers protection for the membrane modules by removing any scaling particulates or wax crystals (Bhore et al., 1999; Gould et al., 1994).

Details of the feed intake, preconditioning, pretreatment filters and pumps are provided in the following subsections.

4.2.1 Filtrate feed tank (V-901)

The tank volume of V-901 was determined as a function of filtrate feed, $\dot{V}$, residence time, t_H, and freeboard volume percentage, FB (Sinnott, 2005). The feed flow rate to the vessel is equal to 480 m^3/h. The residence time for V-901 is assumed as 7.5 minutes but may range between 5 to 10 minutes. In addition, a freeboard volume of 10% was chosen in case of spillages due to agitation and

fluctuations in feed flowrate (Walas, 1988). Furthermore, V-901 is a horizontal tank with a length-to-diameter ratio (LD_{Ratio}) of 3 but may reach up to 5 (Ulrich and Vasudevan, 2004).

4.2.2 Preconditioning tank (V-902) and heating element (E-901)

V-902 is a cylindrical, horizontal vessel fitted with a freeboard volume of 10% (Walas, 1988). Furthermore, V-902 has a length-to-diameter ratio (LD_{Ratio}) of 3 but may reach up to 5 (Ulrich and Vasudevan, 2004).

Three 300 mm-thick concrete slabs with width equal to the diameter of the vessel was chosen as vessel support. The vessel is manufactured from 304-type stainless-steel (SS) with a 7.6 mm thickness. The insulation is 50 mm mineral fiber which will reduce heat lost to the environment by 7.2 kW (Thermon, 2018).

Preconditioning requires the permeation of 20 L clean solvent per m^2 membrane area. For three concentrating stages including 64, 62, 50 pressure vessels per stage, one polishing stage of 28 parallel pressure vessels and a 20% overdesign of membrane modules, the total preconditioning solvent is 823 m^3. Preconditioning is carried out over 48 hours which results in a solvent feed rate of 17.1 m^3/h.

The tank is heated with ceramic withdrawable elements. A ceramic element is inserted into a 304-type SS tubing which is mounted into the tank. The advantage of the design is that elements can be replaced without having to drain the tank (Thermon, 2018).

A heat calculation was carried out to determine the total heating requirement for E-901. Total heat involves heating the preconditioning solvent from room temperature to 50°C and compensation for the heat lost to the environment. As per a representative from Thermon, a 75% thermal efficiency and a heating period of 1 hour could be assumed. This would result in a total heat requirement of 250 kW. A withdrawable heating element from Thermon can maintain 20 kW and is 4 meters in length and 53 millimeter in diameter yielding a total radiant area of 4 m^2 and power density of 2.9 W/cm^2. To maintain the heating requirement, 13 withdrawable elements are required. A Type K thermocouple and a Gefran 600 PID controller was included as per recommendation of Thermon Africa.

4.2.3 Pretreatment filters (F-901)

Prefilters remove any scale or wax crystals that might be present in the feed stream (Bhore et al., 1999). This protects OSN membranes against particulate fouling which if present could cause irreversible membrane damage. For an industrial example in the oil refining industry, the addition of bag filters was found to increase the useful life of coalescing filters from 2 weeks to 2 months (The Filtrate Specialists, Inc.).

Germ Africa (PTY) Ltd. offers solutions for filtration, dosing pumps and industrial lubricant production (Germ Africa, 2018). A Flowrite filter housing equipped with five FSI filter bags was recommended to treat the dewaxed filtrate feed described in Table 4.1. The filter bags are manufactured from a polypropylene polymer with a 5-micron size-exclusion. The size rating corresponds to the minimum size of paraffin wax crystals (Mokhlif et al., 2014; Mansoori et al., 2003). The filter housing is fitted with swing-bolt cover for easy access during bag replacement. Additional information regarding the operating specifications and material of construction (MOC) is presented in Table 4.2.

Table 4.2: Properties of the prefilter designed and quoted for by Germ Africa.

Property	Description or value
Filter bag MOC	Polypropylene
Filter vessel MOC	304 Stainless steel
Operating pressure	825 kPa
Maximum feed flow	90 m^3 /h
Number of bags per vessel	5

For a 480 m^3/h feed, at least 6 prefilters operating in parallel were necessary to maintain the filter feed below the maximum flowrate of 90 m^3/h. Six additional backup filters were included to reduce plant downtime when filters required replacement or maintenance.

4.2.4 Low pressure solvent recovery and preconditioning pump (P-901 and P-902)

P-901A/B/C was to maintain the 825 kPa forward differential pressure feeding the prefilter, F-901. P-902 would provide the 3 to 5 bar initial pressure for preconditioning.

Rhine Ruhr Pumps & Valves have a good reputation for petrochemical processes and has worked alongside PetroSA, Engen and Chevron (Rhine Ruhr Pumps and Valves, 2018). Rhine Ruhr Pumps offers a vertical in-line, process pump that can deliver the required pressure for pretreatment and preconditioning (RuhRPumpen Selection Guide, 2011). The centrifugal pump has a single suction, closed impeller that can handle feed capacities from 2.5 to 500 m^3/h. The discharge and suction size range from 25 to 300 mm. The material of construction (MOC) follows the API 610 standards. For lubricant oil processes below 230°C, the s-1 material class is recommended. The full compliance and trim material is steel and cast-iron (API Standard 610, 2010). Furthermore, the pressure casing is made from carbon steel, the impeller from cast iron, and shaft is manufactured with carbon steel (API Standard 610, 2010).

For pretreatment with F-901, an additional pump was included as a backup. No backup was included for preconditioning since P-902 is not as frequently used as P-901 and is therefore believed to require less maintenance. In addition, the pumping efficiency was assumed to be 65%.

4.3 Membrane skid

Spiral wound modules were chosen due to their increased effective membrane area relative to their floor footprint (Schwinge et al., 2004). The modular nature of the design allows for the expansion from one to multiple modules in series, contained in a pressure vessel (Buonomenna, 2013). The stacking of multiple pressure vessels in parallel is a common technique used for large-scale membrane plants to lower plant footprint (Werth et al., 2017b; Micovic et al., 2014; Gould et al., 1994). The result is an organized group of tubular pressure vessels that can be fixed to framework.

Membrane module manufacturers provide a recommended feed flowrate at which concentration polarisation and pressure drop in the feed channel are at a minimum. In addition, to maintain the feed to a pressure vessel at the recommended flowrate a portion of the retentate leaving a stage is recycled to the stage inlet (Peck, 2017).

Tapering refers to the cascading of parallel pressure vessels in a descending order. This was necessary since the feed to the following stage will decrease due to the solvent recovered by the previous stage (Schwinge et al., 2004). For solvent recovery, the concentrated product from a stage becomes the feed to the following stage. To purify the final recovered solvent, the feed to the additional membrane stage would be the overall permeate recovered during solvent recovery. However, if the solvent recovery is too high the oil concentration in the residual feed might become more than the solubility limit. When this occurs oil will precipitate from the solution and cause irreversible membrane damage.

4.3.1 Pressure vessel

The pressure vessel is designed to withstand the feed-side pressure for OSN operations ranging between 20 and maximum 60 bar (Evonik Resource Efficiency GmbH, 2017). Figure 4.2 provides the dimensions of a Pentair Codeline pressure vessel design containing seven 203 mm diameter by 1016 mm in length modules.

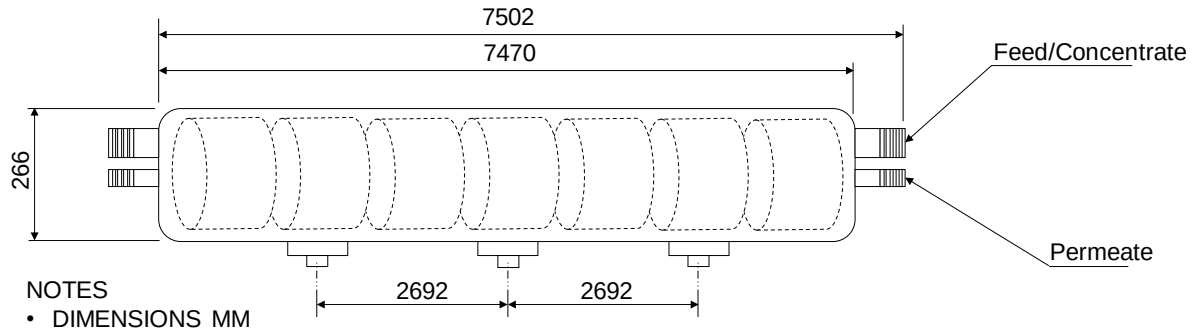

Figure 4.2: Schematic of pressure vessel design with dimensions (based on Pentair Codeline 40E100 high-pressure membrane housing model (2017)).

Referring to Figure 4.2, permeate is drawn from both ends, whereas the feed and concentrate enter and exit on either side. The initial design was constructed with glass reinforced plastic. However, type 304 SS is preferred for the application at an oil refinery (Callister and Rethwisch, 2011).

The modeling approach in Chapter 3 did not included hydrodynamic fluid calculations that describe the pressure drop through the membrane modules and pressure vessel. A constant pressure drop was therefore based on Werth et al. (2017b) who assumed a pressure drop of 3.5 bar for vessels containing up to 8 spiral wound membrane modules.

4.3.2 Membrane modules

An 8040- type spiral wound membrane module from Evonik including polyimide OSN membranes was chosen for the conceptual OSN unit. Through correspondence with Evonik, the pressure drop through an 8040-type module would not be more than 1 bar (Evonik, 2018). The specifications are provided in Table 4.3.

Table 4.3: Specifications for the spiral wound membrane module for the conceptual OSN plant design to recover dewaxing solvent (Evonik Resource Efficiency GmbH, 2017).

Design aspect	Value
Module type	8040*
Nominal diameter	203 mm
Nominal length	1016 mm
Effective membrane area	24.0 m^2
Recommended feed flowrate	7.5 m^3/h
Standard feed spacer height	0.76 mm
Operating pressure range	20-40 bar

Table 4.3 (continued): Specifications for the spiral wound membrane module for the conceptual OSN plant design to recover dewaxing solvent (Evonik Resource Efficiency GmbH, 2017).

Design aspect	Value
Maximum pressure	60 bar
Maximum temperature	50 °C

* 8040 refers to an 8.0" (diameter) by 40" (length) module

4.3.3 Feed pumps for solvent recovery and preconditioning (P-903, P-904 and P-908)

For high pressure feed, SCE OH2 (API 610), horizontal process pumps from RuhRPumpen was chosen since it is suitable for petroleum refining (RuhRPumpen Selection Guide, 2011). The OSN feed pump, P-903, and polishing pump, P-908, each includes two parallel pumps in operation plus one additional backup pump. The high-pressure preconditioning pump, P-904, is only one pump without a backup. The centrifugal pump can produce a pressure head up to 480 m water, maximum capacity of 3 200 m^3/h and 90 bar pressure and is thermally stable between -120 to 450°C. In addition, the discharge and suction flange size may vary between 25 and 300 mm.

4.3.4 Booster pumps (P-905, P-906 and P-907)

Although the purpose of a pressure vessel is to maintain a constant internal pressure, pipe connections and internal vessel design may contribute to pressure losses (Cengel and Cimbala, 2014). A booster pump compensates for the pressure loss across a stage and is located after the recycled retentate connection, at the start of each stage.

The single stage SCE OH2 (API 610), horizontal process pump manufactured by Rhine Ruhr Pumps & Valves was selected. During solvent recovery, preliminary calculations showed that the pressure head for booster pumps will remain at 480 m or below, even if no pressure drop is observed. However, for preconditioning the head may exceed 480 m since the density of the solvent mixture is lower than the mixed dewaxed filtrate feed. Choosing a system pressure that is lower than the 60 bar maximum for OSN like 41.5 bar will reduce the head requirement and mitigate the issue. Furthermore, no backup pump was considered for the booster pumps since OSN model predictions showed that a pressure vessel pressure drop of 3.5 bar would lower flux by no more than 6%.

4.3.5 Permeate collection tank (V-903)

During preconditioning, the permeate was collected in the permeate collection tank equipped with a transparent fitting on the outlet line enabling a visual assessment of stream colour. The permeated solvent will turn colourless once all the preservative has been removed (Evonik Resource Efficiency GmbH, 2017). A residence time of 7.5 minutes, freeboard volume of 10%, and length-to-diameter ratio of 3 was chosen for the horizontal tank (Walas, 1988).

4.3.6 Skid dimensions

Pressure vessels grouped in stages are arranged on skids to minimise plant floor area. To determine the height, width and depth of the membrane skids, the following assumptions are made:

- The minimum horizontal and vertical spacing between each pressure vessel on a skid was one times the diameter of the pressure vessel, which is approximately 270 mm.
- Skid depth was taken as 10 m which was based on a pressure vessel length of 7.5 meters plus a 1.25-meter compensation for pipe fittings on each side of the vessel.
- A 10-meter horizontal clearance was included behind each skid for pressure vessel maintenance.
- A 3-meter horizontal clearance was included in front of the skid for the replacement of membrane modules.
- A horizontal clearance of 2 meters was maintained between adjacent skids.
- A 20% over design factor was included for the three concentration stages resulting in 76, 74 and 60 pressure vessels per stage (Owen et al., 1995).
- A 20% over design factor was also included for the polishing stage to yield a total of 34 pressure vessels.
- Each individual membrane stage was mounted to a skid.
- No more than 6 pressure vessels were stacked on top of each other to yield a skid height of 3 meters.

The floor area for the membrane system including minimum clearance in front, between and behind skids was 635 m^2. A front view of each skid is presented in Figure 4.3 and a top view of the entire membrane system is shown in Figure 4.4.

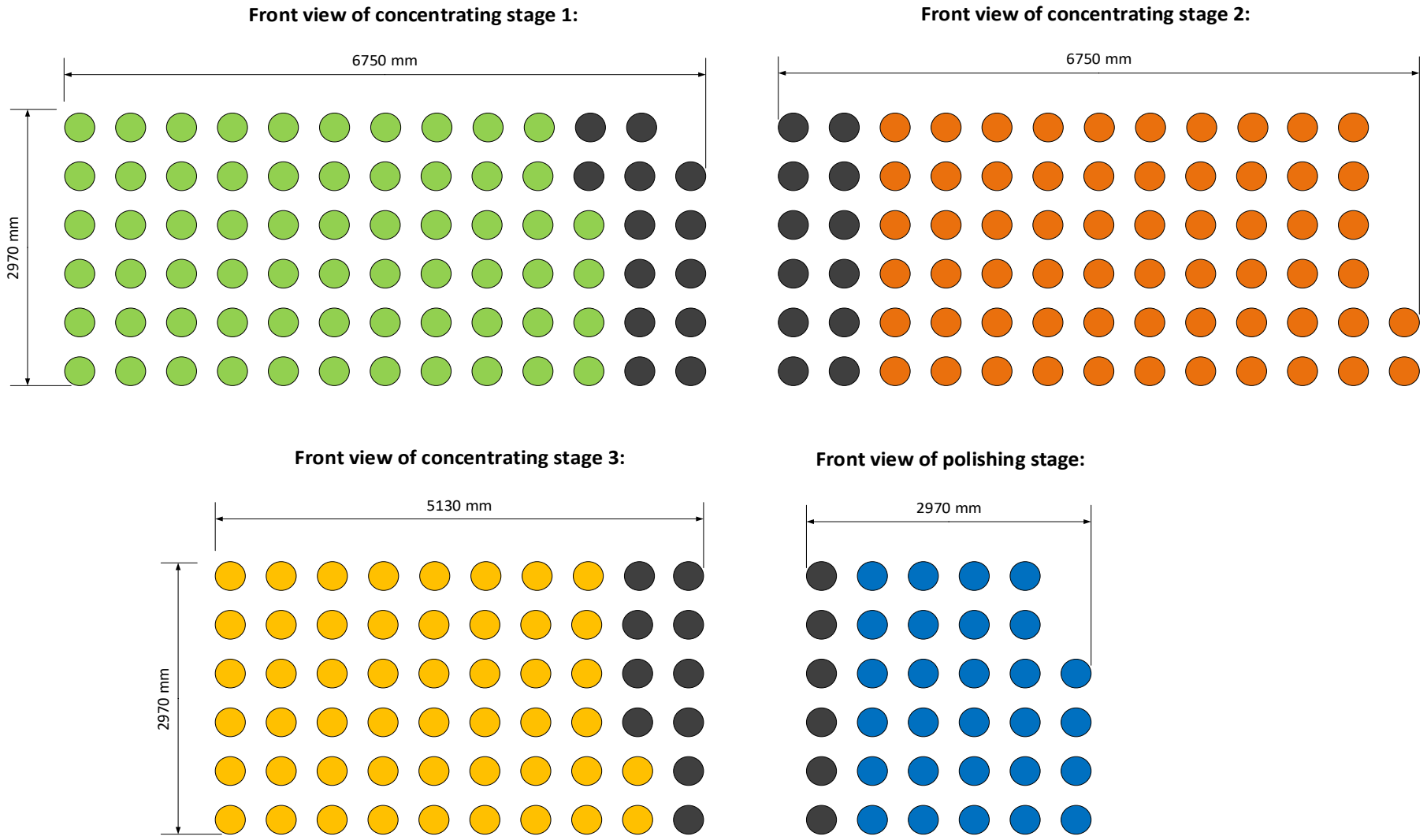

Figure 4.3: Front view of skid designs. The first stage is represented by ●, the second stage is ●, the third stage is ●, the polishing stage is ● and the back-up pressure vessels are indicated as ●.

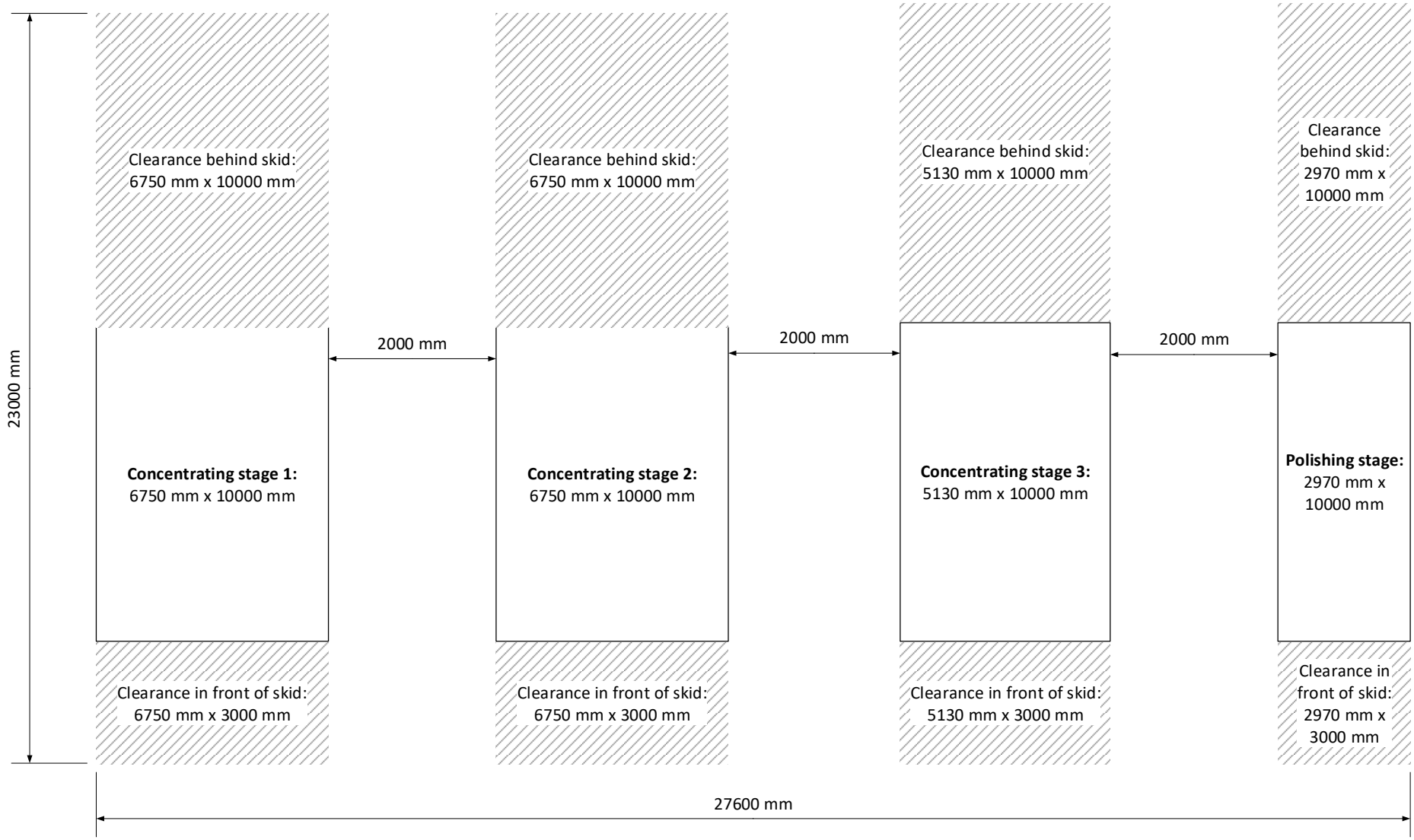

Figure 4.4: Top view of membrane skids including minimum clearance in front, between and behind skids.

4.4 Instrumentation for monitoring flowrate, temperature and differential pressure

Instrumentation was taken into consideration to measure the liquid level in tanks (V-901, V-902 and V-903), differential pressure across prefilters (F-901) and pressure vessels, the temperature of dewaxed filtrate and preconditioning solvent to the feed intake, and the flowrate of the fresh filtrate (Stream 4), mixed feed, total permeate product (Stream 8) and concentrated product (Stream 7) from a skid.

The selection and sizing of the relevant sensors was acquired through conversing with a supplier from Endress & Hauser. The identification code, output signal and sensor range are listed with permission from Endress & Hauser (2018).

Table 4.4: Measurement, output and range specifications for sensors considered for the conceptual OSN plant design (based on quote from Thermon, 2018).

Equipment ID	Measurement	Output signal (mA)	Range (overload)
Cerebar PMP21 IA1U1HBWJJ	Pressure	4 to 20	1 bar (4 bar)
Cerebar PMP21 IA1U1MBWJJ	Pressure	4 to 20	4 bar (16 bar)
Cerebar PMP21 IA1U1SBWJJ	Pressure	4 to 20	40 bar (160 bar)
RTD-assembly TLSR2	Temperature	-	-5 to 200^{o}C
Prosonic Flow 92F80 Inline, DN80 3”	Flowrate	4 to 20	0 to 181 m^3/h

From Table 4.4, two Cerebar PMP21 probes measuring in the 1 bar-range were chosen to determine liquid level in tanks V-901, V-902 and V-903. One probe is submerged in the liquid while the other is placed above the liquid level in the gaseous phase. The sensors’ signal is sent to a programmable logic computer (PLC) which calculates the liquid level (Seborg et al., 2011).

The bag filters in F-901A/B require replacement when the pressure drop across the cartridge exceeds 1 bar (The Filter Specialists, Inc., 2018). Two Cerebar PMP21 probes measuring in the 4 bar-range were attached to the inlet and outlet of F-901 to determine the differential pressure across the prefilter. Pressure drop across the pressure vessels was determined in a similar manner to that of the prefilter, however the Cerebar PMP21 probe measuring in the 40 bar-range was selected (Endress & Hauser, 2018). In addition, to lower costs one set of differential pressure meters was assigned to a group of 10 pressure vessels.

Temperature control is important for process control purposes (Seborg et al., 2011). The temperature is measured with a TLSR2 South African style RTD sensor with a cable probe (Endress & Hauser, 2018).

Flowrate sensors are the most expensive compared to the pressure and temperature probes (Endress & Hauser, 2018). This is due to design improvements with regards to system integration. The Cerebar PMP21 probes require a PLC and SCADA (supervisory control and data acquisition) to process the measured information. Alternatively, the Prosonic Flow 92F80 Inline sensor can process and transmit information via a wireless LAN; accessible to plant operators on their personal computers, tablets and even cellular devices (Endress & Hauser, 2018). The sensor is also designed using Heartbeat Technology enabling permanent self-monitoring and diagnostics for reduced maintenance and quick remediation.

4.5 Summary of equipment specification

A summary of each group of equipment is shown in Table 4.5 for tanks, Table 4.6 for the heater, Table 4.7 for the prefilter, Table 4.8 for membrane modules, Table 4.9 for pressure vessels and Table 4.10 for the pressure pumps.

Table 4.5: Design specifications for the tanks (V-901, V-902 and V-903).

Vessels	**V-901**	**V-902**	**V-903**
Temperature (°C)	-5	50	-5 to 50
Pressure (bar)	1.01	1.01	1.01
Orientation	Horizontal	Horizontal	Horizontal
MOC* (Insulation MOC)	CS**	CS (Organically bonded glass fiber, 50mm thick)	CS
Height/Length (m)	9.1	6.0	6.0
Diameter (m)	3.0	2.0	2.0

* Material of construction ** Carbon-steel

Table 4.6: Design specification of heater (E-901).

Heater	**E-901**
Type	Electric
MOC*	Ceramic element in 304SS** tubing
Thermal efficiency	75%
Maximum power rating per element (kW)	20
Overall heat demand (kW)	252
Number of withdrawable heating elements	13
Convective area (m^2)	4.01
Tube pressure (bar)	1.01

* Material of construction ** Type-304 stainless-steel

Table 4.7: Design specification of prefilters (F-901A/B).

Filter	**F-901**
Type	Bag filter
Filter bag MOC*	Polypropylene
Filter housing MOC*	304SS**
Micron rating	5
Effective filter area (m^2)	2.27
Working pressure (bar)	8.25
Change-out pressure (bar)	0.6 – 1.01
Percentage backups	100%

* Material of construction ** Type-304 stainless-steel

Table 4.8: Design specifications of membrane modules (MM).

Membrane module	**MM**
Type	SWMM*
Temperature (^oC)	-5
Pressure (bar)	41.5
Membrane MOC**	Polyimide
Flowrate ($m^{3/}h$)	7.5
Effective membrane area (m^2)	24.0
Length (m)	1.02
Outer diameter (m)	0.20

* Spiral wound membrane module ** Material of construction

Table 4.9: Design specifications of pressure vessels (PV).

Pressure vessel	**PV**
Temperature (^oC)	-5
Pressure (bar)	41.5
Orientation	Horizontal
MOC*	304SS**
Length (m)	7.5
Diameter (m)	0.27

* Material of construction ** Type-304 stainless-steel

Table 4.10: Specifications of pumps (P-901A/B, P-902, P-903A/B, P-904, P-905, P-906, P-907 and P-908).

Pumps	**P-901 (A/B)**	**P-902**	**P-903 (A/B/C)**	**P-904**	**P-905**	**P-906**	**P-907**	**P-908 (A/B/C)**
Flowrate per pump (m^3/h)	480	17.1	240	17.1	480	465	376	105
Fluid density (kg/m^3)	862	826	862	826	862	865	867	856
Power per pump (kW)	148.4	2.9	330.8	26.7	71.8	69.6	56.3	181.8
Type/Drive	Centrif.*/ Electric	Centrif.*/ Electric	Centrif.*/ Electric	Centrif.*/ Electric	Centrif.*/ Electric	Centrif.*/ Electric	Centrif.*/ Electric	Centrif.*/ Electric
Efficiency	65%	65%	65%	65%	65%	65%	65%	65%
MOC**	CS***	CS***	CS***	CS***	CS***	CS***	CS***	CS***
Inlet temperature (^oC)	-5	50	-5	50	-5	-5	-5	-5
Inlet pressure (kPa)	101	101	725	500	3804	3804	3804	101
Outlet pressure (kPa)	825	500	4154	4154	4154	4154	4154	4154
Percentage spares	100%	-	100%		-	-	-	100%

* Centrifugal ** Material of construction *** Carbon-steel

CHAPTER 5: COST AND ENERGY CONSUMPTION OF THE CONCEPTUAL OSN UNIT

The cost and energy consumption of the conceptual OSN unit developed in Chapter 4 was is estimated and discussed with regards to:

- **Capital cost:** Direct equipment cost (purchasing, erection, piping, electrical, instruments and process buildings) and indirect costs (engineering, contractor's fees and contingency).
- **Operating cost**: Direct costs (raw materials, utilities, operating labour, supervision, maintenance and repairs, laboratory work, membrane replacement and operating supplies), fixed costs (plant overhead) and general expenses (administration and laboratory charges).
- **Total annual cost (TAC):** Annualised capital plus operating cost per m^3 solvent recovered per year.
- **Specific energy consumption (SEC):** Overall energy demand per m^3 solvent recovered per hour.

Table 5.1 provides a breakdown of the system properties affecting capital cost, operating cost, total annual cost and specific energy demand.

Table 5.1: Breakdown of properties of the system that affects either operating cost, capital cost, total annualised cost or energy demand.

Operating cost	Capital cost	Total annual cost	Specific energy demand
Preconditioning solvent	Purchased cost of membrane and non-membrane equipment	Operating cost	Pump energy
Utilities	Erection	Capital cost	Heating energy
Operating labour	Electrical	Annual average solvent recovered	Annual average solvent recovered
Supervisory labour	Instrumentation	Flux decline*	Flux decline*
Laboratory work	Process buildings		
Membrane replacement*	Engineering		
Maintenance and repairs of non-membrane equipment	Contractor's fees		
Operating supplies	Contingency		
Administration costs			
Laboratory charges			

* Dependent on membrane life

Assumptions for the estimation of cost and energy consumption is presented in Section 5.1, followed by a sensitivity in Section 5.7. The remaining sections will address SEC, capital cost, operating cost and TAC.

5.1 Assumptions for cost and energy estimation

In order to estimate the cost of and energy consumed by the OSN unit, the following assumptions were made:

- The OSN unit is an addition to an existing process. Thus, the cost of raw material and finished products storage, ancillary buildings like offices and workshops, land or site preparation are omitted.
- The OSN unit is a continuous process operating 24 hours a day and 332 days per annum which is equivalent to 91% of the total hours available in a year (Sinnott, 2005).
- The feed is like that of the Max-Dewax unit at 480 m^3/h, 46.5% MEK, 34.7% toluene and 18.8% lube-oil, at -5°C and 1 atmospheric pressure (Bhore et al., 1999; White & Nitsch, 2000).
- The operating pressure for each membrane stage is 41.5 bar.
- Pentacosane ($C_{25}H_{52}$) is the reference component for lube-oil. (White and Nitsch, 2000; Kong et al., 2006).
- Long-term membrane stability is based on stability tests performed with the Max-Dewax unit over 14 months (Bhore et al., 1999). The average flux decline observed for Max-Dewax over a 1.5-year membrane life was 27%.
- The membrane permeate rates for MEK was 360 mm/h, 91 mm/h for toluene and lube-oil was 1 mm/h (White and Nitsch, 2000).
- Temperature is assumed to be constant between across membrane modules and pressure vessels.
- The purchasing price of pumps and tanks were based on the cost correlations in Turton et al., (2012).
- The membrane module price is initially 3 200 ZAR/m^2 from Werth et al. (2017b) but quotes of 4120 ZAR/m^2 and 10 000 ZAR/m^2 have been obtained from SolSep BV (2018) and Evonik (2018).
- The purchasing price for a pressure vessel containing seven membrane modules was quoted for 42 000 ZAR (Stainless Crazy, 2018).
- Direct equipment expenses such as the cost for piping, erection, electrical, instruments and process buildings are included and based on the Lang factors (Sinnott, 2005).

- Indirect capital costs for engineering, contractor's fees and contingency are respectively 30%, 5% and 10% of the overall direct equipment cost (Sinnot, 2005).
- Assets are depreciated over 25 years at and interest rate of 7% (SARS, Interpretation note: No.47, 2009; Werth et al., 2017b; Owen et al., 1995).
- Preconditioning solvent contains 59% MEK and 41% toluene. The cost is 21 120 ZAR per ton (S&P Global, 2018; Hashmi, 2018).
- A total of 26 plant operators are required per year based on the correlations by Alkhayat and Gerrard (1984) for one particulate and two non-particulate processing steps. An average salary per operator is R13 160 (Indeed, 2018).
- The cost of electricity is 1.32 ZAR/kWh (Eskom, 2017/2018).
- Historic costs are updated to 2019 using the CEPCI (chemical engineering plant cost index. The CEPCI values for 1999 is 390.6, 2014 is 591.9, 2017 is 588.4, 2018 is 593.8 and 2019 is 600.8 (Vatavuk, 2002; Mignard, 2014).
- The exchange rate from South African rand to US dollar is 14 ZAR/USD and 16 ZAR/EUR to the Euro (Bloomberg, 2018).
- The effective membrane area is 24 m^2 per module (Evonik Resource Efficiency GmbH, 2017).
- Membrane life is 2 years but can range between 1.5 and 3 years (Bhore et al., 1999; Werth et al., 2017; Owen et al., 1995; Micovic et al., 2014).
- No energy is recovered within the process.

5.2 Specific energy consumption (SEC) research and technique

Energy is consumed during the following process steps in the OSN unit:

- Heating the preconditioning solvent from 25°C (i.e. room temperature) to 50°C, and
- Increasing the pressure with low-pressure, high-pressure and interstage booster pumps.

The energy demand is expressed as the **specific energy consumption (SEC)** in kW per m^3 solvent recovered per hour. This section will provide the research design and technique used to estimate the SEC of the conceptual OSN unit. For supplementary information regarding energy calculations, the reader is referred to Appendix B.

Heating of preconditioning solvent:

Heater E-901 increases the temperature of preconditioning solvent from room temperature (25°C) to 50°C using electrical energy (Thermon, 2018; Heiligenstein and Neubert, 1998). Preconditioning is carried out once a new membrane module has been installed to wash out the preservative. A temperature of 50°C ensures that the preservative remains in solution (Evonik, 2017). The membrane

life determines how frequently preconditioning is performed. The duration of preconditioning the entire membrane system is assumed to be 48 hours (Evonik, 2017).

Pump power for pretreatment, preconditioning, OSN feed and interstage boosters:

The mechanical efficiency of all pressure pumps was set to 65%. The energy demand during preconditioning includes the low-pressure pump, P-902, and high-pressure pump, P-904. The remaining pumps, P-901, P-903, P-905, P-906, P-907 and P-908 are in operation during the recovery of solvent.

Specific energy consumption of the OSN unit for the recovery of solvent:

Overall energy consumption is expressed as power per volume solvent recovered per hour. Peshev & Livingston (2013) used SEC since it is independent of feed flowrate and membrane area. The SEC of the OSN unit in the present investigation is exclusively dependent on the amount of solvent recovered. A mathematical definition for SEC is presented in Equation 5.1 (Peshev & Livingston, 2013).

$$SEC = \frac{Q_{Heating} + W_{Pumping}}{\dot{V}_{SR}} \quad [5.1]$$

The distribution of SEC for the conceptual OSN unit is shown in Table 5.1.

Table 5.1: Distribution of SEC over the OSN unit for the recovery of solvent.

Equipment ID	Function	SEC (kWh/m^3)	Distribution
E-901	Heating preconditioning solvent	1.81	15%
P-901	Pressure increase for prefilters	1.06	9%
P-902	Low-pressure preconditioning pump	0.02	0%
P-903	High-pressure feed pump	4.74	40%
P-904	High-pressure preconditioning pump	0.19	2%
P-905	Interstage pressure booster for first stage	0.51	4%
P-906	Interstage pressure booster for second stage	0.50	4%
P-907	Interstage pressure booster for third stage	0.40	3%
P-908	Interstage pressure booster for polishing stage	2.60	22%
TOTAL:		**11.83 kWh/m^3 solvent recovered**	

Through Table 5.1 it is seen that the most to least energy intensive operations are pumping and heating. Membrane units for water treatment often includes the recovery of energy from the high-pressure concentrated stream leaving a stage. Recovering pump energy would reduce the overall SEC since pumping is the most energy intensive process of the OSN unit. The energy consumed during

heating could also be reduced by integrating excess heat downstream to the solvent recovery unit from reboilers and heat exchangers or by means of recovery through condensers and chillers (Werth et al., 2017b; Luo et al., 2015).

Peshev & Livingston (2013) estimated a SEC for an OSN unit of 3 kWh/m^3 at a 70% pump efficiency. The SEC only included the power to maintain OSN feed pressure. For the OSN unit in the present investigation, at a 70% pump efficiency the SEC is 4 kWh/m^3. The relative difference of 32% might be because the membrane permeate rate of toluene is 91 L/m^2/h compared to 420 L/m^2/h used in Peshev & Livingston (2013). A higher membrane permeate rate would lead to an increased solvent transport through the membrane which will result in a decrease in SEC.

5.3 Capital cost research and technique

The capital investment for the conceptual OSN unit includes direct and indirect equipment costs:

- Direct costs are expenses that are dependent on the operating capacity such as the cost to purchase, install, cost of piping, electrical, instruments and process buildings.
- Indirect costs are independent on the operating capacity, but adds respectively 30%, 5% and 10% of the total direct equipment cost for engineering, contractor's fees and contingency.

Purchased equipment costs were based on quotes where possible. Quotes for heating elements, instruments for membrane modules and pressure vessels, prefilters, membrane modules and pressure vessels were supplied by Thermon, Endress & Hauser, Germ Africa, Evonik, SolSep BV, PROXA or Stainless Crazy. These costs are presented in Table 5.2.

Table 5.2: Quotes to purchase heating elements, prefilters, membrane modules, instruments and pressure vessels.

Equipment ID/location	Function	Description	Supplier	Quote (for 2018)
Heater (E-901)	Heating the preconditioning solvent	Ceramic withdrawable heater	Thermon South Africa (Pty) Ltd. (2018)	115 200 ZAR
Prefilter (F-901A/B)	Prefilters to remove scale and wax particles in feed	Bag filters and stainless-steel housing	GERM Africa (2018)	161 891 ZAR
Liquid level sensor	Measures the liquid level in tanks V-901, V-902 and V-903	Cerabar PMP 21 IA1U1HBWJJ differential pressure sensors	Endress & Hauser (2018)	15 788 ZAR
Differential pressure sensor	Measures the differential pressure across prefilters (F-901A/B) and pressure vessels	Cerebar PMP 21 IA1U1M(B/S) WJJ differential pressure sensor	Endress & Hauser (2018)	14 682 ZAR
Temperature sensor	Measures the temperature of streams 5 and 6*	RTD-assembly TLSR2	Endress & Hauser (2018)	536 ZAR

Table 5.2 (continued): Quotes to purchase heating elements, prefilters, membrane modules, instruments and pressure vessels.

Equipment ID/location	Function	Description	Supplier	Quote (for 2018)
Flowmeter	Measures volumetric flowrate of streams 4, 8 and 7*	Prosonic flow 92F80 Inline, DN80 3”	Endress & Hauser (2018)	128 712 ZAR
Control panel for heater (E-901)	Controlling the heater	Type K thermocouples with a Gefran 600 PID controller	Thermon South Africa (Pty) Ltd. (2018)	47 000 ZAR
Membrane modules	Contains OSN membrane sheets	Spiral wound, polymer membrane modules	Evonik (2018), and SolSep BV (2018)	Evonik: 10 000 ZAR/m^2** SolSep: 4 120 ZAR/m^2**
Pressure vessel	Contains 7 serial membrane modules	Stainless-steel vessel	Proxa (2018) and Stainless Crazy (2018)	42 000 ZAR

* See Figure 4.1

** Exchange rate of 16 ZAR/EUR

The bare module costing technique was used for the remaining equipment - estimated with cost correlations based on historic cost data compiled by Guthrie (1974) and Ulrich & Vasudevan (2004) and summarized in Turton et al. (2012). It should be mentioned that the bare module costing technique is only +/- 50% accurate (Turton et al., 2012).

Once the purchased cost of all equipment was obtained, multiplication factors were applied to include the cost of installation, piping, electrical, instruments for non-membrane equipment and process buildings. These multiplication factors are referred to as Lang factors and are shown in Table 5.3 (Sinnott, 2005). The indirect costs for engineering, contractor’s fees and contingency are independent of the operating capacity but is respectively 30%, 5% and 10% of the total direct equipment cost. These costing methods are referred to as the *bare module costing technique* and has been used to estimate the cost of traditional process equipment (i.e. pumps, heat exchangers, vessels, evaporators and distillation columns) included in membrane systems (Lee et al., 2017; Peddie et al., 2017; Werth et al., 2017; Micovic et al., 2014). Details regarding the cost estimation procedure can be viewed in Appendix C.

Table 5.3: Lang factors to estimate the overall fixed capital of a fluid process (Sinnott, 2005).

Item	Lang factor
Total purchased cost for equipment (PCE)	
Equipment erection	0.40
Piping	0.70
Instrumentation	0.20
Electrical	0.10
Process buildings	0.15
Total physical plant cost (PPC)	**PPC = PCE x (1 + 0.4 + 0.7 + 0.2 + 0.1 + 0.15)**
Design and engineering	0.30
Contractor's fee	0.05
Contingency	0.10
Fixed capital investment (FCI)	**FCI = PPC x (1 + 0.3 + 0.05 + 0.10)**

The equivalent annual cost (EAC) is a way of representing the annual cost of owning, operating and maintaining assets over their lifespan (Owen et al., 1995). EAC treats the FCI as an annualised cost invested at an interest rate, i, over n years. A numerical definition was provided in Equation 2.6 (Owen et al., 1995; Werth et al., 2017b).

A depreciation rate of 7% is chosen over a period of 25 years, based on the write-off period for assets at a water purification and distillation plant (SARS, Interpretation note: No.47, 2009).

A summary of the capital costs for the conceptual OSN unit is presented in Table 5.4.

Table 5.4: Summary of the capital costs for the conceptual OSN unit for the recovery of solvent. The solvent recovery was 51% for a feed capacity is 480 m^3/h.

Item	Equipment ID	Physical plant cost (ZAR)	Fixed capital investment (ZAR)	Distribution
Feed tank	V-901	1 925 000	2 791 000	0.5%
Prefilter pump	P-901 *	1 875 000	2 719 000	0.5%
Prefilters	F-901 *	4 954 000	7 184 000	1.3%
High-pressure feed pump	P-903 *	5 234 000	7 589 000	1.4%
Preconditioning feed tank	V-902	844 000	1 224 000	0.2%
Heater	E-901	294 000	426 000	0.1%
Low-pressure preconditioning pump	P-902	155 000	224 000	0.0%

Table 5.4 (continued): Summary of the capital costs for the conceptual OSN unit for the recovery of solvent. The solvent recovery was 51% for a feed capacity is 480 m^3/h.

Item	Equipment ID	Physical plant cost (ZAR)	Fixed capital investment (ZAR)	Distribution
High-pressure preconditioning pump	P-904	332 000	481 000	0.1%
Booster pump for concentrating stage 1	P-905	575 000	834 000	0.1%
Booster pump for concentrating stage 2	P-906	565 000	819 000	0.1%
Booster pump for concentrating stage 3	P-907	496 000	719 000	0.1%
Booster pump for permeate polishing stage	P-908 *	3 264 000	4 733 000	0.8%
Solvent recovered tank	V-903	854 000	1 238 000	0.2%
Membrane modules		335 670 000	486 722 000	86.9%
Pressure vessels		26 240 000	38 048 000	6.8%
Instrumentation		3 080 000	4 466 000	0.8%
TOTAL EAC:**		**48 072 000 ZAR/year**		
TOTAL specific EAC:		**43 ZAR/m^3 solvent recovered per year**		
TOTAL specific TAC:		**210 ZAR/m^3 solvent recovered per year**		

* Capital cost includes that of backup equipment ** Depreciated over 25 years at 7%

Table 5.4 shows that the fixed capital investment (FCI) for membrane modules makes the largest contribution. An 87% contribution is substantially more than a 10% value for solvent resistant recovery from active pharmaceutical ingredients (Vanneste et al., 2013), 10-20% to treat dye house effluents (Samhaber and Nguyen, 2014) and 22% for a reverse osmosis (RO) membrane plant treating wastewater (Sommariva et al., 2003).

Grouping all the equipment involved with pretreatment and preconditioning yields a total contribution of 4%. This is 2.5 times less than for RO plants since OSN requires no chemical dosing or CIP (cleaning-in-place) (Sommariva et al., 2003; Evonik Resource Efficiency GmbH, 2017). Furthermore, pumps for RO plants typically contribute 10% towards plant capital which more than the 3.4% contribution for the OSN unit (Sommariva et al., 2003). However, RO feed pressures range from 40 to 80 bar for seawater treatment whereas the maximum pressure for OSN is 60 bar. The higher

operating pressures for RO compared to OSN would pump cost and lead to a larger contribution towards overall FCI.

The EAC of the conceptual OSN unit was 43 ZAR/m^3 solvent recovered per year compared to 7 ZAR/m^3 for the Max-Dewax for the same depreciation rate and period. The cost of Max-Dewax was adjusted to 2019 by assuming an exchange rate of 14 ZAR/USD and a 54% increase in capital cost since 1999. It was found that the EAC of the OSN unit in this investigation would be equal to that of the Max-Dewax unit if membrane costs are between 57 and 170 ZAR/m^2, if the estimations for capital cost is +/- 50% accurate. This would yield the following distribution of the FCI:

Table 5.5: Summary of the capital costs for the conceptual OSN unit for the recovery of solvent if membrane costs are 57 and 170 ZAR/m^2. The solvent recovery was 51% for a feed capacity is 480 m^3/h.

Item	**57 ZAR/m^2 membrane cost**		**170 ZAR/m^2 membrane cost**	
	FCI (ZAR)	**Distribution**	**FCI (ZAR)**	**Distribution**
Feed tank	2 791 000	3.4%	2 791 000	2.8%
Prefilter pump	2 719 000	3.3%	2 719 000	2.7%
Prefilters	7 184 000	8.8%	7 184 000	7.2%
High-pressure feed pump	7 589 000	9.3%	7 589 000	7.6%
Preconditioning feed tank	1 224 000	1.5%	1 224 000	1.2%
Heater	426 000	0.5%	426 000	0.4%
Low-pressure preconditioning pump	224 000	0.3%	224 000	0.2%
High-pressure preconditioning pump	481 000	0.6%	481 000	0.5%
Booster pump for concentrating stage 1	834 000	1.0%	834 000	0.8%
Booster pump for concentrating stage 2	819 000	1.0%	819 000	0.8%
Booster pump for concentrating stage 3	719 000	0.9%	719 000	0.7%
Booster pump for permeate polishing stage	4 733 000	5.8%	4 733 000	4.8%
Solvent recovered tank	1 238 000	1.5%	1 238 000	1.2%
Membrane modules	8 518 000	10.4%	25 858 000	26.0%
Pressure vessels	38 048 000	46.4%	38 048 000	38.3%
Instrumentation	4 466 000	5.4%	4 466 000	4.5%
TOTAL EAC:	**6.34 ZAR/m^3 solvent recovered**		**7.66 ZAR/m^3 solvent recovered**	

* Capital cost includes that of backup equipment ** Depreciated over 25 years at 7%

Table 5.5 shows that membrane cost has a significant influence on the PPC of an OSN unit.

5.4 Operating cost research and technique

The operating costs of the OSN unit includes:

- **Direct expenses** – costs that are directly proportional to the solvent recovered (e.g. raw materials, utilities, operating labour, supervision, maintenance and repairs, membrane replacement, laboratory work and operating supplies),
- **Fixed expenses** – charged at constant rates regardless of whether the plant is operational or not (e.g. plant overhead), and
- **General expenses** – activities that are not directly related to the production rate (e.g. administrative costs and laboratory charges).

The specific cost of raw material, utilities and direct labour were based on current market values from S&P Global (2018), Indeed (2018) and Bloomberg (2018). The remaining operating expenses (excluding membrane replacement cost) are fractions of the total plant capital for which the percentage values were taken from Sinnot (2005), Szklo and Schaeffer (2007), Ulrich (1984), Valle-Riestra (1983), Peters and Timmerhaus (1991), Lee et al. (2017) and Owen et al. (1995).

Direct costs:

- Raw material: Clean, preconditioning solvent was identified as the only raw material. The composition was based on the ratio of MEK to toluene in the dewaxed filtrate feed (White and Nitsch, 2000). A preconditioning solvent cost of 21 120 ZAR/t was based on 2,088 USD/mt for MEK, 731 USD/t for toluene and a ZAR/USD conversion of 14 (S&P Global 2018; Hashmi, 2018; Bloomberg, August 2018).
- Utilities: Electricity is the only utility for the conceptual OSN unit and is used for the pumps and preconditioning heater. The cost of electricity is 1.32 ZAR/kWh based on Eskom's 2018/2019 tariffs and charges for urban tariffs for non-local authorities (Eskom, 2018).
- Operating labour: The cost of operating labour was based on the number of hired operators earning an average monthly salary of 13 160 ZAR (Indeed, September 2018). To determine the required number of hired operators, a correlation developed by Alkhayat and Gerrard (1984) was used. Using the correlation for one particulate step and two non-particulate steps, at least 6.2 operators are required per shift. An operator may work five 8-hour shifts a week yielding a total of 245 shifts per operator per year assuming there are 49 weeks in a year (Turton et al., 2012). An oil refinery operating 24 hours a day, 332 days a year will result in 996 shifts per year (Sinnot, 2005). Thus, the total requirement for the membrane plant is 26 plant operators per year.

- Supervision: An operating team involves four to five plant operators and one supervisor (Sinnot, 2005). Support personnel oversee administrative and engineering activities during a shift. If an operation team includes 5 plant operators and one supervisor, the cost of supervision will be 20% of the total cost of operating labour.
- Laboratory work: Another labour expense is the cost of laboratory work to examine the composition of samples taken from the feed and product streams to and from the OSN unit. The total cost of laboratory work was assumed to be 15% of the total operating labour cost (Valle-Riestra, 1983).
- Membrane replacement: OSN membranes have a finite life which is based on the decline in flux over membrane life. Gould et al. (2001), Micovic et al. (2014) and Werth et al. (2017b) based the membrane life of polymeric OSN membranes in the petrochemical industry between 1.5 to 2 years. Vanneste et al. (2013) assumed a longer lifetime of 5 years for OSN membranes in the pharmaceutical industry. Owen et al. (1995) also stated that the life of polymeric nanofiltration membranes could range betwen 3 to 5 years, however this was for a water treatment plant. Thus, for a lifetime of 2 years membrane replacement will contribute 50% of the purchased cost for membrane modules each year.
- Maintenance and repairs: The cost to maintain and repair traditional process equipment (i.e. pumps, heat exchangers, vessels, evaporators and distillation columns) was chosen as 10% but may range from 5 to 15% of the total capital of a chemical plant according to Sinnot (2005). Petrobras, a Brazilian oil refinery, allocated 11% towards maintenance and repairs (Szklo and Schaeffer, 2007).
- Operating supplies: As for operating supplies**,** 10% of the total cost for maintenance and repairs made provision for additional expenses like chart paper, PPE, lubricants and miscellaneous chemicals (Ulrich, 1984; Valle-Riestra, 1983; Peters and Timmerhaus, 1991).

Fixed costs:

- Plant overhead: Is the catch-all cost associated with the auxiliary facilities that support the conceptual OSN unit. These costs go towards fire protection and safety services, general engineering and medical services (Peters and Timmerhaus, 1991). A value of 60% was chosen but this may vary between 50 and 70% of the total cost for operating labour, supervision and maintenance and repairs (Peters and Timmerhaus, 1991).

General expenses:

- Administrative: Administration costs cover salaries, administrative buildings and other admin-related activities and are assumed to be 15% of the total operating labour, supervision, and maintenance and repairs cost (Sinnot, 2005).
- Laboratory charges: For routine tests to determine the composition of for example the filtrate, mixed feed, permeate and concentrate streams. Laboratory charges contribute 5% of the overall operating cost (Turton et al., 2012).

Operating cost of OSN unit for the recovery of solvent:

A summary of all operating costs is presented in Table 5.6 for a feed flowrate of 480 m^3/h and solvent recovery of 51% at a 99% purity.

Table 5.6: Summary of the operating costs of the conceptual OSN unit for the recovery of solvent.

Item	Direct costs (ZAR)	Fixed costs (ZAR)	General expenses (ZAR)	Distribution
Raw materials	7 175 000			3.9%
Utilities	12 006 000			6.4%
Operating labour	343 000			0.2%
Supervision	69 000			0.0%
Laboratory work	52 000			0.0%
Membrane replacement (every 2 years)	52 655 000			28.3%
Maintenance and repairs	56 021 000			30.1%
Operating supplies	5 603 000			3.0%
Plant overhead		33 859 000		18.2%
Administration costs			8 465 000	4.5%
Laboratory charges			9 955 000	5.3%
TOTAL:	**167 ZAR/m^3 solvent recovered per year**			

Werth et al. (2017b) estimated a specific operating cost including only the cost of membrane replacement and electricity for an OSN unit recovering solvent from oil. The specific cost for

membranes were 200 EUR/m^2 (3 200 ZAR/m^2) The operating cost of the OSN unit in this investigation was 1 965 ZAR/m^2 compared to 1 836 ZAR/m^2 effective membrane area in Werth et al. (2017b). The conceptual OSN unit is thus within 6% of that in Werth et al. (2017b).

5.5 Total annual cost research and technique

The total annual cost (TAC) is the sum of the operating cost and EAC (equivalent annual cost). The distribution of the TAC for the conceptual OSN unit for the recovery of solvent is presented in Table 5.7.

Table 5.7: Summary of the total annualised cost (TAC) of the conceptual OSN unit for the recovery of solvent. The solvent recovery is 51% for a feed of 480 m^3/h.

Item	Total annual cost (TAC) (ZAR)	Distribution
EAC *	48 072 000	20.5%
Raw material	7 175 000	3.1%
Utilities	12 006 000	5.1%
Operating labour	343 000	0.1%
Supervision	69 000	0.0%
Laboratory work	52 000	0.0%
Membrane replacement (every 2 years)	52 655 000	22.5%
Maintenance and repairs	56 021 000	23.9%
Operating supplies	5 603 000	2.4%
Plant overhead	33 859 000	14.5%
Administration costs	8 465 000	3.6%
Laboratory charges	9 955 000	4.2%
TOTAL:	**210 ZAR/m^3 solvent recovered per year**	

* Equivalent annual cost (EAC) includes a depreciation rate of 7% over 25 years.

Membrane replacement makes the second largest contribution towards the life cycle cost next to maintenance and repairs. This is within the range of RO systems for which membrane replacement ranges between 15 – 25% (Owen et al., 1995; Samhaber and Nguyen, 2014).

A single set of assumptions was used to simulate the cost and energy consumption of the conceptual OSN unit. Comparing the estimated cost and energy consumption of the OSN unit with literature sources revealed similarities in the range of 6% to 84%. Thus, it was of interest to see how the cost and energy consumption of the conceptual OSN unit might change if the values of certain simulation assumptions were adjusted.

A sensitivity analysis investigates how changes in assumptions influence the conclusions drawn from a simulation. The procedure involves changing the value of a single assumed value while fixing the remaining properties at their initial values. A sensitivity analysis was therefore performed and discussed in the following section.

5.6 Sensitivity analysis of the conceptual OSN unit for the recovery of solvent

The assumed values of variables are tentative for any model, including the plant properties assumed to simulate the conceptual OSN unit in this investigation (Pannell, 1997). Permutations to the assumed values of certain variables were based on upper and lower adjustments from the initial value.

The literature review revealed that permselectivity (the membrane permeate rate of MEK or toluene relative to the membrane permeate rate of lube-oil), membrane life, flux decline and operating pressure affects OSN membrane performance. In Sections 5.3 to 5.5 it was shown that the cost of membrane equipment was both uncertain and had a significant influence on the cost of an OSN unit. The initial values and their permutations are presented in Table 5.8.

Table 5.8: Initial and permutation values of permselectivity, flux decline, membrane module cost, pressure vessel cost, electricity price, membrane life and operating pressure for the conceptual OSN unit to recover solvent from lube-oil.

Decision variable	Lower adjustment	Base-case value	Upper adjustment	References
Permselectivity ($\alpha = \frac{b_{solvent}}{b_{solute}}$)	$\alpha_{MEK/Oil}$ = 180 $\alpha_{Toluene/Oil}$ = 46	$\alpha_{MEK/Oil}$ = 360 $\alpha_{Toluene/Oil}$ = 91	$\alpha_{MEK/Oil}$ = 540 $\alpha_{Toluene/Oil}$ = 137	White and Nitsch (2000) and Werth et al. (2017b)
Average decline in membrane flux after 15 936 hours (2 years) membrane life	14%	28%	42%	White and Nitsch (2000) and Bhore et al. (1999)
Specific membrane module price (ZAR/m^2)*	1 600	3 200	4 800	Werth et al. (2017b), Evonik (2018), SolSep BV (2018) and Owen et al. (1995)
Pressure vessel cost (ZAR)	21 000	42 000	63 000	Stainless Crazy (2018)
Electricity price (ZAR/kWh)	0.66	1.32	1.98	Eskom (2018/2019 Tariffs)
Membrane life (years)	0.5	2	3.5	Werth et al. (2017b), Vanneste et al. (2013), Owent et al. (1995) and Bhore et al. (1999)
Operating pressure (kPa)	2 077	4 154	6 231	White & Nistch (2000) and Evonik (2017).

* ZAR/EUR = 16 (Bloomberg, August 2018)

Pannell (1997) showed that following simplistic methods to perform sensitivity analyses may be as suitable for optimisation and simulation as more complex methods. One recommended method is to estimate the sensitivity indices, SI, of each variable. The SI is determined with Equation 5.2 (Pannell, 1997).

$$SI = \frac{|O_{MAX} - O_{MIN}|}{O_{MAX}} \quad [5.2]$$

The method is applied to estimate the difference between the output, O_{MAX}, at the upper adjustment, and O_{MIN}, at the lower adjustment, followed by dividing by O_{MAX} (Pannell, 1997). The approach is highly simplistic but is recommended for identifying variables with the most significant influence to assist with optimisation.

The following subsections will address the sensitivity of SEC, capital cost, operating cost and TAC when the values of permselectivity, average flux decline, specific membrane module cost, pressure vessel cost, electricity price, membrane life and operating pressure are adjusted.

5.6.1 Sensitivity of specific energy consumption (SEC)

The sensitivity of SEC to adjustments of the assumed values for simulation is shown in Figure 5.1. The SI-value of a variable is presented within brackets in the legend of each plot.

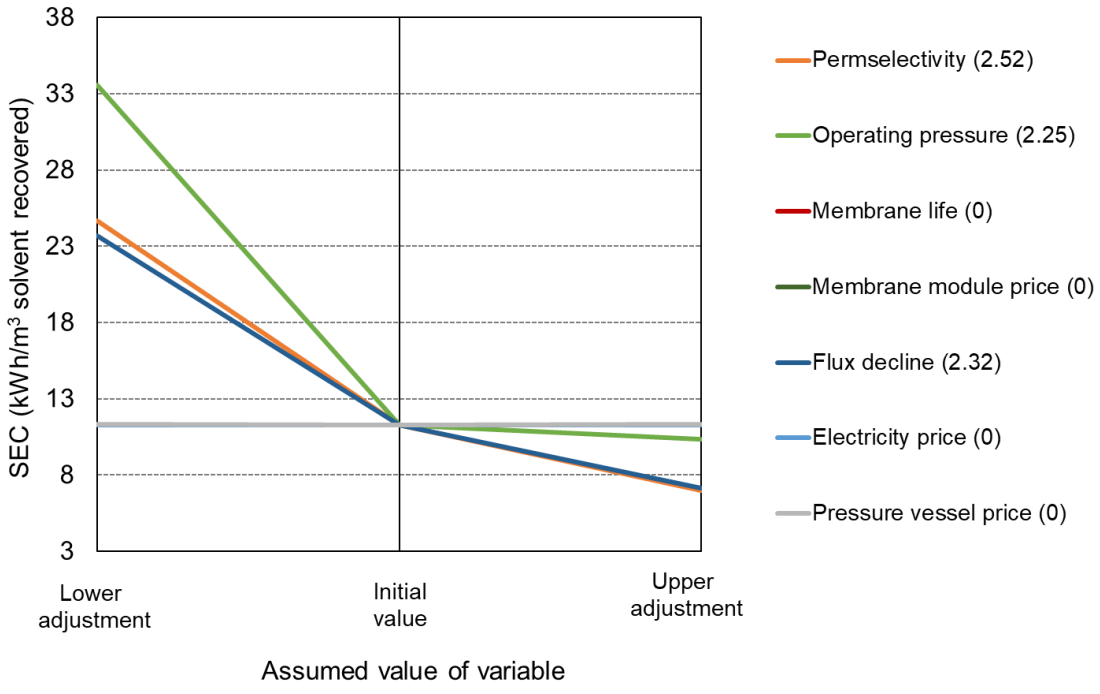

Figure 5.1: Sensitivity in specific energy consumption (SEC) presented as a spider diagram for conceptual OSN unit.

In Figure 5.1, it is seen that adjustments to the permselectivity, operating pressure and flux decline had the most significant impact on the SEC. A positive adjustment of permselectivity, operating pressure and flux decline lead to an increase in permeate flux since:

1. Improved permselectivity leads to a higher membrane permeate rate of solvent through the membrane relative to the lube-oil,
2. A higher operating pressure increases the driving force across a membrane which increases the solvent transport through the membrane, and
3. Reducing flux decline yields a higher overall permeate flowrate over time.

Micovic et al. (2014) and Motelica et al. (2012) both observed improved energy savings for increased membrane permselectivity. Fontalvo (2014) also showed that improved membrane permselectivity reduced the overall energy consumption of hybrid-OSN solvent recovery units.

5.6.2 Sensitivity of operating cost

Figure 5.2 shows the sensitivity of the operating cost to permutations in the initial values. The SI-value of a variable is presented in brackets in the legend.

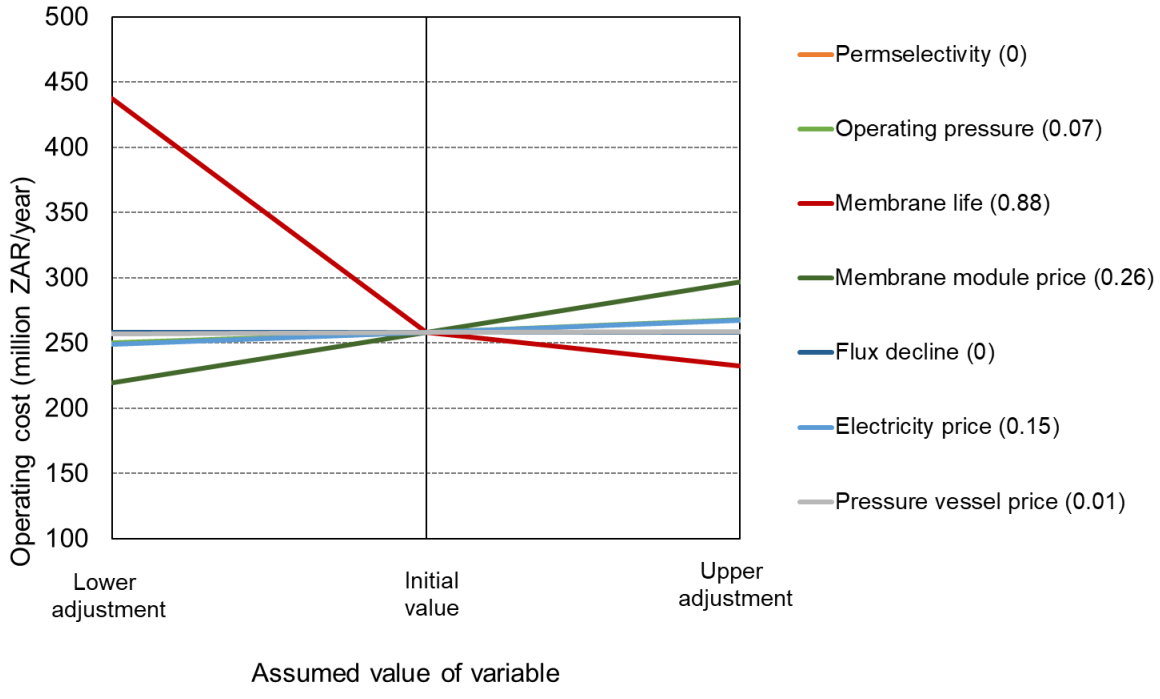

Figure 5.2: Sensitivity in operating cost presented as a spider diagram for conceptual OSN solvent recovery unit.

Figure 5.2 reveals that membrane life had the most significant effect on the operating cost of the OSN unit. Recall from Section 5.4 that the cost to replace membrane modules made the second largest contribution towards operating cost next to maintenance and repairs. Thus, the influence of membrane module price will also affect the total operating cost as was shown in Figure 5.2. Unfortunately, no literature studies have confirmed that a longer membrane life could decrease overall operating cost. Nonetheless, keeping membranes on stream for longer periods would reduce the membrane replacement frequency, and for the conceptual OSN unit this would significantly reduce the operational costs.

The influence of operating pressure and electricity price can also be seen in Figure 5.2. Both variables have similar SI- indices which suggests that electricity price and operating pressure may be correlated. This is because increased operating pressure will increase the energy consumption which in turn will increase the utility cost for electricity. The increase in the electricity price will also increase the utility cost for electricity. Lee et al. (2017) also showed that the operating cost of a membrane-based separation process will increase when the driving force is increased.

5.6.3 Sensitivity of capital cost

The sensitivity of the capital cost to adjustments to the initial values assumed for the conceptual OSN unit is shown in Figure 5.3. The SI-value of a variable is presented within brackets in the legend.

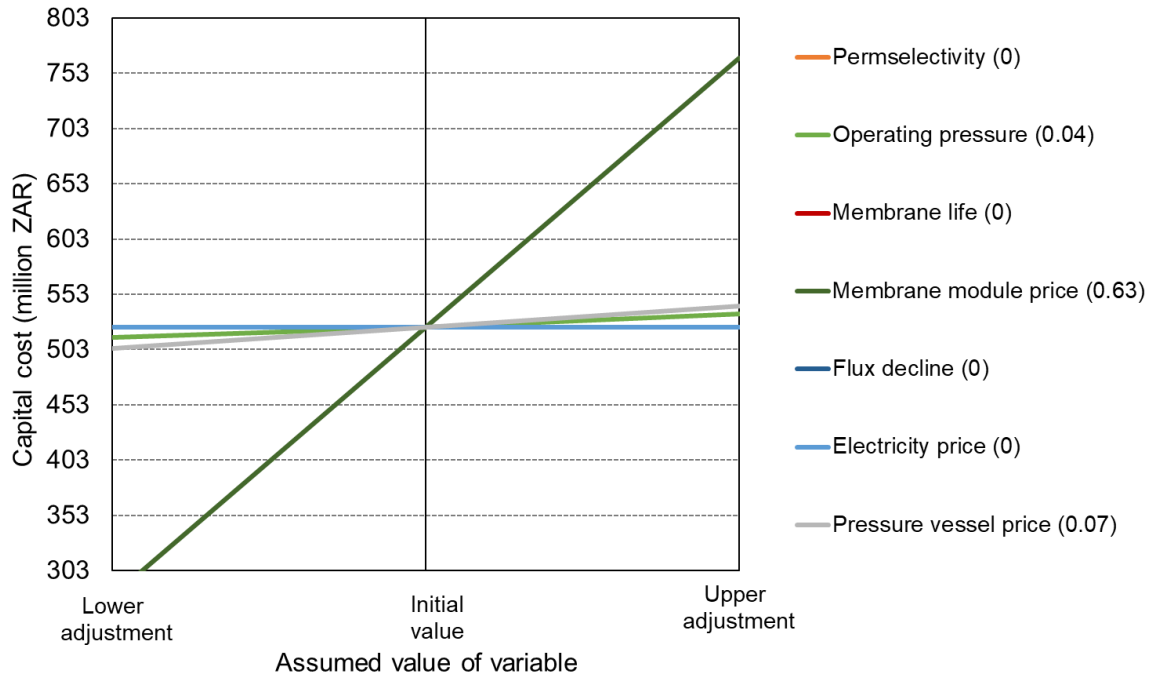

Figure 5.3: Sensitivity in capital cost presented as a spider diagram for conceptual OSN solvent recovery unit.

Figure 5.3 shows that the most significant variable affecting the capital cost of the OSN unit was the membrane module price. In Section 5.3 it was shown that the capital investment for membrane modules is the highest cost, contributing 80% towards the total capital cost. Micovic et al. (2014), Werth et al. (2017b) and Lee et al. (2017) concluded that the specific cost of membrane modules is very uncertain. Thus, all three studies looked at the effect of membrane module cost on overall cost. The trends they observed was the same as is shown in Figure 5.3 where capital cost increases for increased membrane module price.

5.6.4 Sensitivity in total annual cost (TAC)

The sensitivity of the TAC to adjustments in values initially assumed for the OSN unit is shown in Figure 5.4. The SI-value of a variable is presented within brackets in the legend.

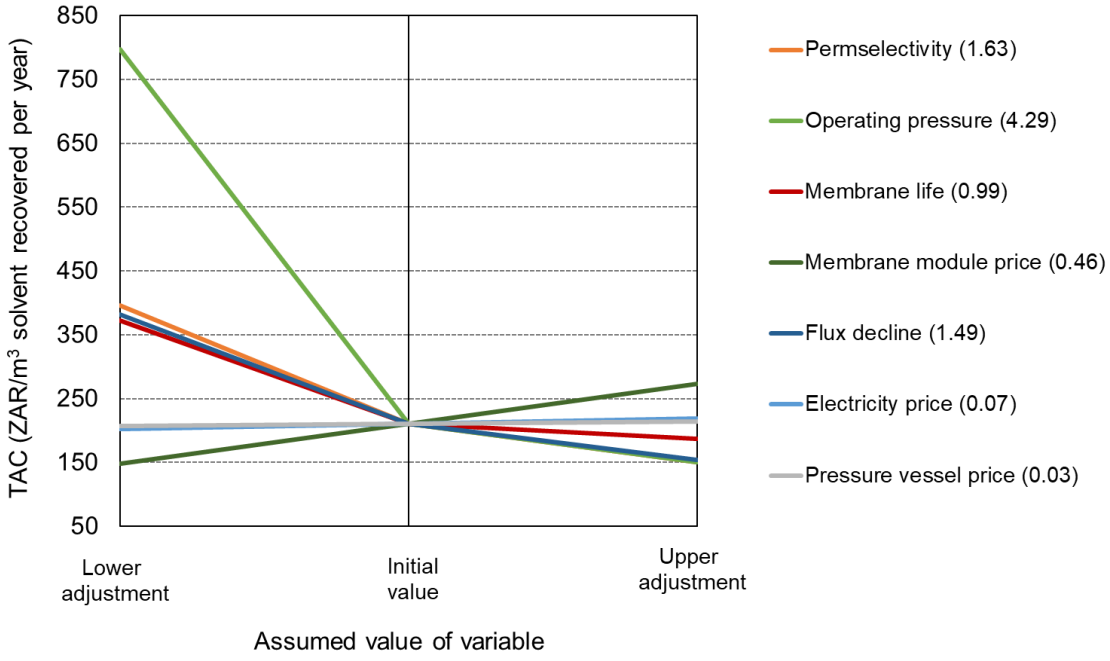

Figure 5.4: Sensitivity in total annual cost (TAC) of the OSN unit.

The trends shown in Figure 5.4 show that operating pressure, permselectivity, flux decline, membrane cost and membrane life had the most significant influence on the TAC of the OSN unit. The most significant response in TAC was for increased operating pressure. This was also observed by Lee et al. (2017). This trend was due to increased drivining force as operating pressure increased resulting in a higher membrane permeate rate of solvent through the membrane. However, increasing operating pressure will also increase electricity cost.

The reduction in TAC due to improved membrane permselectivity was due to increased solvent membrane permeate rate relative to oil. Micovic et al. (2014) showed that membranes with higher permselectivities reduced the TAC of a hybrid-OSN distillation unit per ton solvent recovered. Finally, membrane life would have a significant effect on TAC since it was shown in Table 5.7 that membrane replacement made the second largest contribution towards TAC.

Micovic et al. (2014), Werth et al. (2017b), Peshev & Livingston (2013) and Bhore et al. (1999) all compared the energy consumption and/or cost of classical separations to OSN separation. Micovic et al. (2014), Werth et al. (2017b) and Bhore et al. (1999) all developed hybrid-OSN units since the maximum amount of solvent recovered through stand-alone OSN was not enough.

The following chapter the TAC and SEC will be simulated and compared for a classical and hybrid-OSN unit for the recovery of solvent from dewaxed lube-oil.

CHAPTER 6: COMPARISON IN COST AND ENERGY OF A HYBRID-OSN AND CLASSICAL SOLVENT RECOVERY UNIT

It was shown that the conceptual OSN unit could recover 51% solvent at a 99% purity and to increase the recovery to 98% would require additional separation. The Max-Dewax OSN unit was designed as a preliminary separation to recover 50% solvent followed by evaporation and distillation to recover the remaining solvent (Bhore et al., 1999). Micovic et al. (2014) developed a hybrid-OSN process configuration including an OSN unit followed by a distillation column to recover 98% solvent. Werth et al. (2017b) assessed the potential cost and energy savings when the first step in a two-step evaporation unit was replaced with an OSN unit. Therefore, in this chapter the total annualised cost (TAC) and specific energy consumption (SEC) of a hybrid-OSN unit will be compared to a classical unit for the recovery of solvent.

The process flow of the hybrid-OSN unit is shown in Figure 6.1a and the classical solvent recovery unit is shown in Figure 6.1b. Both process configurations were simulated in Aspen Plus to obtain the energy consumed and size of equipment not included in the OSN unit. The operating conditions for the hybrid-OSN unit and classical unit are provided in Table 6.1.

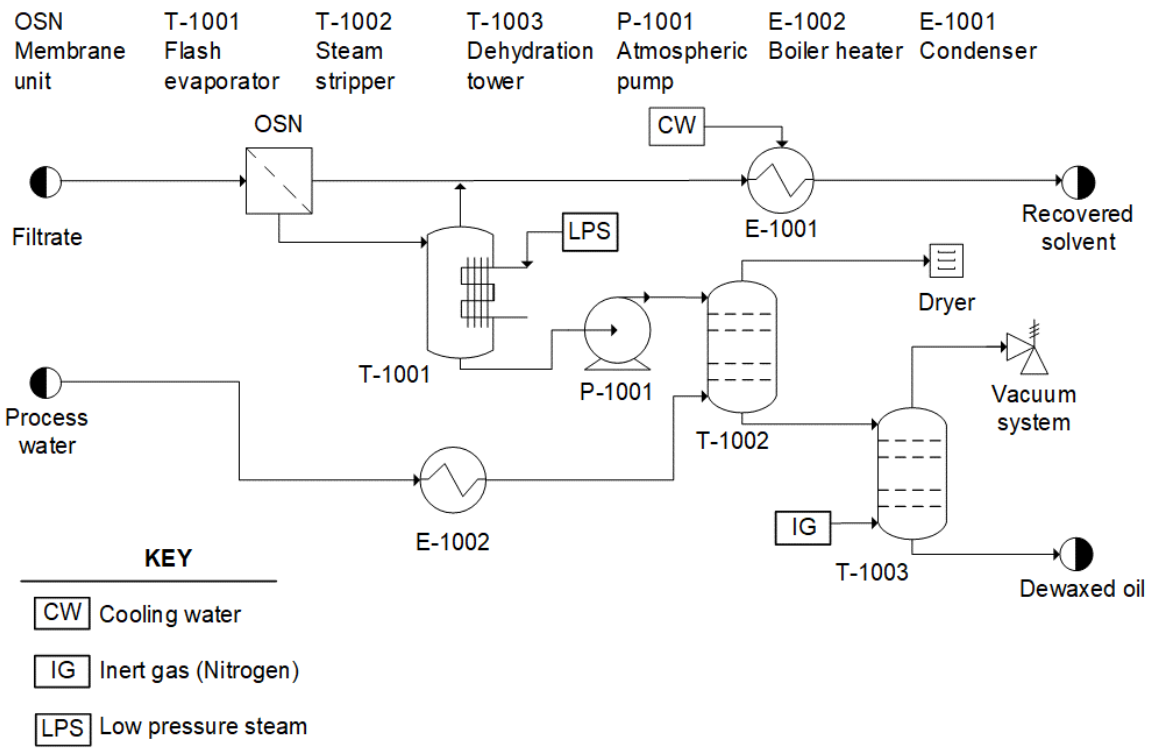

Figure 6.1a: Process configuration of conceptual hybrid-OSN unit to recover solvent.

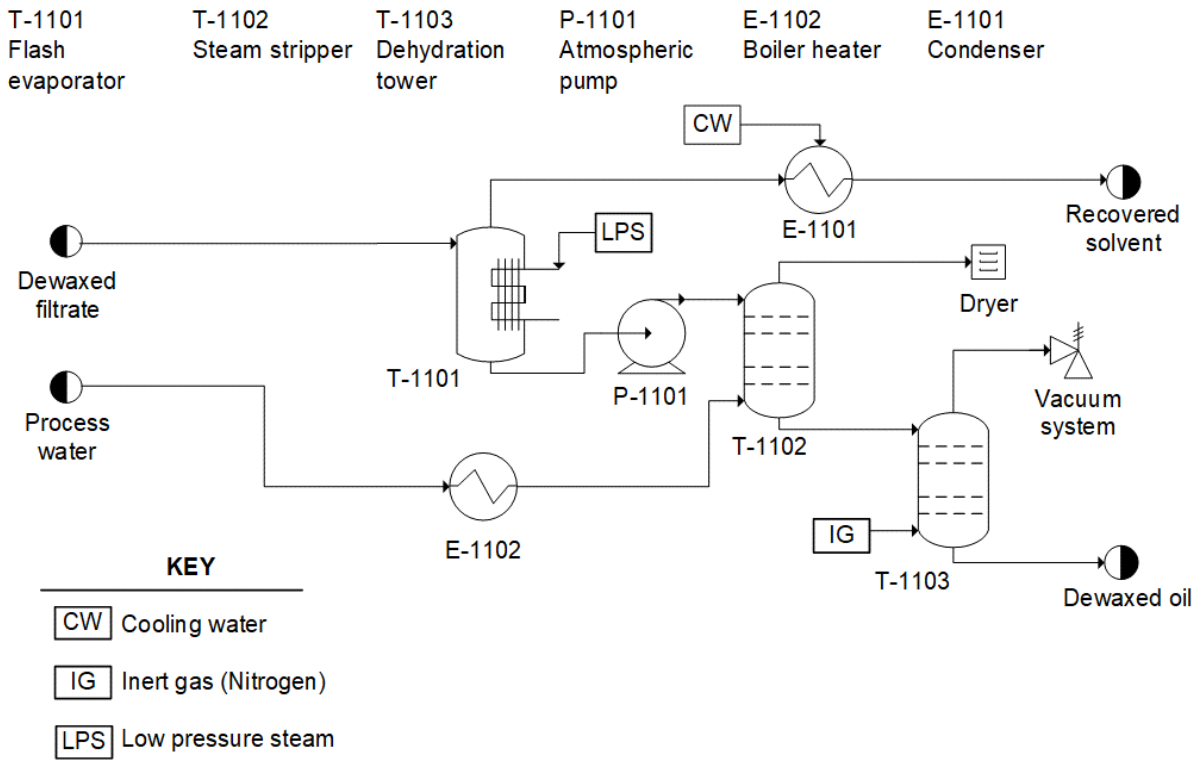

Figure 6.1b: Process configuration of conceptual classical unit to recover solvent.

Table 6.1: Operating conditions for Aspen Plus simulation

Property	Hybrid-OSN unit	Classical unit	Reference
OSN unit:	**OSN**		
MEK permeate flowrate (kg/s)	15.73 *		Simulated at base-case conditions (See Section 5.1)
Toluene permeate flowrate (kg/s)	7.88 *		Simulated at base-case conditions (See Section 5.1)
Lube-oil permeate flowrate (kg/s)	0.02 *		Simulated at base-case conditions (See Section 5.1)
Flash evaporator:	**T-1001**	**T-1101**	
Temperature (°C)	109	102	Sequeira (1991)
Pressure (atm)	0.25	0.33	Sequeira (1991)
Utility	Low pressure steam (125°C and 232 kPa)	Low pressure steam (125°C and 232 kPa)	Werth et al. (2017b)
Atmospheric pump:	**P-1001**	**P-1101**	
Discharge pressure (atm)	1	1	
Pump efficiency	0.75	0.75	

Table 6.1 (continued): Operating conditions for Aspen Plus simulation

Property	Hybrid-OSN unit	Classical unit	Reference
Boiler heater:	**E-1002**	**E-1102**	
Temperature (°C)	250	250	Sequeira (1991)
Pressure (atm)	1	1	Sequeira (1991)
Stripping column:	**T-1002**	**T-1102**	
Number of stages	5	5	Sequeira (1991)
Condenser	None	None	
Reboiler	None	None	
Feed stream position	On-stage 1	On-stage 1	
Steam stream position	Above-stage 6	Above-stage 6	
Top stage pressure (atm)	1	1	Sequeira (1991)
Condenser:	**E-1001**	**E-1101**	
Pressure (atm)	1	1	
Vapor fraction	0	0	
Utility	Cooling water (20°C and 1atm)	Cooling water (20°C and 1atm)	Aspen Plus V8.8 default settings
Dehydration tower:	**T-1003**	**T-1103**	
Number of stages	2	2	Sequeira (1991)
Condenser	None	None	
Reboiler	None	None	
Feed stream position	Above-stage 1	Above-stage 1	
N_2 stream position	Above-stage 3	Above-stage 3	
Top stage pressure (psia)	3	3	Sequeira (1991)

* Subject to change during process evaluations

For both processes, a total solvent recovery of 98% at a 99% solvent purity was achieved for a 480 m^3/h feed. The feed was a dewaxed filtrate containing 48% MEK, 34% toluene and 18% lube-oil by mass. Pentacosane was chosen as the reference component for lube-oil (White and Nitsch, 2000; Kong et al., 2006).

The fixed capital cost of each process included the purchased cost for equipment based on quotes (see Table 5.2) or the bare module costing technique in Turton et al. (2012), ancillary costs for piping, erection, electrical, instrumentation and process buildings based on Lang factors in Sinnott (2005),

and indirect costs for engineering, contractor's fees and contingency. The following assumptions were made for estimating the capital cost:

- All capital costs were adjusted to the year 2019 using CEPCI projections.
- The equivalent annual cost (EAC) was based on a depreciation rate of 7% over 25 years (Werth et al., 2017; SARS, Interpretation note: No.47, 2009).
- Engineering and design, contractor's fees and contingency were 30%, 5% and 10% of the direct capital costs (Sinnott, 2005).
- The bare module costing technique was +/- 50% accurate (Turton et al., 2012).

The operating cost included direct costs (i.e. raw material, utilities, operating labour, supervision, laboratory work, membrane replacement, maintenance and repairs and cost of operating supplies), fixed costs such as plant overhead, and general expenses for administrative and laboratory work. The following assumptions were made for the estimation of the operating costs:

- The cost of preconditioning solvent was 21.12 ZAR/kg (S&P Global 2018; Hashmi, 2018; Bloomberg, August 2018).
- A cost of 0.70 ZAR/m^3 for cooling water and 0.11 ZAR/MJ for low pressure steam were taken from Werth et al. (2017b).
- The cost of 1.32 ZAR/kWh was based on Eskom tariffs for 2018/2019 and the cost of 0.47 ZAR/kL for process water related to the water tariffs for Johannesburg for 2018/2019.
- The cost of 0.4 ZAR/m^3 for nitrogen gas was based on market research by Purity Gas, Canada (Styles, 2017).
- 26 Plant operators were required per year (Alkhayat & Gerrard, 1984). It was assumed that the number of plant operators would remain the same even though the hybrid-OSN configuration has more process units than the classical process. The monthly salary per operator was 13 160 ZAR (Indeed, 2018). 20% of the direct labour cost was required for supervision (Sinnott, 2005).
- Laboratory work was 15% of the direct labour cost (Turton et al., 2012).
- The cost for maintenance and repairs was 10% of the FCI (fixed capital investment) (Turton et al., 2012).
- The cost of operating supplies was 10% of the maintenance and repairs (Turton et al., 2012).
- Plant overhead is 60% of maintenance and repairs, supervision plus direct labour cost (Turton et al., 2012).
- Administration cost is was 15% of maintenance and repairs, supervision plus direct labour cost (Turton et al., 2012).

- Laboratory charges were 5% of the total operating cost (Turton et al., 2012).

The sensitivity analysis in Section 5.7 revealed that for the OSN unit, membrane life, permselectivity (i.e. membrane permeate rate of solvent relative to the membrane permeate rate of lube-oil), operating pressure, flux decline and specific membrane module cost have the most significant influence on TAC and SEC. Process simulations were therefore performed in this chapter for varying values of each variable to observe for which conditions a hybrid-OSN unit might compete with a classical unit based on TAC and SEC. The base-case values for each variable was:

- Membrane permselectivity: 360 for MEK and 91 for toluene (White & Nitsch, 2000)
- Operating pressure: 42 bar (White & Nitsch, 2000)
- Membrane life: 2 years (Werth et al., 2017b; Micovic et al., 2014)
- Specific membrane module cost: 3 200 ZAR/m^2 (Werth et al., 2017b)
- Average flux decline over membrane life: 28% after 15 936 hours (2 years) (see Equation 2.4) (Bhore et al., 1999).

Simulations were performed for various combinations of each sensitivity variable. The most critical and interesting simulated results are presented and discussed in Sections 6.1 to 6.5. The remaining simulated results are presented in Appendix D.

6.1 The influence of membrane permselectivity

The effect of permselectivity on the TAC and SEC was explored on three levels. The lowest level was referred as the “lower adjustment” and is 180 for MEK and 46 for toluene. The base-case permselectivity was 360 for MEK and 91 for toluene (White & Nitsch, 2000). The higher level was referred to as the “upper adjustment” at a permselectivity of 540 for MEK and 137 for toluene. To prove that the upper adjusted permselectivity for MEK was not unreasonable, Werth et al. (2017a) reported an even higher permselectivity for n-hexane. Werth et al. (2017a) estimated a permselectivity of 661 for n-hexane relative to triolein.

The lower, base-case and upper adjusted permeate rate values were evaluated for varying operating pressure, membrane life, specific membrane module cost and average flux decline. It was observed that for certain instances of permeate rate and average flux decline, the TAC and SEC of the hybrid-OSN unit might be the same as the classical solvent recovery unit. The influence of permeate rate on TAC and flux decline on SEC is presented in Figure 6.2 and Figure 6.3 respectively. The remaining evaluations can be seen in Appendix D.

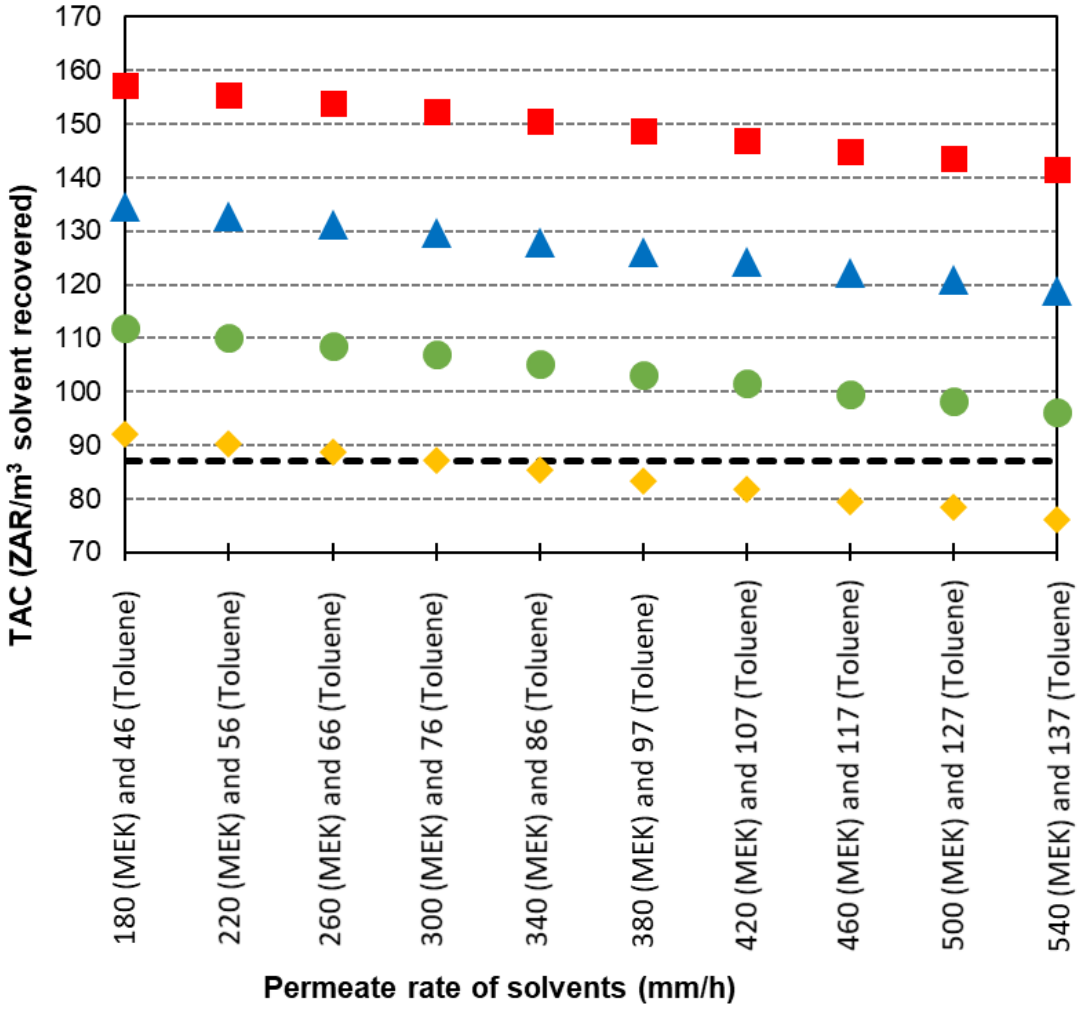

Figure 6.2: Total annual cost (TAC) of the classical solvent recovery unit (---) compared to a hybrid-OSN unit with a specific membrane cost of 200 ZAR/m^2 (◆) 1600 ZAR/m^2 (●), 3200 ZAR/m^2 (▲), and 4800 ZAR/m^2 (■) for varying membrane permeate rate.

From Figure 6.2, the TAC of the hybrid-OSN unit might be the same as the classical unit if the permeate rate was at least 300 mm/h for MEK and 76 mm/h for toluene at a specific membrane cost of 200 ZAR/m^2. In addition, Figure 6.2 shows that a membrane with a lower permselectivity should also have a lower specific cost. Micovic et al. (2014) and Werth et al. (2017b) also showed that at a specific cost of 1920 ZAR/m^2, hybrid-OSN would be have a lower TAC than a classical solvent recovery unit. However, the permeate rated used in Micovic et al. (2014) and Werth et al. (2017b) were higher than those used in this investigation. Thus, if membranes with an even higher permselectivity than the upper adjustment were available, specific membrane module costs larger than 200 ZAR/m^2 might still lead to a lower TAC than a classical solvent recovery unit.

The influence of average flux decline was evaluated for the lower adjusted (i.e. 180 for MEK and 46 for toluene), base-case (i.e. 360 for MEK and 91 for toluene) and upper adjusted permeate rate (i.e. 540 for MEK and 137 for toluene). The simulated SEC is shown in Figure 6.3.

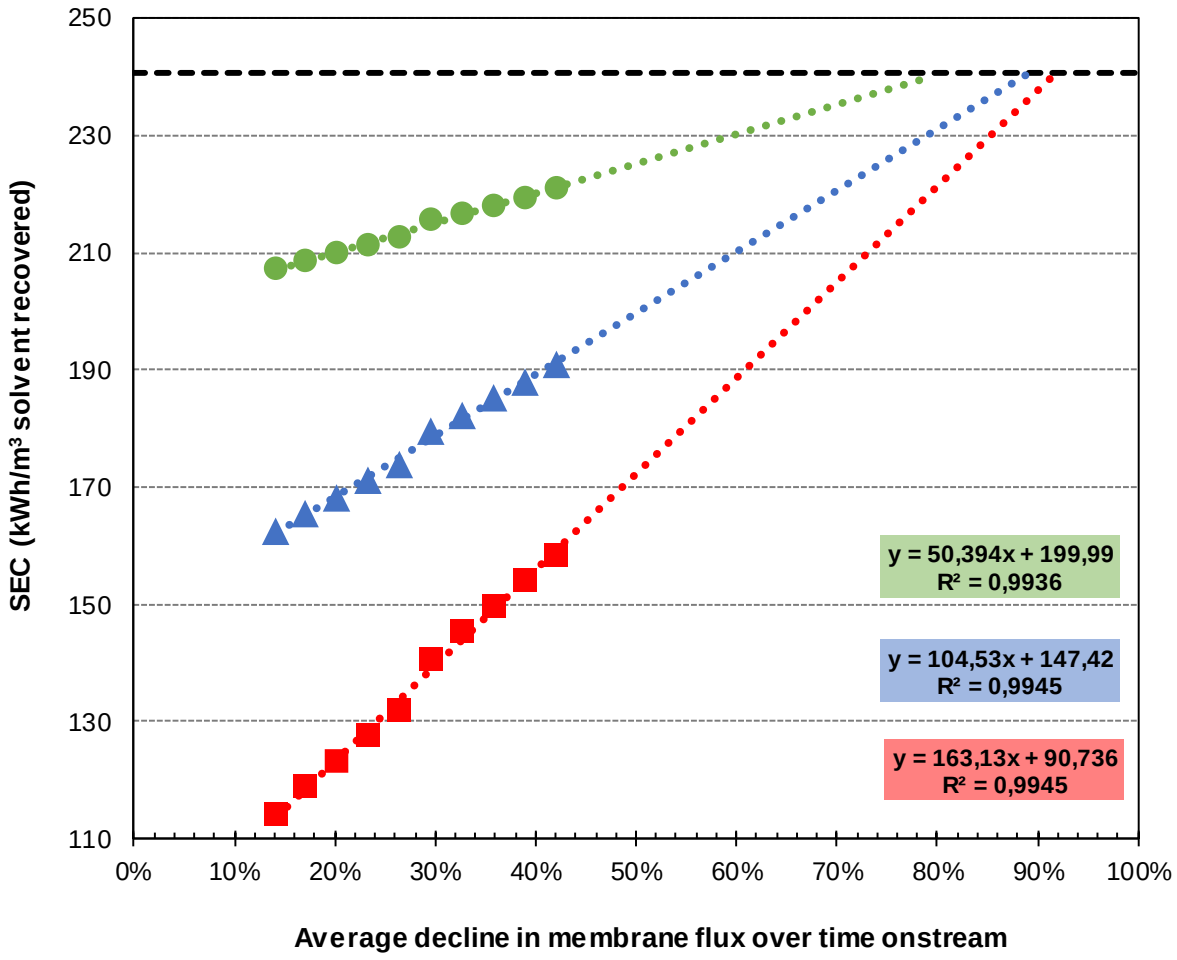

Figure 6.3: Specific energy consumption (SEC) of the classical solvent recovery unit (---) compared to a hybrid-OSN unit with a MEK and toluene permeate rate of 180 and 46 mm/h (●), 360 and 91 mm/h (▲), and 540 and 137 mm/h (■) for varying average decline in membrane flux over membrane life.

Figure 6.3 shows that the SEC of the hybrid-OSN unit will remain lower than the classical unit if the average flux decline does not exceed 79% for the lower adjusted permselectivity, 89% for the base-case and 92% for the upper adjusted case. However, for an 89% decline in membrane flux, the membrane would have to be kept on stream for a very long time. Even if the membrane at the base-case permselectivity was kept on stream for 5 years, the decline in flux would only be 31%. It is therefore unlikely that flux decline would reach 79% to 92%, unless the membrane is damaged for operating pressures above 60 bar or due to fouling when the solvent recovery is too high.

6.2 The influence of operating pressure

The recommended operating pressure for OSN membranes range from 20 bar to 40 bar. Evonik warns users to not exceed 60 bar as this could cause irreversible damage to the membranes (Evonik, 2017). Membrane telescoping is the longitudinal unravelling of membrane sheets in a spiral wound membrane module that is under too high pressure (Bhore et al., 1999). Thus, the TAC and SEC of the hybrid-OSN unit is evaluated for three levels of operating pressure: 20 bar (lower adjusted), 42 bar (base-case) and 56 bar (upper adjusted).

Membrane units for water treatment often includes the recovery of energy from the concentrated stream that was still under a high pressure. Recovering pump energy would reduce the overall SEC and thus operating costs. However, energy recovery by means of pressure exchangers was not taken into consideration for the present investigation.

The TAC and SEC was simulated at varying permselectivity, membrane life, specific membrane module cost and flux decline for each level of operating pressure. It was observed that the specific membrane module cost had the biggest influence on TAC. In addition, flux decline had the most significant influence on the SEC of the hybrid-OSN unit. The trend in TAC for varying operating pressure and in SEC for flux decline is shown in Figure 6.4 and Figure 6.5. The response in TAC to changes in membrane life, permselectivity and flux decline, and SEC to changes in membrane life and permselectivity are shown in Appendix D.

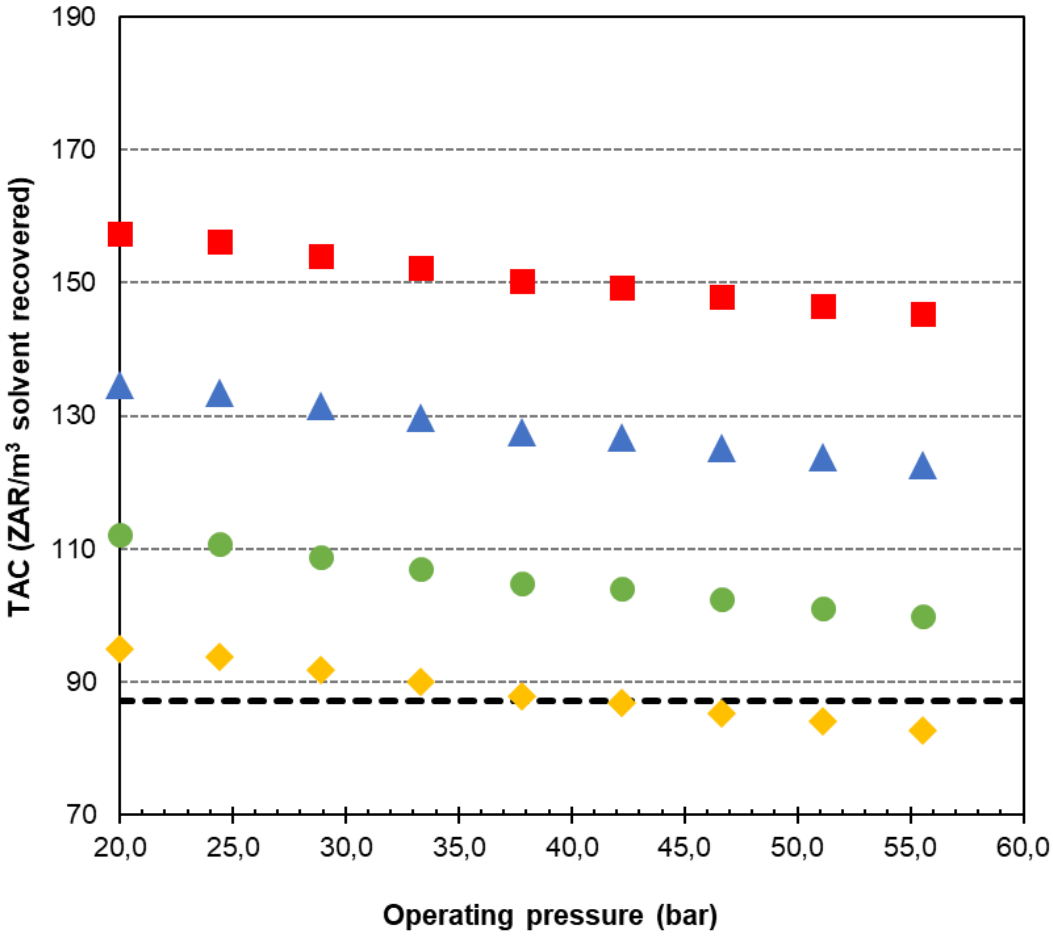

Figure 6.4: Total annual cost (TAC) of the classical solvent recovery unit (---) compared to a hybrid-OSN unit for a specific membrane cost of 400 ZAR/m^2 (◆) 1600 ZAR/m^2 (●), 3200 ZAR/m^2 (▲), and 4800 ZAR/m^2 (■) for varying operating pressure.

Figure 6.4 shows that the TAC of the hybrid-OSN unit decreased as operating pressure increased. A higher operating pressure will increase the driving force for solute transport through the membrane. Higher permeate flowrates will lead to an increase in the overall amount of solvent recovered. Since more solvent is recovered, the TAC will decrease because it is expressed as cost per volume of solvent recovered per year. Owen et al. (1995) also observed a decrease in the specific TAC of a RO (Reverse Osmosis) membrane plant when the operating pressure was increased.

It was also shown in Figure 6.4 that the cost of hybrid-OSN might become competitive with the classical solvent recovery unit when the operating pressure is at least 42 bar at a specific membrane cost of 400 ZAR/m^2.

As mentioned earlier, it was observed that the variable with the most significant influence on the SEC of the OSN unit was flux decline over membrane life. The influence of flux decline on SEC is shown in Figure 6.5.

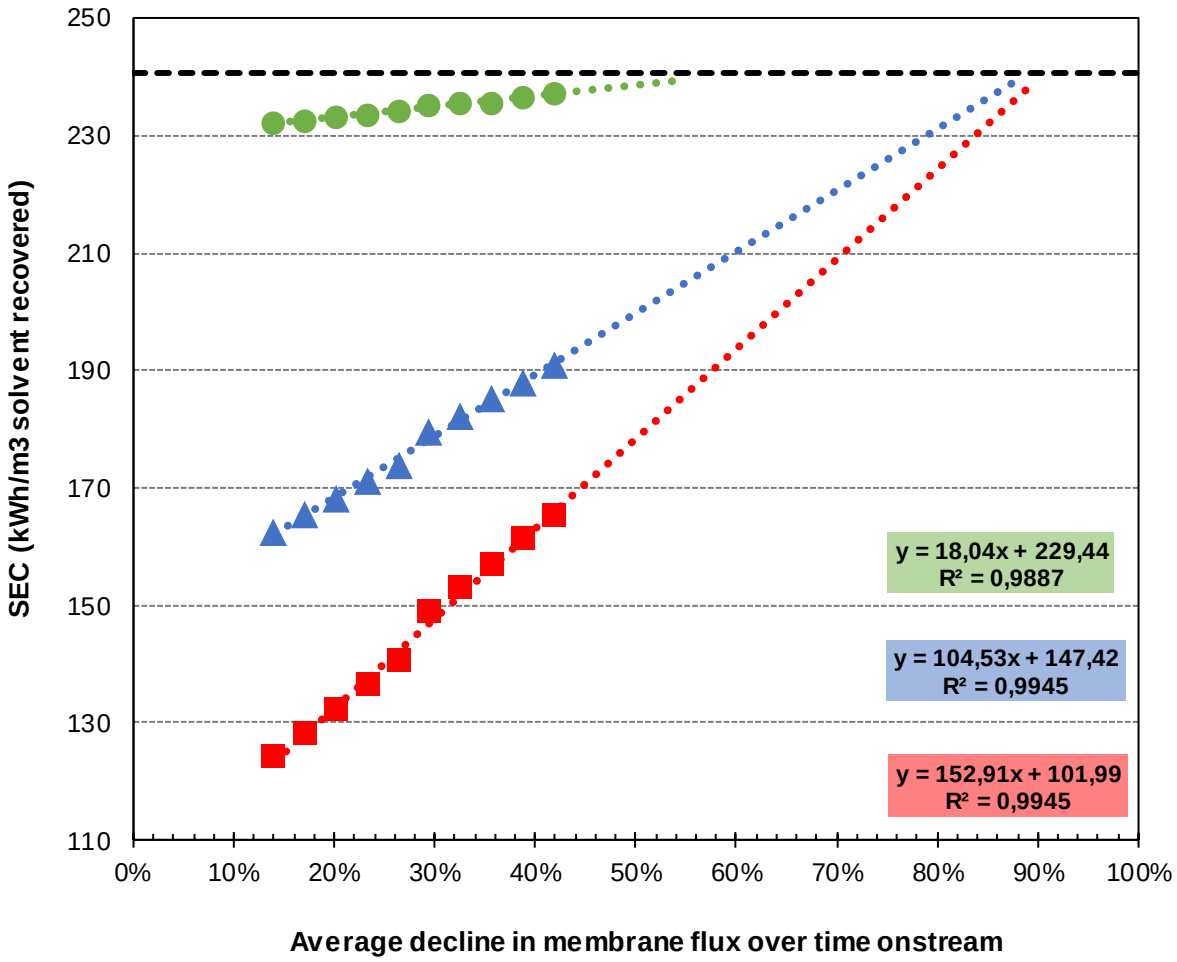

Figure 6.5: Specific energy consumption (SEC) of the classical solvent recovery unit (---) compared to a hybrid-OSN unit at an operating pressure of 20 bar (●), 42 bar (▲), and 56 bar (■) for varying average membrane flux decline over membrane life.

Figure 6.5 shows that the SEC of the hybrid-OSN unit operating at 20 bar, 42 bar and 56 bar remains less that classical solvent recovery if the average flux decline does not exceed 55%. However, it is unlikely that the decline in flux would reach 55% unless the membrane is damaged due to operating pressures over 60 bar or fouling when the solvent recovery is too high.

6.3 The influence of membrane life

Long-term demonstrations with the Max-Dewax unit have shown that membrane performance decreases over membrane life. For example, the Max-Dewax unit recovered 27% less solvent after a membrane life of 18 months compared to the first month (Bhore et al., 1999).

In Chapter 5, TAC estimations showed that membrane replacement makes the second largest contribution. Process simulations revealed that for fixed membrane life, varying the specific membrane module cost had the most significant effect on the TAC of the hybrid-OSN unit. In addition, average flux decline over membrane life had the largest effect on SEC for fixed membrane life. The simulated trends in TAC for varying permselectivity, membrane flux and operating pressure, and in SEC for varying permselectivity and operating pressure are shown in Appendix D.

Figure 6.6 shows the influence of membrane life for a specific membrane cost of 300, 1600, 3200 and 4800 ZAR/m^2 on TAC of the hybrid-OSN unit.

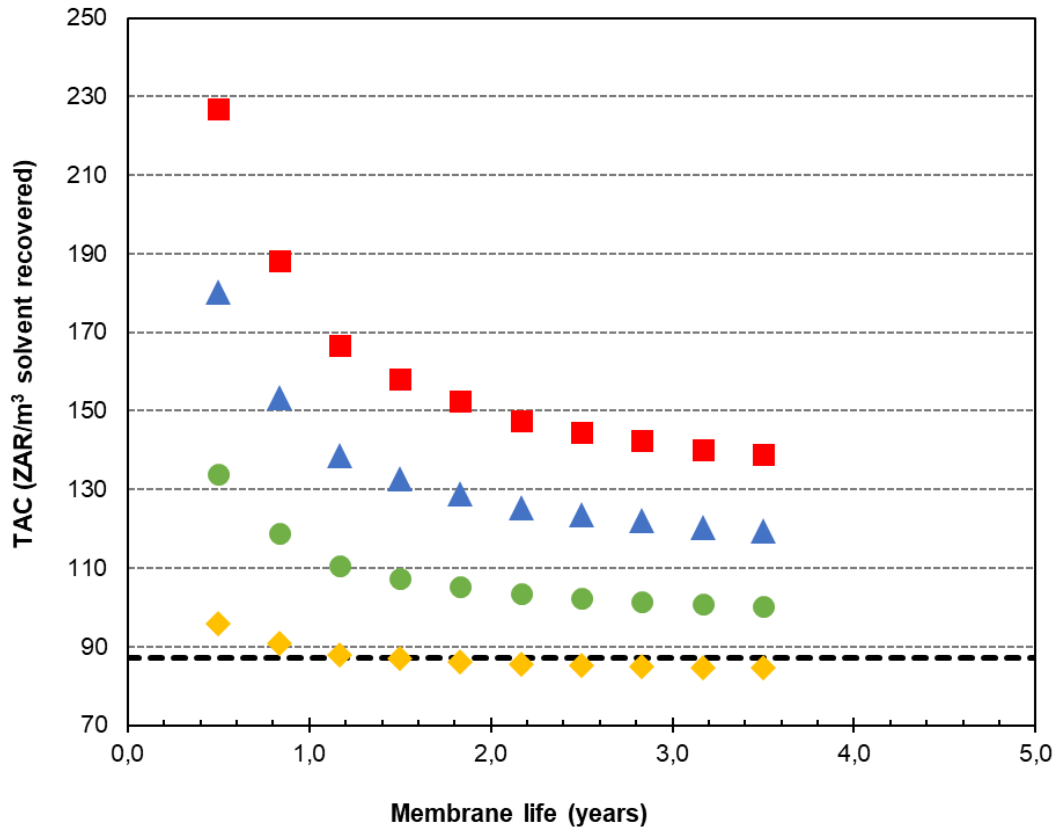

Figure 6.6: Total annual cost (TAC) of the classical solvent recovery unit (---) compared to a hybrid-OSN unit for a specific membrane cost of 300 ZAR/m^2 (◆) 1600 ZAR/m^2 (●), 3200 ZAR/m^2 (▲), and 4800 ZAR/m^2 (■) for varying membrane life.

In Figure 6.6 it is shown that membrane modules with a longer lifetime results in lower TAC. The rate at which TAC increases as the specific membrane module cost increases is also more severe when membranes are replaced every 6 months compared to the 24 and 42 months. In Chapter 5 it was shown that the contribution of membrane replacement cost towards total TAC was the second largest annual expense. Thus, membrane life has a significant effect. In addition, at a specific membrane cost of 300 ZAR/m^2, the membrane life should be at least a year.

As previously mentioned, flux decline over membrane life had the most significant effect on SEC of the hybrid-OSN unit at the three levels of membrane life. The trend in SEC for varying average flux decline is shown in Figure 6.7.

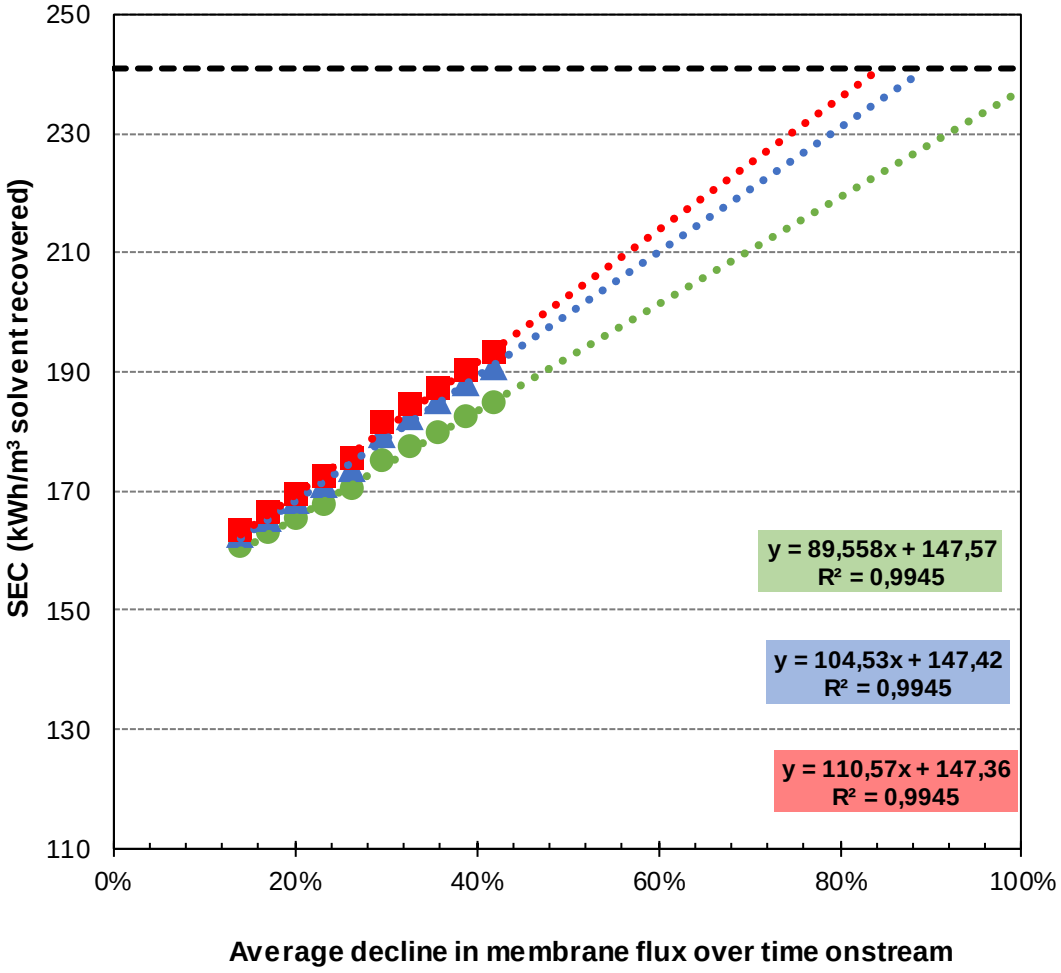

Figure 6.7: Specific energy consumption (SEC) of the classical solvent recovery unit (---) compared to a hybrid-OSN unit for a membrane life of 6 months (●), 24 months (▲), and 42 months (■) for varying average membrane flux decline over membrane life.

Figure 6.7 shows that increasing average flux decline and membrane life, will lead to an increase in SEC. At a flux decline rate of 84%, the reduction in permeate flowrate for a membrane life of 42 months will be more than for 24 and 6 months since the membranes are kept on stream for longer. Since SEC is expressed as kW per volume solvent recovered per hour, a reduction in permeate flowrate will increase SEC.

6.4 The influence of average membrane flux decline over membrane life

The long-term demonstrations with the Max-Dewax unit showed that the permeate flowrate reduced by 27% after 12 500 hours (18 months) on stream compared to the initial permeate production during the first 100 hours (Bhore et al., 1999). The reduction was due to membrane compaction or fouling which becomes more severe over membrane life (White & Wildemuth, 2006). Membrane compaction is the physical compression of the membrane material whereas fouling is the obstruction of pores in the membrane.

The hybrid-OSN unit TAC was simulated at three levels of flux decline over membrane life for varying specific membrane module cost and is shown in Figure 6.8. Additional simulations over varying permselectivity, membrane life and operating pressure is presented in Appendix D.

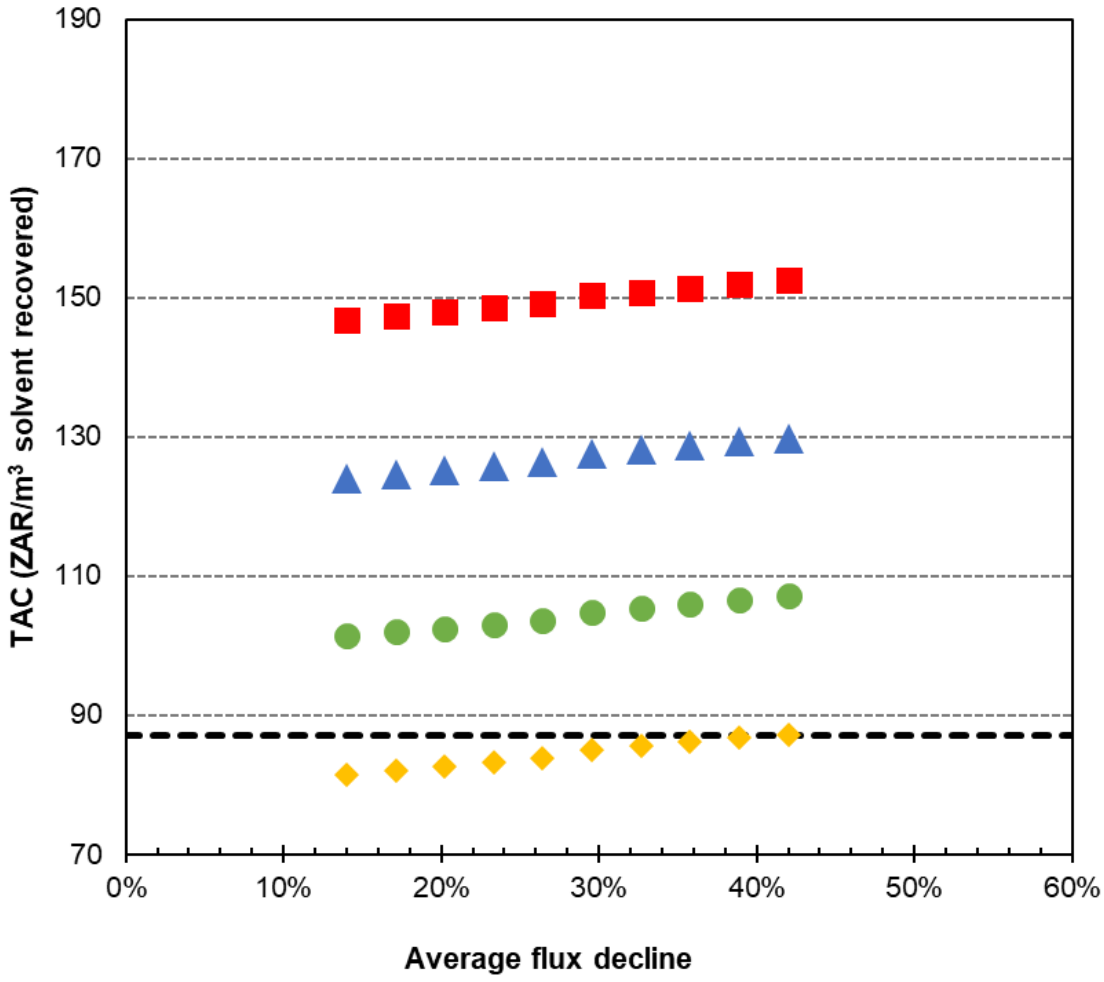

Figure 6.8: Total annual cost (TAC) of the classical solvent recovery unit (---) compared to a hybrid-OSN unit for a specific membrane cost of 900 ZAR/m^2 (◆) 1600 ZAR/m^2 (●), 3200 ZAR/m^2 (▲), and 4800 ZAR/m^2 (■) for varying flux decline.

Figure 6.9 shows that the TAC of the hybrid-OSN unit decreases as the average flux decline over membrane life is less. At a specific membrane module price of 1 000 ZAR/m^2, a flux decline of 14% per year would yield a lower TAC than at a flux decline of 28%. Membranes undergo treatment to improve their long-term stability and performance, but this will increase the manufacturing costs of membrane modules. In addition, hybrid-OSN starts to compete with classical solvent recovery if the specific cost of a membrane module is 900 ZAR/m^2 and the flux decline is less than 42% after a 2-year membrane life.

CHAPTER 7: CONCLUSIONS

The present investigation assessed whether an OSN membrane separation is more cost and energy effective than classical separation for the recovery of solvent from dewaxed lube-oil. At first glance, the literature highlights the lower energy consumption associated with OSN units compared to classical separations such as evaporation and distillation. Through process simulation, it was found that for the present investigation, including an OSN unit as an initial processing step could reduce the specific energy consumption (SEC) of a conceptual solvent recovery unit by 26% from 240 kWh/m^3 to 177 kWh/m^3 solvent recovered. The reduced energy consumption would lead to a lower utility demand and carbon emissions which makes OSN a more environmentally friendly separation than classical separation.

The conceptual stand-alone OSN unit could recover 51% solvent at a purity of 99%. The extent of solvent recovery by OSN depends on the operating pressure limits. Therefore, a hybrid-OSN unit was considered for a 98% recovery of solvent. The hybrid-OSN unit included an OSN unit followed by evaporation and distillation to recover additional solvent from the concentrated dewaxed lube-oil feed.

However, the literature shows that the total annual cost (TAC), which refers to the sum of operating and annualised capital cost, of such a hybrid-OSN unit is larger than stand-alone evaporation and/or distillation. This was confirmed in the present investigation through simulating the TAC for a hybrid-OSN and classical solvent recovery unit, which was respectively 127 ZAR/m^3 and 87 ZAR/m^3 solvent recovered.

A closer observation revealed that the specific annualised capital for the hybrid-OSN unit was 14 ZAR/m^3 more than the classical unit. The capital invested for membrane modules contributed 84% towards the overall annualised capital of the hybrid-OSN unit. However, this contribution depended on the actual cost for OSN membranes for real-life applications. Many authors in literature have expressed their concern regarding the uncertainty of membrane module prices. Even quotes from actual membrane manufacturers obtained in this investigation ranged from 258 EUR/m^2 (4 130 ZAR/m^2) up to 625 EUR/m^2 (10 000 ZAR/m^2).

A sensitivity analysis was performed to identify other variables that could also have a significant influence on TAC and SEC of the OSN unit. These variables included the following:

- Membrane life - how often membranes are replaced,
- Membrane permeate rate – rate at which species move through the membrane,
- Operating pressure – the applied OSN feed pressure, and

- Average decline in flux over membrane life.

Process simulations for different combinations of membrane permeate rate, operating pressure, membrane life, average flux decline and membrane cost were performed for the hybrid-OSN unit. Typical combinations that would yield a simulated TAC equal to that of the classical solvent recovery unit are presented in Table 7.1.

Table 7.1: Typical results of the cost (TAC) and energy (SEC) of a hybrid-OSN unit for the recovery of solvent. The energy demand and cost of a classical separation* unit was 240 kWh/m^3 and 87 ZAR/m^3 solvent recovered.

	Membrane permeate rate (mm/h)	**Membrane life (months)**	**Operating pressure (bar)**	**Average decline in flux**	**Membrane module cost (ZAR/m^2)**	**SEC** (kWh/m^3)**	**TAC*** (ZAR/m^3)**
Case 1:	MEK: 540 Toluene: 137 Lube-oil: 1	24	42	28%	950	140	87
Case 2:	MEK: 360 Toluene: 91 Lube-oil: 1	24	56	28%	1 120	150	87
Case 3:	MEK: 360 Toluene: 91 Lube-oil: 1	42	42	30%	1 150	180	87
Case 4:	MEK: 360 Toluene: 91 Lube-oil: 1	78	42	32%	1 600	177	87
Case 5:	MEK: 360 Toluene: 91 Lube-oil: 1	24	42	14%	560	163	87

* Evaporation and distillation ** Energy consumed per volume solvent recovered

*** Total operating costs plus annualised capital at 7% over 25 years.

The simulated results from the present investigation shows that under certain conditions, OSN membrane units bare the potential to assist classical solvent recovery units. However, the cost effectiveness will largely depend on the cost of membrane modules. It is also recommended that the long-term stability of OSN membranes be determined for future commercial application.

REFERENCES

A guide to cost-effective membrane technologies for minimising wastes and effluents. 1997. Scotland: Accepta. Available at: http://www.spice3.eu/GR/component/docman/doc_download/336-accepta-membrane-technology.

Alkhayat W.A. and Gerrard, A.M. 1984. Estimating manning levels for process plants. *Association for the Advancement of Cost Engineering Transactions*: I.2.1-I.2.4.

API Standard 610. September 2010. *Centrifugal pumps for petroleum, petrochemical and natural gas industries.* [Online]. Available: http://www.karoonkhozestan.com/images/upload_image/1455617220_api-610-11th.pdf. Accessed: 05 March 2018.

Baerns, M. 2006. *Technische Chemie.* Weinheim: Willey-VCH Verlag.

Bhore, N., Gould, R.M., Jacob, S.M., Staffeld, P.O, McNally D., Smiley, P.H. & Wildemuth, C.R. 1999. New membrane process debottlenecks solvent dewaxing unit. *Oil & Gas Journal,* 97(46):67.

Bloomberg: Currencies. 2018. [Online] Available at: https://www.bloomberg.com/markets/currencies. [2018, August 2]

Buonomenna, M. G. 2013. Membrane processes for a sustainable industrial growth, *RSC Advances*, 3(17): 5694.

Callister, W.D. Jr. and Rethwisch, D.G. 2011. *Material science and engineering.* Hoboken: John Wiley & Sons, Inc.

Cengel, Y.A. and Cimbala, J.M. 2014. *Fluid mechanics: Fundamentals and applications.* 3rd Edition. McGraw-Hill Education.

Chen, D., Yuan, X., Xu, L., Yu., K. 2013. Comparison between different configurations of internally and externally heat-integrated distillation by numerical simulation. *Ind. Eng. Chem. Res.* 52 (16): 5781–5790.

CoLan, 2010. *Cape-Open Standard* [Online]. Available at: http://www.colan.org. [2017, June 26].

Cuperus, F.P. 2018. SolSep membranes, e-mail to P. Cuperus [Online], 26 February. Available e-mail: cuperus@solsep.com.

Darvishmanesh, S. et al. 2011. Performance of solvent resistant nanofiltration membranes for purification of residual solvent in the pharmaceutical industry: Experiments and simulation, *Green Chemistry*, 13(12): 3476–3483.

Eghbali, M. H., Nazar, A. R. S. and Tavakoli, T. 2013. An Experimental Study on the Operational Factors Affecting the Oil Content of Wax during Dewaxing Process: Adopting a DOE Method, *Iranian Journal of Oil & Gas Science and Technology*, 2(1): 1–8.

Endress & Hauser. 2018. Membrane plant instrumentation. Email to G Robertson [Online] September 17. Available email: gavin.robertson@za.endress.com

Environment and Infrastructure Services. March 15, 2018. *Amendment of tariff charges for water services and sewerage and sanitation services: 2018/2019.* Available at: https://www.joburg.org.za/services_/Documents/rates%20and%20taxes/2018-19%20APPROVED%20TARIFFS%20FOR%20COJ.pdf. Accessed on: 09 May 2019.

Eskom. 2018. Tariffs & Charges 2018/2019. [Online] Available at: http://www.eskom.co.za/CustomerCare/TariffsAndCharges/Pages/Tariffs_And_Charges.aspx

Evonik. 2018. OSN membrane module enquiry, E-mail to Christine Frisch [Online], 6 August. Available email: christine.frisch@evonik.com

Evonik Resource Efficiency GmbH. 2017. PuraMem 280 and s600 membrane module: Instruction for use. [Online] Available at: https://duramem.evonik.com/sites/lists/RE/DocumentsHP/Flyer%20PuraMem%20Membrane%20Module%20Instruction%20for%20use%2003-2017.pdf

Filmtec membranes. N.d. High pressure pump: System design. [Online] Available at: http://msdssearch.dow.com/PublishedLiteratureDOWCOM/dh_0036/0901b803800362f7.pdf?filepath=liquidseps/pdfs/noreg/609-02060.pdf&fromPage=GetDoc.

Filter Specialists, Inc. 2018. *Tools & Resources: Oil Refinery* [Online]. Available: http://www.fsifilters.com/tech-tools/applications/oil-and-gas/oil-refinery/ Accessed: 05 February 2018.

Fontalvo, J. 2014. Using user models in MATLAB within the Aspen Plus interface with an Excel link. *Ingenieria E Investigacion,* 34(2): 39-43.

Geraldes, V., Semião, V. & De Pinho, M. N. .2002. Flow management in nanofiltration spiral wound modules with ladder-type spacers', *Journal of Membrane Science*, 203(1–2): 87–102.

Germ Africa. 2018. Prefilter design to filter solidified wax. Email to T Beatty [Online] September 21. Available email: tia@germafrica.com

Gilat, A. and Subramaniam, V. 2011. *Numerical methods – An introduction with applications using MATLAB.* Hoboken: John Wiley & Sons.

Gould, R. M., White, L. S. and Wildemuth, C. R. 2001. Membrane separation in solvent lube dewaxing, *Environmental Progress*, 20(1): 12–16.

Gould, R.M., Heaney, W.F., Nitsch, A.R. & Spencer, H.E. 1994. Lubricating oil dewaxing using cold solvent recycle process. EU Patent EP0695337 B1.

Guthrie, K.M. 1974. *Process plant estimating evaluation and control.* California: Craftsman Book Co.

Hashmi, S. and Geller, M. (Ed.) 2018. S&P Global Platts. *European methyl ethyl ketone price hits fresh 2018 low on improved availability.* [Online] Available at: https://www.spglobal.com/platts/en/market-insights/latest-news/petrochemicals/040418-european-methyl-ethyl-ketone-price-hits-fresh-2018-low-on-improved-availability.

Heiligstein, A. and Neubert, H. 1998. *Electric tank heating – A general discussion.* [Online] Available at: https://www.chromalox.com/-/media/files/training-manuals/en-us/tm-pt501-tank-heat.pdf

Hirschberg, H.G. 1999. *Handbuch verfahrenstechnik und anlagenbau: Chemie, technik, wirtschaftlichkeit.* Berlin: Springer.

Indeed. 2018. Plant operator salaries in South Africa. [Online] Available at: https://www.indeed.co.za/salaries/Plant-Operator-Salaries

Jones, D. S. J. and Pujado, P. R. 2006. *Handbook of Petroleum Processing*. Edited by D. S. J. S. Jones and P. R. Pujadó. Dordrecht: Springer Netherlands.

Kemper, T.G. 2013. *Solvent Extraction in Edible Oil Processing*. Hamm, W., Hamilton, R.J., Calliauw, G. (Eds.) Chichester: John Wiley & Sons Ltd.

Khan, H. U. et al. 2006. Studies of lubricating oil base stock: characterisation and composition, *Tribotest*, 12(1), pp. 57–65.

Kong, Y., Shi, D., Yu, H., Wang, Y., Yang, J., Zhang, Y. 2006. Separation performance of polyimide nanofiltration membranes for solvent recovery from dewaxed lube oil filtrates, *Desalination*, 191(1–3): 254–261.

Lee, U., Kim, J., Chae, I.S. & Han, C. 2017. Techno-economic feasibility study of membrane-based propane/propylene separation process. *Chemical Engineering & Processing: Process Intensification,* 119 (2017): 62-72.

Luo, Y., Wang, L., Wang, H., Yuan, X. (2015) Simultaneous optimization of heat-integrated crude oil distillation systems. *Chinese Journal of Chemical Engineering*. 23(9): 1518–1522.

Luyben, W.L. 2011. Design and control of the acetone process via dehydration of 2-propanol. *Industrial & Engineering Chemistry Research.* 50: 1206-1218.

Maleka, E.M., Mashimbye, L. & Goyns, P. 2010. South African Energy Synopsis 2010. *Directorate: Energy information management, process design and publication.* Pretoria: Department of Energy.

Mansoori, G. A., Barnes, H. L. and Webster, G. M. 2003. *Fuels and Lubricants Handbook: Technology, Properties, Performance, and Testing*, *Fuels and Lubricants Handbook: Technology, Properties, Performance, and Testing*. Edited by G. Totten, S. Westbrook, and R. Shah. West Conshohocken: ASTM International.

Marchetti, P. and Livingston, A. G. 2015. Predictive membrane transport models for Organic Solvent Nanofiltration: How complex do we need to be? *Journal of Membrane Science*. 476: 530–553.

Marchetti, P., Jimenez-Solomon, M.F., Szekely, G. & Livingston, A.G. 2014. Molecular separation with organic solvent nanofiltration: A critical review. *Ind. Chem. Rev*. 114:10735-10806.

MATLAB: Language reference manual: Version 5. 1997. Natick: The MathWorks Inc. Available at: https://ub.cbm.uam.es/publications/teaching/master.../MATLAB_REFBOOK.pdf

Matley, J. 1984. *Modern cost engineering: Methods and data: Volume II*, *Chemical Engineering.* New York: McGraw-Hill.

Micovic, J., Werth, K. & Lutze, P. 2014. Hybrid separations combining distillation and organic solvent nanofiltration for separation of wide boiling mixtures. *Chemical Engineering Research and Design,* 92(11): 2131-2147.

Mokhlif, N. D., Al-Kayiem, H. H. and Baharom, M. Bin. 2014. Numerical model to predict wax crystal size distribution in solvent dewaxing unit. *International Journal of Chemical Engineering and Applications.* 5(1): 73–78. doi: 10.7763/IJCEA.2014.V5.354.

Morris, H. C. and Nixon, J. I. 1969. Separation of solvent from raffinate phase in the solvent refining of lubricating oil stocks with n-methyl-2-pyrrolidone. US Patent, US3470089.

Motelica, A., Bruinsma, S.L., Kreiter, R., den Exter, M., Vente, J.F. 2012. Membrane retrofit option for paraffin/olefin separation-a technoeconomic evaluation, *Industrial and Engineering Chemistry Research*. 51(19): 6977–6986.

Namvar-Mahboub, M. and Pakizeh, M. 2013. Development of a novel thin film composite membrane by interfacial polymerization on polyetherimide/modified SiO2 support for organic solvent nanofiltration, *Separation and Purification Technology*, 119 (2013): 35–45.

Oatley-Radcliffe, D. L. *et al.* (2017) Nanofiltration membranes and processes: A review of research trends over the past decade, *Journal of Water Process Engineering*. 2017. 19: 164–171.

Owen, G., Bandi, M., Howell, J.A. & Churchouse, S.J. 1995. Economic assessment of membrane process for water and waste water treatment. *Journal of Membrane Science,* 102(1995): 77-91.

Pannell, D.J. 1997. Sensitivity analysis of normative economic models: Theoretical framework and practical strategies, *Agricultural Economics,* 16: 139-152.

Peck, A. 2017. *Guidelines for sizing and designing a reverse osmosis system,* AXEON Water Technologies. [Online] Available at: https://www.axeonwater.com/blog/guidelines-for-sizing-and-designing-a-reverse-osmosis-system/

Peddie, W. L., van Rensburg, J.N., Vosloo, H.C.M., van der Gryp, P. 2017. Technological evaluation of organic solvent nanofiltration for the recovery of homogeneous hydroformylation catalysts, *Chemical Engineering Research and Design*. Institution of Chemical Engineers. 121: 219–232.

Peeva, L. G. et al. 2004. Effect of concentration polarisation and osmotic pressure on flux in organic solvent nanofiltration, *Journal of Membrane Science*, 236(1–2): 121–136.

Peshev, D. & Livingston, A.G. 2013. OSN designer, a tool for predicting organic solvent nanofiltration technology performance using Aspen One, MATLAB and CAPE OPEN. *Chemical Engineering Science,* 104 (2013): 975-987.

Peters, A. and Timmerhaus, K.D. 1991. *Plant design and economics for chemical engineers,* 4th Ed. New York: McGarw-Hill.

Pitman, H. J. and Harrison, C. W. 1982. Solvent Dewaxing Process. US Patent, US4354921.

Pokorny, O.S. & Speer, G.A. 1956. Methyl-ethyl ketone dewaxing process. US Patent US2740746.

Proxa Water. 2018. High pressure membrane housing. Email to M Mahlangu [Online] March 27. Available email: Mmahlangu@proxawater.com

Richter, F., Van Zyl Visser, A. & Swiegers, G.G. 2001. Production of lubricant base oils. US Patent US6315891 B1.

RuhRPumpen. 2011. *Selection guide*. [Online]. Available: http://rrpumps.co.za/wp-content/uploads/2017/05/Selection_Guide.pdf. Accessed: 05 March 2018.

S&P Global. 2018. Platts global toluene index. [Online] Available at: https://www.platts.com.es/news-feature/2014/petrochemicals/pgpi/toluene

Samhaber, W. M. and Nguyen, M. T. 2014. Applicability and costs of nanofiltration in combination with photocatalysis for the treatment of dye house effluents, *Beilstein Journal of Nanotechnology*, (5): 476–484.

Santos, R.G., Loh, W., Bannwart, A.C. & Trevisan O.V. 2014. An overview of heavy oil properties and its recovery and transportation methods. *Brazilian Journal of Chemical Engineering.*31(2014): 571-590

SARS. Interpretation note: No. 47 (3). November 2, 2012. *Schedule of write-off periods acceptable to SARS: Water distillation and purification plant.* Available at: https://www.sars.gov.za/AllDocs/LegalDoclib/Notes/LAPD-IntR-IN-2012-47%20-%20Wear%20And%20Tear%20Depreciation%20Allowance.pdf. Date accessed: 09 May 2019.

Schäfer, A. I., Fane, A. G. and Waite, T. D. 2005. Nanofiltration: Principles and Applications, *American Water Works Association Journal* 97(11): 121.

Schwinge, J., Neal, P. R., Wiley, D. E., Fletcher, D. F. and Fane, A. G. 2004. Spiral wound modules and spacers: Review and analysis, *Journal of Membrane Science*, 242 (1–2): 129–153.

Seborg, D.E., Edgar, T.F., Mellichamp, D.A., Doyle III, F.J. 2011. *Process dynamics and control.* 3rd Edition. Hoboken: John Wiley & Sons, Inc.

Sequeira A, Jr. 1991. Solvent dewaxing of lubricating oils. US5,006,222.

Shi, B., Peshev, D., Marchetti, P., Zhang, S., Livingston, A. 2016. Multi-scale modelling of OSN batch concentration with spiral-wound membrane modules using OSN Designer. *Chemical Engineering Research and Design*. 109: 385–396.

Sholl, D. & Lively, R. 2016. The comment: Seven chemical separations to change the world, *Nature,* 532: 435-437.

Silberberg, M.S. 2013. *Principles of General Chemistry.* 3rd Ed. New York: McGraw-Hill.

Silva, P., Peeva, L. G. and Livingston, A. G. 2010. Organic solvent nanofiltration (OSN) with spiral-wound membrane elements-Highly rejected solute system, *Journal of Membrane Science*, 349(1–2): 167–174.

Sinnott, R. K. 2005. *Coulson & Richardson's Chemical Engineering Design*, Vol.6, 4th Ed. Oxford: Elsevier

Sommariva, C., Hogg, H. and Callister, K. 2003. Maximum economic design life for desalination plant: The role of auxiliary equipment materials selection and specification in plant reliability. *Desalination.* 153(1–3): 199–205.

Stamatialis, D. F., Stafie, N., Buadu, K., Hempenius, M., Wessling, M. 2006. Observations on the permeation performance of solvent resistant nanofiltration membranes, *Journal of Membrane Science*, 279(1–2): 424–433.

Styles, C. August 21, 2017. *Costs of nitrogen gas - how much should you be paying?* Available at: https://puritygas.ca/nitrogen-gas-costs/. Accessed on: 09 May 2019.

Szekely, G., Jimenez-Solomon, M.F., Marchetti, P., Kim J.F. & Livingston, A.G. 2014. Sustainability assessment of organic solvent nanofiltration: From fabrication to application. *Green Chemistry*. 16: 4440-4473.

Szklo, A. and Schaeffer, R. 2007. Fuel specification, energy consumption and CO2 emission in oil refineries. *Energy.* 32(7): 1075–1092.

The Kirkpatrick chemical engineering achievement award. 1999. [Online]. Available at: https://www.chemengonline.com/kirkpatrick-award/. [2018, July 15].

Thermon. 2018. Heating system for dewaxing solvent. Email to M Kriess [Online] October 5. Available email: manfred.kriess@thermon.com

Tsarkov, S., Malakhov, A. O., Litvinova, E. G., Volkov, A. 2013, *Pet. Chem*. 53 (2013): 537.

Turton, R., Bailie, R.C., Whiting, W.B., Shaewitz, J.A., Bhattacharyya, D. 2012. *Analysis, synthesis, and design of chemical processes,* 4th Ed. New Jersey: Pearson Education.

Ulrich, G. D. 1984. *A Guide to Chemical Engineering Process Design and Economics.* New York: Wiley.

Ulrich, G.D. and Vasudevan, P.T. 2004. *Chemical Engineering Process Design and Economics: A practical guide.* 2nd Ed. Durham: Process Pub.

US Department Energy Advanced Manufacturing Office. 2015. *Bandwidth Study on Energy Use and Potential Energy Saving Opportunities in U.S. Petroleum Refining* [Online]. Available at: https://www.energy.gov/sites/prod/files/2015/08/f26/petroleum_refining_bandwidth_report.pdf [2018, August 14].

Vandezande, P., Gevers, L.E.M. and Vankelecom, I.F.J. 2008. Solvent resistant nanofiltration Separation on a molecular level. *Chemical Society Reviews,* 37(2): 365-405.

Vanneste, J., Ormerod, D., Theys, G., Van Gool, D., Van Camp, B., Darvishmanesh, S., Van der Bruggen, B. 2013. Towards high resolution membrane-based pharmaceutical separations. *Journal of Chemical Technology and Biotechnology*. 88(1): 98–108.

Vos, B. 2018. *SS 304 Drukvat koste*, e-mail to B. Vos [Online], 30 July. Available e-mail: stainlesscrazy@gmail.com.

Walas, S.M. 1988. *Chemical Process Equipment: Selection and Design*. Newton: Butterworth-Heinemann.

Werth, K., Kaupenjohann, P., Knierbein, M. and Skiborowski, M. 2017a. Solvent recovery and deacidification by organic solvent nanofiltration: Experimental investigation and mass transfer modeling, *Journal of Membrane Science*. 528(2017): 369–380.

Werth, K., Kaupenjohann, P., Skiborowski, M. 2017b. The potential of organic solvent nanofiltration process for oleochemical industry. Separation and Purification Technology, 182 (2017): 185-196.

White, L. S. 2006. Development of large-scale applications in organic solvent nanofiltration and pervaporation for chemical and refining processes. *Journal of Membrane Science*. 286(1–2): 26–35. doi: 10.1016/j.memsci.2006.09.006.

White, L. S. and Nitsch, A. R. 2000. Solvent recovery from lube oil filtrates with a polyimide membrane, *Journal of Membrane Science*, 179(1–2): 267–274.

White, L. S. and Wildemuth, C. R. 2006. Aromatics enrichment in refinery streams using hyperfiltration, *Industrial and Engineering Chemistry Research*, 45(26): 9136–9143.

White, L. S., Wang, I. and Minhas, B. S. 1993. Polyimide membrane for separation of solvents from lube oil. US Patent, US5264166.

Woods, D.R. 2007. *Rules of thumb in engineering practice.* Weinheim: Wiley-VCH Verlag GmbH & Co.

Yuan, B. et al. 2014. Preparation of a polyimide nanofiltration membrane for lubricant solvent recovery', Journal of Applied Polymer Science, 131(11): 1–8.

APPENDIX A: SOLUTION APPROXIMATION

The solution methodology was based on a brute-force grid-search technique. A solution has converged when the following is true: $J^{dif} \leq E$ (accepted error). If no solution has converged, a new compositional fraction (indexed by i or j) is investigated. The process continues until the sum of the least squares is at a minimum. This is the optimum approximate solution.

The MATLAB code used to obtain an approximate solution is provided below:

```
function[VFPV,J_volume,xMF1,xMF2,FMF,xP1i,xP2i,FP,xC1,xC2,FC,VMF,VC,VP,CT,J_mass,di
fJ,PO1,PO2,PO3,SR]=SD_test(VF,xFF1,xFF2,xFF3,d1,d2,d3,MW1,MW2,MW3,Papp,T,NPV,NSM,RR
,b1,b2,b3,A)
%SolutionDiffusion solves transport equations to estimate the total and
%individual flux of each spiecies for an OSN feed stream.
t = cputime;
%Convertions and convergence
error = 0.1;
maxi = 1000;
DFF = (1/((xFF1/d1)+(xFF2/d2)+(xFF3/d3)));  %density of fresh feed in kg/m^3
FF=VF*DFF;          %fresh feed (kg/h)
%VF=FF/DFF;
v1 = MW1/(1000*d1); %molar volume in cum/mol
v2 = MW2/(1000*d2);
v3 = MW3/(1000*d3);
Rc = 8.314;         %universal gas constant in J/mol/K
%Initial guess for permeate composition -> LOOP No.1
SRi = 0.1;          %initial guess is a 22% permeate recovery
Ri = 0.3;           %initial guess is a 97% solute rejection
countR = 0;
difR = inf;

while countR < maxi && difR > error


    M = [];     %empty matrix for modelled data
    S = [];     %empty matrix for solution data

    JR_1 = 0.00000001:0.001:1;        %m/m fractions
    JR_2 = 0.00000001:0.0001:1;

    FPi=FF*SRi*(1-xFF3)/(1-(xFF3*(1-Ri)));    %initial permeate flowrate (kg/h)

    for i = 1:length(JR_1)
        for j = 1:length(JR_2)
            %calculate mass flows
            xP1i = JR_1(i);
            xP2i = JR_2(j);
            xP3i=1-xP1i-xP2i;

            FMF = (FF-FPi*RR)/(1-RR);
            xMF1= ((xFF1*FF)-(xP1i*FPi*RR))/(FMF*(1-RR));
            xMF2= ((xFF2*FF)-(xP2i*FPi*RR))/(FMF*(1-RR));
            xMF3 = 1-xMF1-xMF2;
            Ri=1-(xP3i/xMF3);

            %Calulate concentration flows
            NP1 = xP1i*FPi*1000/MW1;
            NP2=xP2i*FPi*1000/MW2;
            NP3=xP3i*FPi*1000/MW3;
            NP=NP1+NP2+NP3;
            DP=(1/((xP1i/d1)+(xP2i/d2)+(xP3i/d3)));
            CP=NP/(FPi/DP);
            nP1=NP1/NP; nP2=NP2/NP; nP3=NP3/NP;
            CP1=CP*nP1; CP2=CP*nP2; CP3=CP*nP3;
```

```
            NMF1 = xMF1*FMF*1000/MW1;
            NMF2 = xMF2*FMF*1000/MW2;
            NMF3 = xMF3*FMF*1000/MW3;     %mol/h
            NMF = NMF1 + NMF2 + NMF3;
            DMF = (1/((xMF1/d1)+(xMF2/d2)+(xMF3/d3)));  %density of fresh feed in
kg/m^3
            CMF = NMF/(FMF/DMF);       %Molar density in mol/m3
            nMF1 = NMF1/NMF;nMF2 = NMF2/NMF;nMF3 = 1-nMF1-nMF2;
            CMF1 = nMF1*CMF;CMF2 = nMF2*CMF; CMF3 = nMF3*CMF;       %solute molar
density at feed channel in mol/m3

            %calculate mechanical and osmotic membrane pressure
            Posmotic1 = (Rc*T)*(CMF1-CP1); %Pa
            P1 = Papp - Posmotic1;
            Posmotic2 = (Rc*T)*(CMF2-CP2); %Pa
            P2 = Papp - Posmotic2;
            Posmotic3 = (Rc*T)*(CMF3-CP3); %Pa
            P3 = Papp - Posmotic3;

            %convert volumetric permeability to mass permeability
            %coefficients
            bm1=b1*d1/1000;
            bm2=b2*d2/1000;
            bm3=b3*d3/1000;

            %Initial flux calculation in kg/m2/h
            J1i = bm1*(xMF1 - xP1i*exp(-(v1*P1)/(Rc*T)));
            J2i = bm2*(xMF2 - xP2i*exp(-(v2*P2)/(Rc*T)));
            J3i = bm3*(xMF3 - xP3i*exp(-(v3*P3)/(Rc*T)));

            if  J1i >=0 && J2i >=0 && J3i >=0
                difJ = inf;
                countJ = 0;
                flag = 0;
                while  countJ < maxi && difJ >= error
                    %Re-calculate permeate stream:
                    Jti=J1i+J2i+J3i;        %Total permeate flux (kg/m2/h)
                    xP1=J1i/Jti; xP2=J2i/Jti; xP3=J3i/Jti;
                    R=1-(xP3/xMF3);         %Membrane rejection
                    As=A*NPV*NSM;           %Effective membrane stage area (m2)
                    FP=Jti*As;              %Permeate flowrate (kg/h)
                    NP1=FP*xP1*1000/MW1;  %Permeate flowrates (mol/h)
                    NP2=FP*xP2*1000/MW2;
                    NP3=FP*xP3*1000/MW3;
                    NP = NP1+NP2+NP3;
                    nP1=NP1/NP; nP2=NP2/NP; nP3=NP3/NP;
                    DP = 1/((xP1/d1)+(xP2/d2)+(xP3/d3)); %density in kg/cum
                    CP=NP/(FP/DP);
                    CP1=CP*nP1; CP2=CP*nP2; CP3=CP*nP3;

                    %Re-calculate mixed feed stream:
                    FMF = (FF-FP*RR)/(1-RR);
                    xMF1= ((xFF1*FF)-(xP1*FP*RR))/(FMF*(1-RR));
                    xMF2= ((xFF2*FF)-(xP2*FP*RR))/(FMF*(1-RR));
                    xMF3 = 1-xMF1-xMF2;
                    NMF1 = xMF1*FMF*1000/MW1;
                    NMF2 = xMF2*FMF*1000/MW2;
                    NMF3 = xMF3*FMF*1000/MW3;     %mol/h
                    NMF = NMF1 + NMF2 + NMF3;
                    DMF = (1/((xMF1/d1)+(xMF2/d2)+(xMF3/d3)));  %density of fresh
feed in kg/m^3
                    CMF = NMF/(FMF/DMF);       %Molar density in mol/m3
                    nMF1 = NMF1/NMF;nMF2 = NMF2/NMF;nMF3 = 1-nMF1-nMF2;
                    CMF1 = nMF1*CMF;CMF2 = nMF2*CMF; CMF3 = nMF3*CMF;

                    if CMF1<0 || CMF2<0 || CMF3<0 || CP1<0 || CP2<0 || CP3<0
                        flag=1;
```

```
                    break
                end

                %Second transmembrane pressure calculation
                Posmotic1 = (Rc*T)*(CMF1-CP1); %Pa
                P1 = Papp - Posmotic1;
                Posmotic2 = (Rc*T)*(CMF2-CP2); %Pa
                P2 = Papp - Posmotic2;
                Posmotic3 = (Rc*T)*(CMF3-CP3); %Pa
                P3 = Papp - Posmotic3;

                %Second flux calculation
                J1 = bm1*(xMF1- xP1*exp(-(v1*P1)/(Rc*T)));
                J2 = bm2*(xMF2- xP2*exp(-(v2*P2)/(Rc*T)));
                J3 = bm3*(xMF3- xP3*exp(-(v3*P3)/(Rc*T)));

                if J1 < 0 || J2 < 0 ||  J3 < 0 || isnan(J1) ||  isnan(J2) ||
isnan(J3)
                    flag =1;
                    break;
                end
                %Check for convergence:
                countJ = countJ +1;
                difJ = (abs(J1i-J1) + abs(J2i-J2) + abs(J3i-J3))/(J1i+J2i+J3i);
                J1i = J1;
                J2i = J2;
                J3i = J3;


                %mass balance around stage
                Jt=J1+J2+J3;
                FP=Jt*As;
                FC=FF-FP;
                xP1=J1/Jt; xP2=J2/Jt; xP3=J3/Jt;
                xC1=((xFF1*FF)-(xP1*FP))/FC;
                xC2=((xFF2*FF)-(xP2*FP))/FC;
                xC3=((xFF3*FF)-(xP3*FP))/FC;
                FMF=(FF-FP*RR)/(1-RR);
                xMF1= ((xFF1*FF)-(xP1*FP*RR))/(FMF*(1-RR));
                xMF2= ((xFF2*FF)-(xP2*FP*RR))/(FMF*(1-RR));
                xMF3 = 1-xMF1-xMF2;
                Jv=(J1*1000/d1)+(J2*1000/d2)+(J3*1000/d3);  %volumetric flux
(L/h/m2)
                DMF = (1/((xMF1/d1)+(xMF2/d2)+(xMF3/d3)));
                VMF= FMF/DMF;       %volumetric mixed feed flowrate (cum/h)
                VFPV = VMF/NPV;     %volumetric flowrate to pressure vessel
                DP = 1/((xP1/d1)+(xP2/d2)+(xP3/d3)); %density in kg/cum
                VP = FP/DP;         %volumetric permeate (cum/h)
                DC = 1/((xC1/d1)+(xC2/d2)+(xC3/d3)); %density in kg/cum
                VC = FC/DC;         %volumetric concentrate (cum/h)
                SR = FP*(1-xP3)/(FF*(1-xFF3));   %overall stage solvent
recovery

%
            end

            if ~flag
                PO1=Posmotic1/100000;   %bar
                PO2=Posmotic2/100000;
                PO3=Posmotic3/100000;
                S = [S;difJ,Jt,Jv,VMF,xMF1,xMF2,FMF,FP, xP1, xP2, FC, xC1,
xC2,VP,VC,SR,PO1,PO2,PO3];
            end
        end

    end
end
if ~isempty(S)
```

```
        [~,s]=min(S(:,1));
        difJ = S(s,1);
        J_mass=S(s,2);      %flux in kg/h/sqm
        J_volume = S(s,3); %flux in L/h/sqm
        VMF=S(s,4); %mixed feed to stage in cum/hr
        VFPV=VMF/NPV; %mixed feed to pressure vessel in cum/hr
        xMF1=S(s,5); %composition of component 1 in kg/kg
        xMF2=S(s,6);
        FMF=S(s,7); %mixed feed to stage in kg/s
        FP=S(s,8); %permeate flowrate from stage in kg/s
        xP1i=S(s,9);
        xP2i=S(s,10);
        FC=S(s,11);
        xC1=S(s,12);
        xC2=S(s,13);
        VP=S(s,14); %permeate flowrate from stage in cum/hr
        VC=S(s,15); %concentrate flowrate from stage in cum/hr
        SR=S(s,16);
        PO1=S(s,17);
        PO2=S(s,18);
        PO3=S(s,19);
    else
        fprintf('No solution was found\n');
    end
    countR = countR+1;
    SRi = SR;

end
CT=cputime -t;
end
```

APPENDIX B: OSN UNIT EQUIPMENT SIZING SAMPLE CALCULATIONS

Vessel sizing (V-901, V-902 or V-903):

Vessel volume was determined with Equation A1 (Sinnott, 2005). Holdup time, t_H, of 7.5 minutes and freeboard volume, FB, of 10% is assumed based on Walace (1988). The feed to the vessel, $\dot{V}$, corresponds to the feed of 480 m^3/h.

$$V = \dot{V} \times t_H \times (1 + FB) \quad [B.1]$$

The vessel diameter is estimated assuming a length-to-diameter ratio, LD_{Ratio}, of 3 (Ulrich and Vasudevan, 2004).

$$D = \sqrt[3]{\frac{4 \times V}{\pi \times LD_{Ratio}}} \quad [B.2]$$

Heat calculation for preconditioning solvent (E-901):

The initial heating requirement delivered by E-901 is to compensate for heat loss associated with V-902. To determine the surface area exposed to the environment, Equations B.3 to B.7 was used with respect to area of the vessel sides, domes and concrete supports. The design variables are tangential length in meter, L, dome height in meters, H_D, concrete slab thickness, S_C, and concrete support width, Z_C, in meters.

$$A_e = A_1 + A_2 - A_3 \quad [B.3]$$

$$A_1 = \pi \times D \times L \quad [B.4]$$

$$A_2 = 2 \times \left(\pi \times \frac{D^2 + 4 \times (H_D)^2}{4}\right) \quad [B.5]$$

$$A_3 = 3 \times (S_C \times Z_C) \quad [B.6]$$

WeatherSA compiled temperature data in Secunda from January 2017 to July 2018 yielding an average summer ambient, T_a, of 30°C and winter ambient of 8°C (WeatherSA, 2018). The heat transfer coefficient of air, h_{air}, is 1.14 W/K/m^2 and was obtained from Heiligenstein and Neubert (1998) involving a 304-type stainless-steel tank with 1" fiberglass insulation. The thermal conductivity of concrete, $k_{concrete}$, was taken from Cengel and Ghajar (2015) and is 1.3 W/K/m. Heat loss to the environment and supports could was estimated with Equations B.7 and B.8 (Cengel and Ghajar, 2015).

$$\mathrm{Q}_{air} = h_{air} \times A_e \times (T_d - T_a) \quad [B.7]$$

$$Q_{concrete} = \frac{A_3 (T_d - T_a)}{\frac{\mathrm{S_c}}{k_{concrete}}} \quad [B.8]$$

The function of V-902 is to maintain a preconditioning solvent (57% MEK and 43% toluene) at a desired temperature, T_d, of 50°C to prevent the formation of wax crystals on the membrane surface.

Equation B.9 was used to calculate the heating requirement for a known specific heating capacity, C_P, and preconditioning solvent density, ρ (Cengel and Ghajar, 2015). The specific heat capacity of a 57% MEK and 43% toluene solvent mixture was 2.05 kJ/kg/K.

$$\mathrm{Q}_{solvent} = \mathrm{C}_{\mathrm{P}_{\mathrm{solvent}}} \times \dot{V} \times \rho_{\mathrm{solvent}} \times (T_d - T_a) \quad \text{[B.9]}$$

The final transferal of heat is to the 7.6 mm-thick (S_{tank}) stainless-steel vessel for which Equation B.10 was used. To estimate the total heat, a density of 7,900kg.m^{-3} and constant heat capacity of 0.477 kJ/kg/K was taken from Cengel and Ghajar (2015).

$$Q_{tank} = \rho \times S_{\mathrm{tank}} \times (A_1 + A_2) \times C_{P_{tank}} \times (T_d - T_a) \quad \text{[B.10]}$$

The net duty for V-902 during preconditioning was calculated with Equations B.11. In addition, a 20% buffer was assumed to compensate for temperature fluctuations.

$$Q_{E-101}^{PC} = \frac{Q_{air}+Q_{concrete}+Q_{preconditioning\ solvent}+Q_{tank}}{1-20\%} \quad \text{[B.11]}$$

Shaft work for pumps (P-901 to P-908):

Pump power was calculated with Equation B.12 for a pump efficiency, η, volumetric flowrate of the mixed feed to a membrane stage, $\dot{V_{MF}}$, in m^3/s and applied pressure, ΔP, in kPa (absolute) (Szekely et al., 2014).

$$W_P = \frac{\dot{V}_{MF} \times \Delta P}{\eta} \quad \text{[B.12]}$$

Pump efficiency for centrifugal pumps were chosen as 65% (Walas, 1988).

Preconditioning solvent demand:

Evonik (2017) recommends that 20 L of clean solvent per effective area (SA_{Ratio}) is necessary for preconditioning. The effective area, A_{eff}, includeed the 20% overdesign assumption for membrane modules. A design involving 3 concentrating tapered stages, j, of 62, 60 and 52 parallel pressure vessels, N_{PV}, and one polishing stage of 28 pressure vessels, each containing 7 membrane modules, N_{MM}, with a 24m^2 effective membrane area, A_{eff}^m, will have an effective area of 41126 m^2. The solvent mass for a density, ρ_{PC}, of 0.826kg/L is determined with Equation B.13.

$$M_{solvent} = \sum_{j=1}^{j} \left(N_{PV} \times N_{MM} \times A_{eff}^m\right) \times SA_{Ratio} \times \rho_{PC} \quad \text{[B.13]}$$

Solvent recovery:

The solvent recovery, ϕ, was determined as a function of effective area, A_{eff}, average permeate flux, J^{ave}, and solvent content in the feed, $\dot{V}_F x_{F,solvent}$. The average permeate flux represents the flux predicted with the OSN membrane model developed in MATLAB, averaged over the number of stages.

$$\phi_{solvent} = \frac{A_{eff} \times J^{ave}}{\dot{V}_F \times x_{F,solvent}} \quad \text{[B.14]}$$

APPENDIX C: BARE MODULE COST ESTIMATION

The capital cost for pumps, heaters, tanks, columns and evaporators was estimated using the bare module costing technique developed by Guthrie (1974) and Ulrich (1984). Cost constants for the bare module technique was taken from Turton et al. (2012). The estimated equipment costs corresponded to 2001, however, to reflect the approximate 2018 cost, the Chemical Engineering Plant Cost Index (CEPCI) was used. The following discussion will address how CEPCI was applied, bare module cost of equipment was estimated, and provide the cost constants for pumps, heaters, tanks, columns and evaporators.

CEPCI values:

The values for CEPCI was taken from Mignard (2014) and Vatavuk (2002) and presented in Table C.1 from 1999 to 2017. The cost index represents a composite index comprising of the weighted average of four sub-indices, namely the equipment, building, engineering and supervision, and the construction labour index (Vatavuk, 2002). Furthermore, the equipment index represents the weighted average of seven types, involving: heat exchangers and tanks; process machinery; pipes, valves and fittings; pumps and compressors; process instruments; electrical equipment; and structural support and miscellaneous (Mignard, 2014).

Table C.1: Chemical Engineering Plant Cost Index values.

Year	CEPCI	Reference	Year		Reference
1999	391	Vatavuk (2002)	2009	521	Turton et al. (2014)
2000	394	Vatavuk (2002)	2010	551	Turton et al. (2014)
2001	394	Turton et al. (2014)	2011	582	Turton et al. (2014)
2002	396	Turton et al. (2014)	2012	-	
2003	402	Turton et al. (2014)	2013	597	Mignard (2014)
2004	444	Turton et al. (2014)	2014	592	Mignard (2014)
2005	468	Turton et al. (2014)	2015	584	Mignard (2014)
2006	500	Turton et al. (2014)	2016	585	Mignard (2014)
2007	525	Turton et al. (2014)	2017	588	Mignard (2014)
2008	575	Turton et al. (2014)	2018	594	Mignard (2014)
			2019	608	Mignard (2014)

The expression in Equation C.1 updates the bare module cost, C_{BM_1}, at year n_1 to the final cost, C_{BM_2}, at the year n_2 (Turton et al., 2012).

$$C_{BM_2} = C_{BM_1}\left(\frac{I_2}{I_1}\right) \quad [C.1]$$

Bare module costing:

The purchased cost, C_P^o, involves base conditions like ambient pressure and carbon-steel as material of construction. For the CAPCOST program, Richardson Engineering Services Inc. (2001) fitted a logarithmic trend to historic cost-against-capacity data gathered by Guthrie (1974) and Ulrich (1984) based on historic equipment costs. The fitted parameters K_1, K_2 and K_3 are unique for the type of equipment having a maximum, A_{Max}, and minimum, A_{Min}, possible capacity within which Equation C.2 may be applied (Turton et al., 2012).

$$\mathrm{Log}_{10} C_P^o = K_1 + K_2 \log_{10} A + K_3 (\log_{10} A)^2 \qquad [C.2]$$

The purchased cost for a piece of equipment is related to its operating capacity, A. Tanks depend on vessel volume in m^3, pumps on shaft power in kW, and mixers on mixing power in kW.

Equipment constructed from a material other than carbon steel is taken into consideration with a material factor, F_M. In addition, operating pressure is accounted for by a pressure factor, F_P. The bare module factor, F_{BM}, combines F_M and F_P with two additional constants, B_1 and B_2, that are equipment-specific (Turton et al., 2012). Equation C.3 was is applied to heat exchangers (E-1002, E-1101, E-1102), process vessels (V-901,V-903), towers (T-1002, T-1003, T-1102, T-1103) and pumps (P-901, P-902, P-903, P-904, P-905, P-906, P-907, P-908, P-1001, P-1101). The bare module cost is the product of F_{BM} and C_P^o.

$$F_{BM} = B_1 + B_2 F_M F_P \qquad [C.3]$$

The mixer (M-901) and evaporators (T-1001, T-1101) are treated differently than heat exchangers, pumps, vessels and towers. The mixer is assigned a F_{BM} based on an impeller design estimated by Guthrie (1974). The evaporator is assigned a F_{BM} for a falling film, scraped wall unit constructed from stainless steel (Werth et al., 2017). Furthermore, the bare module cost is the product of the purchased cost, C_P^o, F_{BM} and F_P (Turton et al., 2012).

The towers (T-1002, T-1003, T-1102, T-1103) involving sieve trays includes a quantity factor, F_q, for N number of trays. The bare module cost is equal to the product of F_q, F_{BM}, N, and the purchased cost, C_P^o (Turton et al., 2012). The bare module factor is a constant for stainless steel sieve trays, and the quantity factor is determined with Equation C.4 (Turton et al., 2012).

$$\mathrm{Log}_{10} F_q = 0.4771 + 0.08516 \log_{10} N + 0.3473 (\log_{10} N)^2 \text{ for } N < 20 \qquad [C.4]$$

Finally, all equipment except the high-pressure pumps (P-903, P-904, P-905, P-906 and P-907) operate at, near or under vacuum pressure and thus assigned a F_P value of 1 (Turton et al., 2012). Alternatively, Equation C.5 was applied to the high-pressure pumps at 34 bar gauge pressure, P, since

the base condition in Chapter 5 is 35 bar. The constants C_1, C_2 and C_3 was based on a centrifugal pump.

$$\mathrm{Log}_{10} F_P = C_1 + C_2 \log_{10} P + C_3 (\log_{10} P)^2 \qquad [C.5]$$

Table C.2: Constants and multiplication factors for all equipment.

ID	K_1	K_2	K_3	F_M*	F_P*	B_1	B_2	F_{BM}	N	F_q
V-901	3.5565	0.3776	0.0905	1.0	1.0	1.49	1.52	3.01		
V-902	3.5565	0.3776	0.0905	3.1	1.0	1.49	1.52	6.20		
V-903	3.5565	0.3776	0.0905	1.0	1.0	1.49	1.52	3.01		
M-901	3.8511	0.7009	-0.0003					1.38		
P-901	3.3892	0.0536	0.1538	1.6	1.0	1.89	1.35	4.05		
P-902	3.3892	0.0536	0.1538	1.6	1.0	1.89	1.35	4.05		
P-903	3.3892	0.0536	0.1538	1.6	1.6	1.89	1.35	5.37		
P-904	3.3892	0.0536	0.1538	1.6	1.6	1.89	1.35	5.37		
P-905	3.3892	0.0536	0.1538	1.6	1.6	1.89	1.35	5.37		
P-906	3.3892	0.0536	0.1538	1.6	1.6	1.89	1.35	5.37		
P-907	3.3892	0.0536	0.1538	1.6	1.6	1.89	1.35	5.37		
P-908	3.3892	0.0536	0.1538	1.6	1.0	1.89	1.35	4.05		
T-1001	5.2366	-0.6572	0.3500		1.0			4.00		
T-1002 (tower)	3.4974	0.4485	0.1074	3.1	1.0	2.25	1.82	7.89		
T-1002 (trays)	2.9949	0.4465	0.3961		1.0			1.80	5	2.328
T-1003 (tower)	3.4974	0.4485	0.1074	3.1	1.0	2.25	1.82	7.89		
T-1003 (trays)	2.9949	0.4465	0.3961		1.0			1.80	2	2.960
E-1002	4.1884	-0.2503	0.1974	1.8	1.0	1.63	1.66	4.62		
P-1001	3.3892	0.0536	0.1538	1.6	1.6	1.89	1.35	5.37		
T-1101	3.9119	0.8627	-0.0088		1.0			4.00		
T-1102 (tower)	3.4974	0.4485	0.1074	3.1	1.0	2.25	1.82	7.89		
T-1102 (trays)	2.9949	0.4465	0.3961		1.0			1.80	5	2.328
T-1103 (tower)	3.4974	0.4485	0.1074	3.1	1.0	2.25	1.82	7.89		
T-1103 (trays)	2.9949	0.4465	0.3961		1.0			1.80	2	2.960
E-1101	4.1884	-0.2503	0.1974	1.8	1.0	1.63	1.66	4.62		
E-1102	4.4646	-0.5727	0.3955	2.7	1.0	1.63	1.66	6.11		
P-1101	3.3892	0.0536	0.1538	1.6	1.0	1.89	1.35	4.05		

* See equipment summary, Table 4.5, for operating conditions

APPENDIX D: RESULTS FROM PROCESS SIMULATIONS

The following cases are presented:

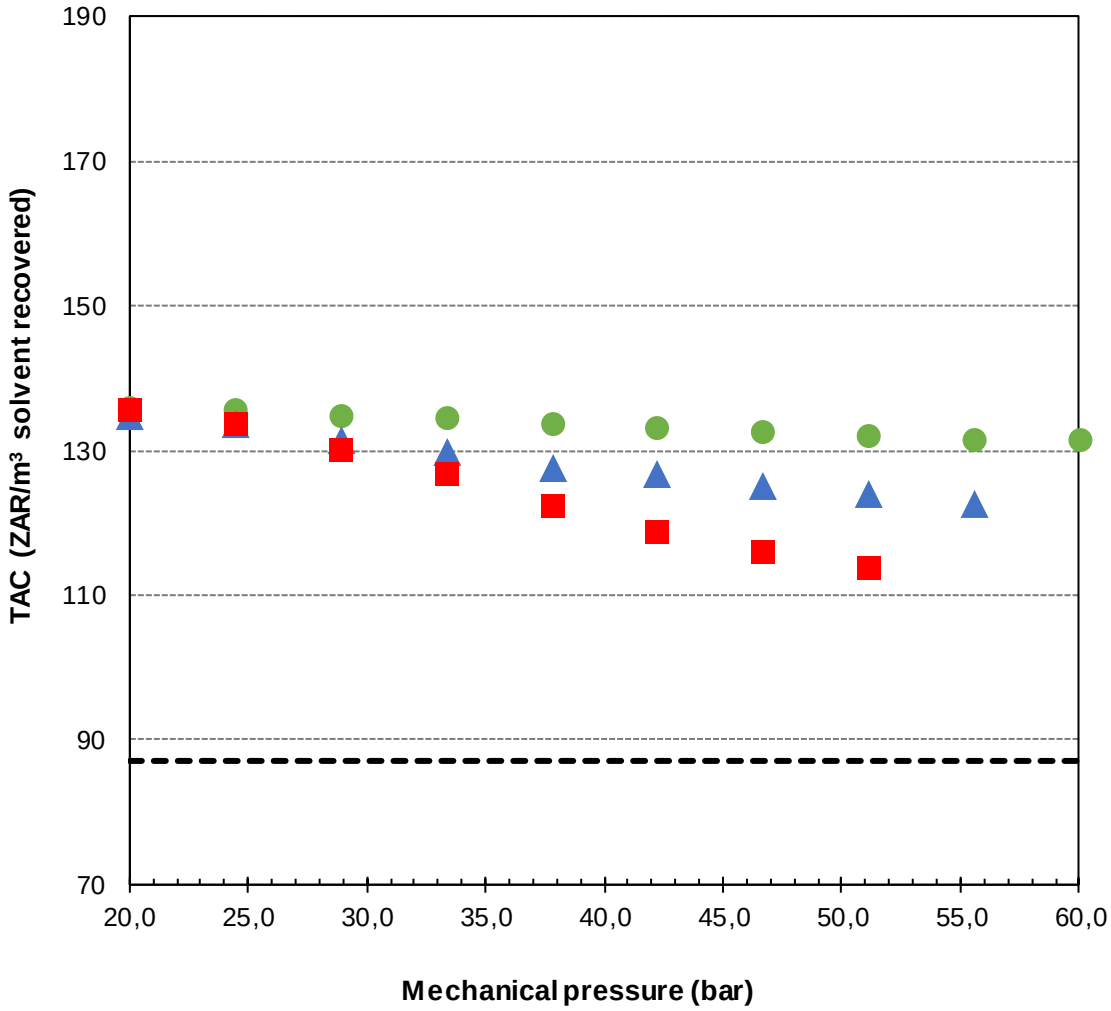

Figure D.1: Total annual cost (TAC) of the classical solvent recovery unit (---) compared to a hybrid-OSN unit with a MEK and toluene permselectivity of 180 and 46 (●), 360 and 91 (▲), and 540 and 137 (■) for varying operating pressure.

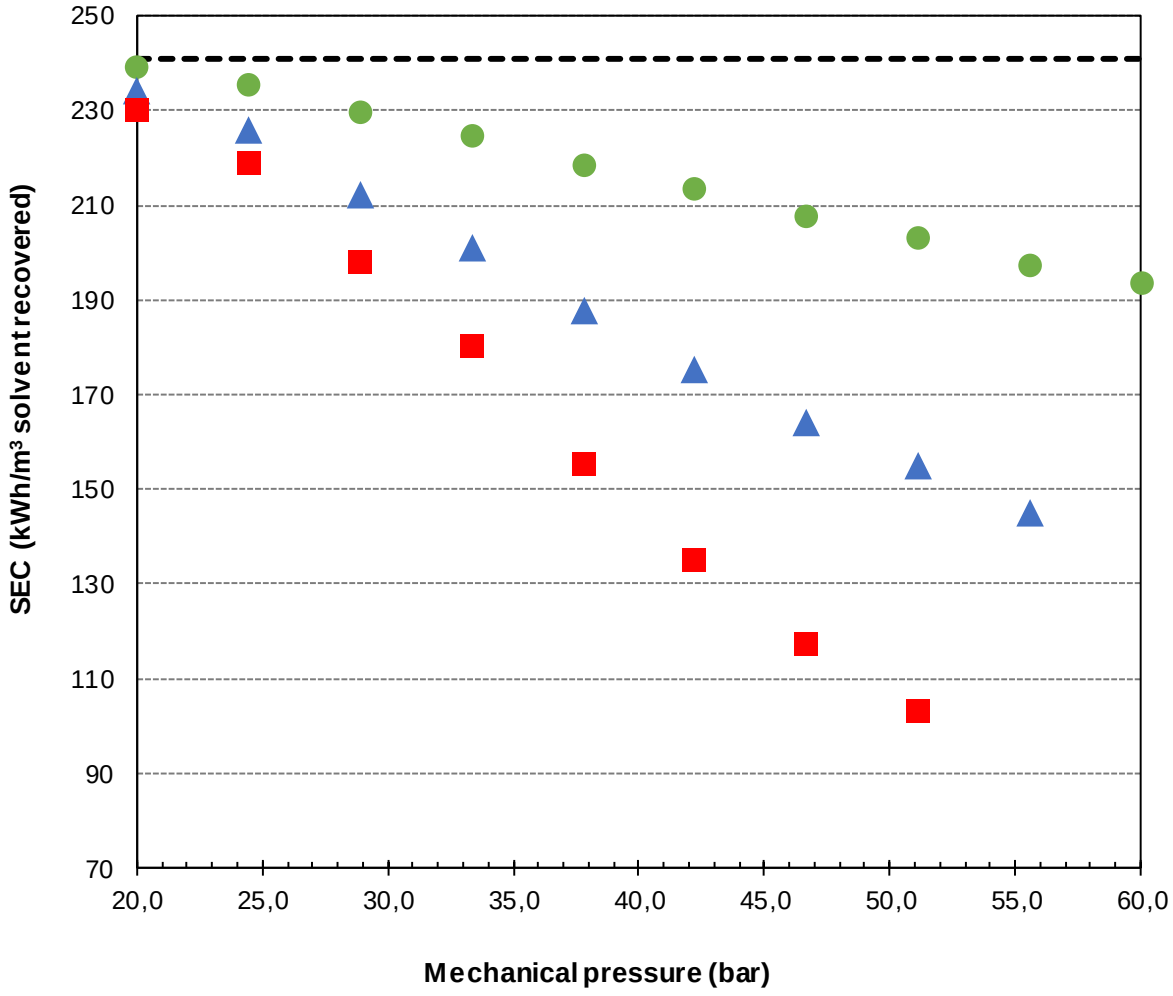

Figure D.2: Specific energy consumption (SEC) of the classical solvent recovery unit (---) compared to a hybrid-OSN unit with a MEK and toluene permselectivity of 180 and 46 (●), 360 and 91 (▲), and 540 and 137 (■) for varying operating pressure.

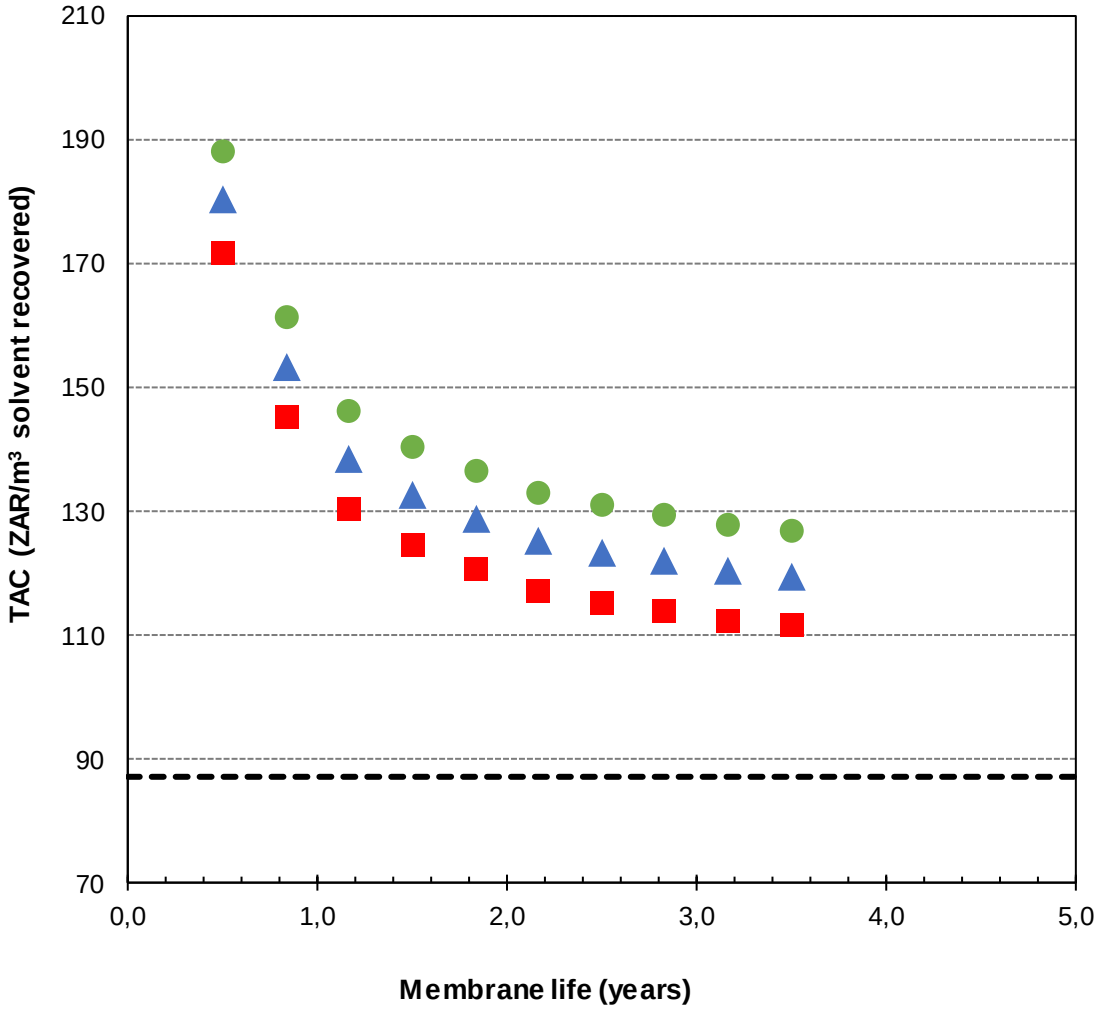

Figure D.3: Total annual cost (TAC) of the classical solvent recovery unit (---) compared to a hybrid-OSN unit with a MEK and toluene permselectivity of 180 and 46 (●), 360 and 91 (▲), and 540 and 137 (■) for varying membrane life.

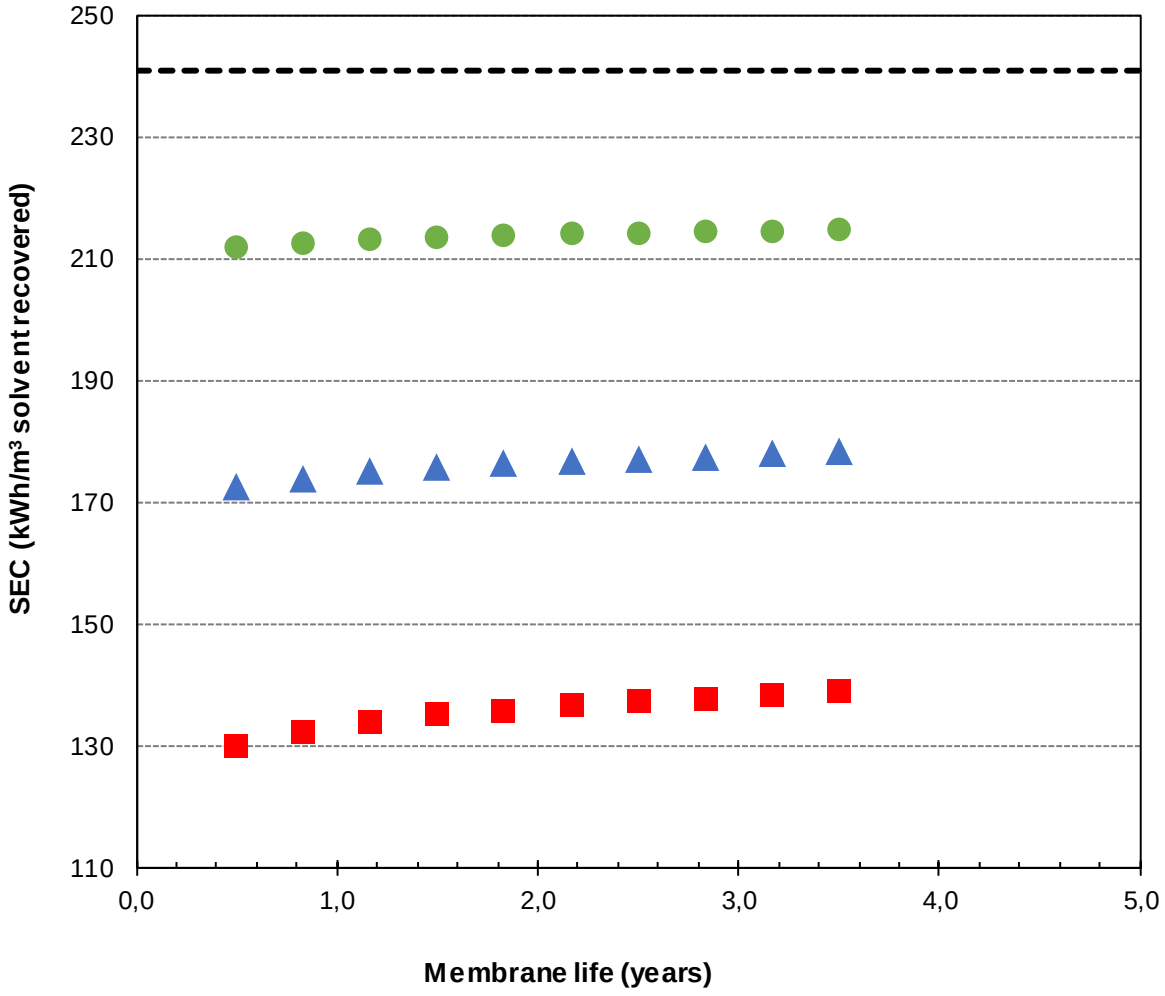

Figure D.4: Specific energy consumption (SEC) of the classical solvent recovery unit (---) compared to a hybrid-OSN unit with a MEK and toluene permselectivity of 180 and 46 (●), 360 and 91 (▲), and 540 and 137 (■) for varying membrane life.

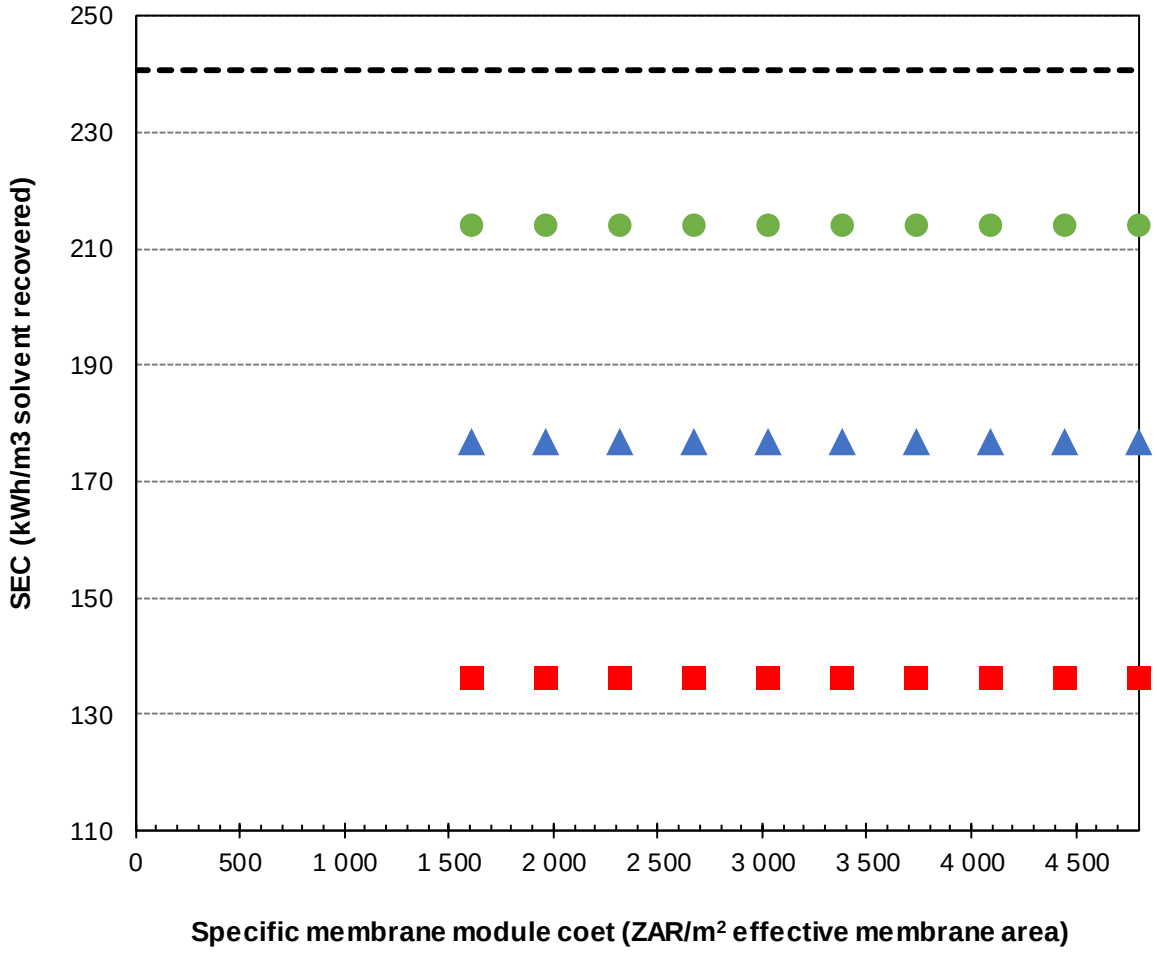

Figure D.5: Total annual cost (TAC) of the classical solvent recovery unit (---) compared to a hybrid-OSN unit with a MEK and toluene permselectivity of 180 and 46 (●), 360 and 91 (▲), and 540 and 137 (■) for varying specific membrane module cost.

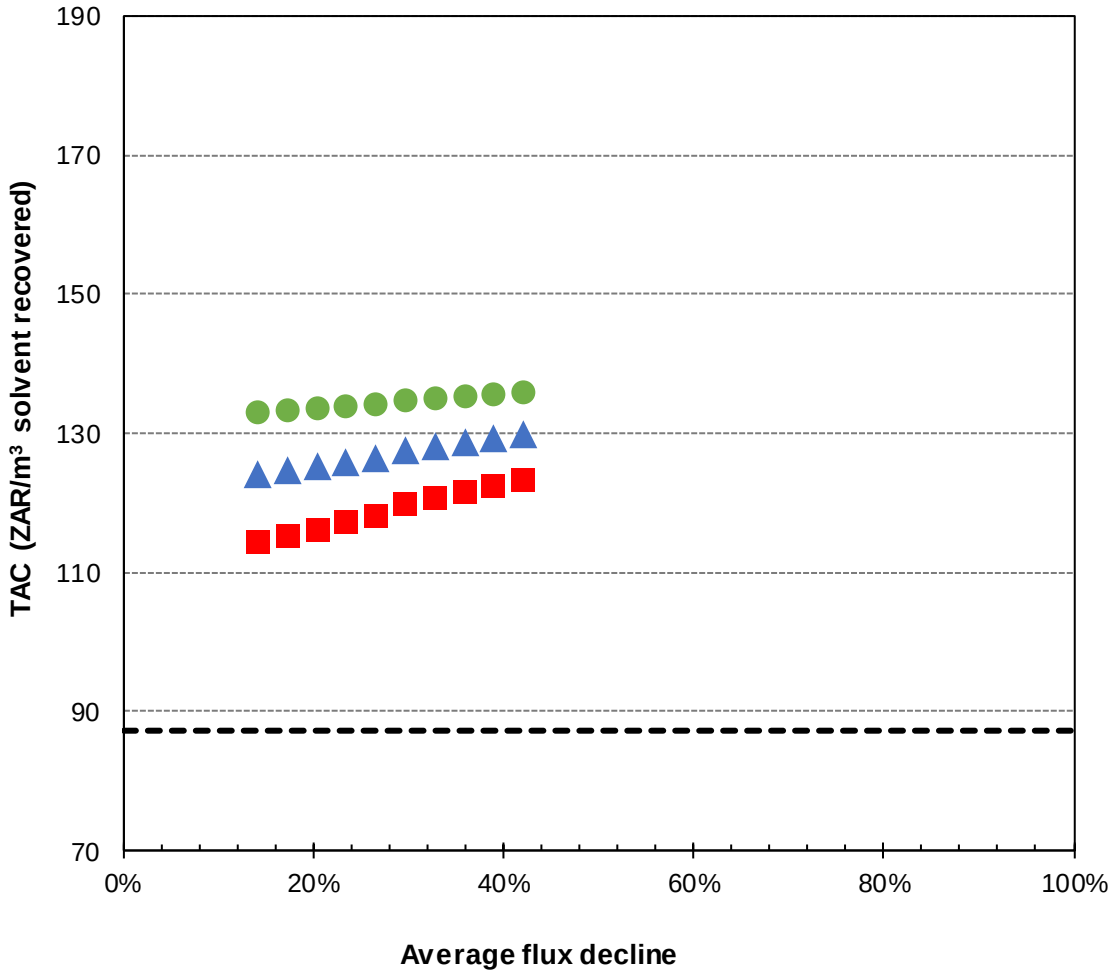

Figure D.6: Specific energy consumption (SEC) of the classical solvent recovery unit (---) compared to a hybrid-OSN unit with a MEK and toluene permselectivity of 180 and 46 (●), 360 and 91 (▲), and 540 and 137 (■) for varying average membrane flux decline over membrane life.

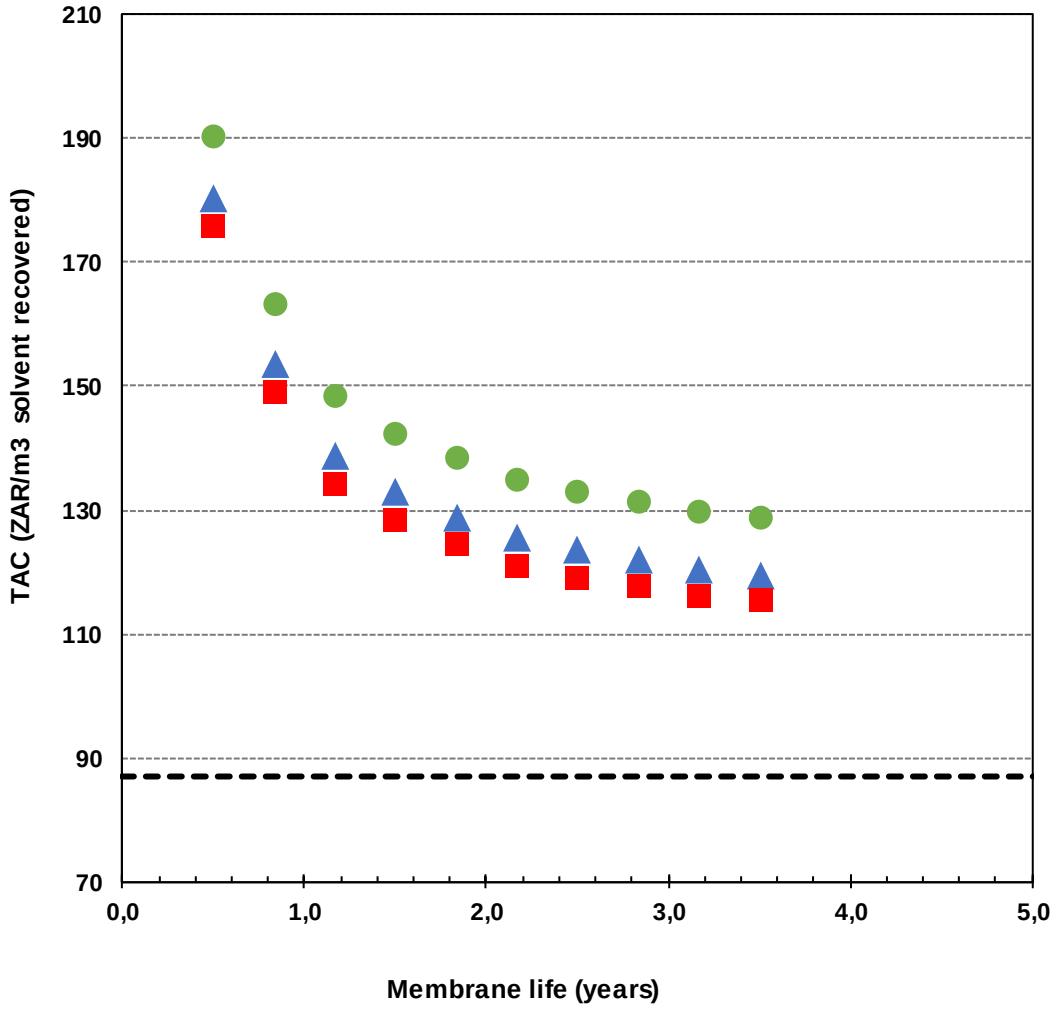

Figure D.7: Total annual cost (TAC) of the classical solvent recovery unit (---) compared to a hybrid-OSN unit at a operating pressure of 20 bar (●), 42 bar (▲), and 56 bar (■) for varying membrane life.

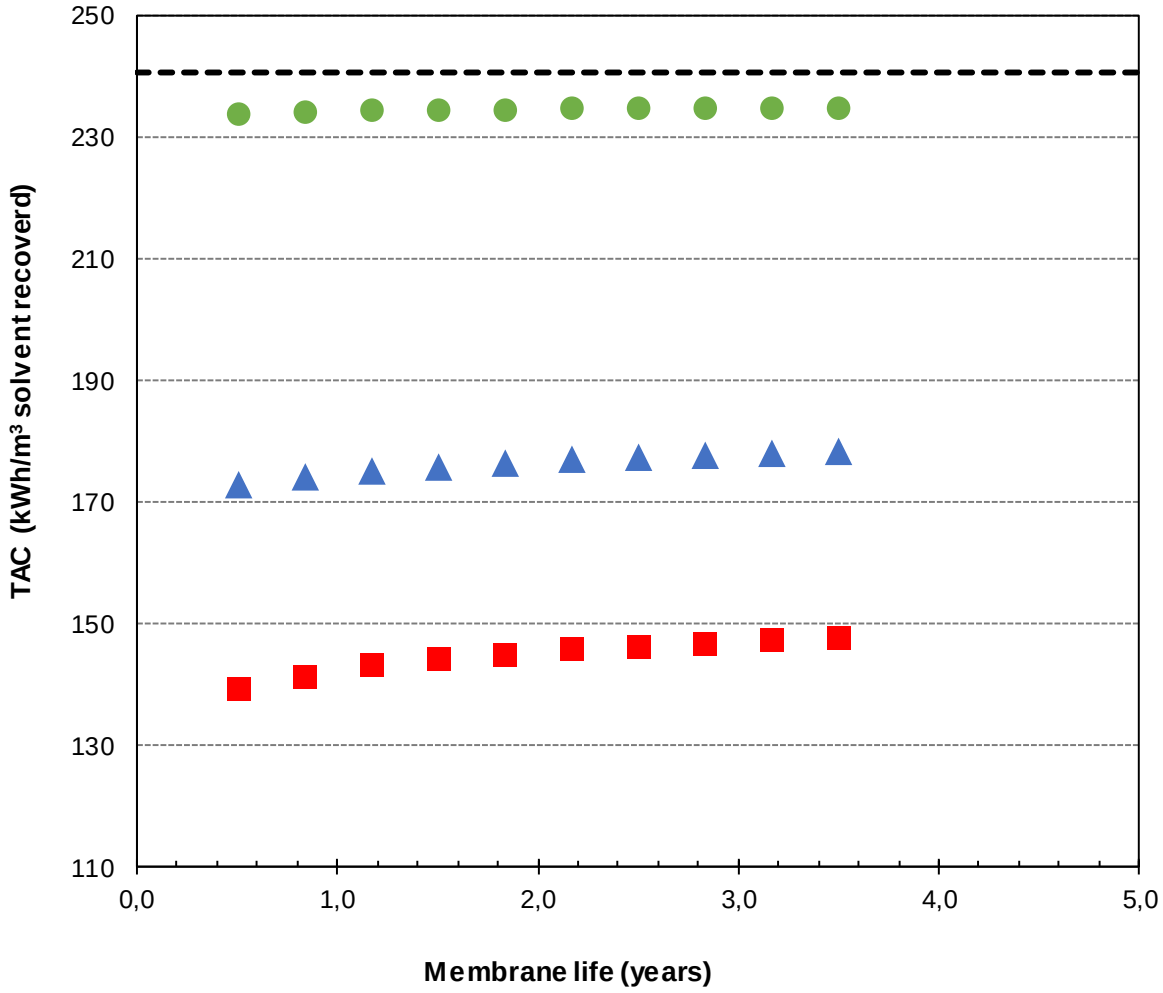

Figure D.8: Specific energy consumption (SEC) of the classical solvent recovery unit (---) compared to a hybrid-OSN unit at a operating pressure of 20 bar (●), 42 bar (▲), and 56 bar (■) for varying membrane life.

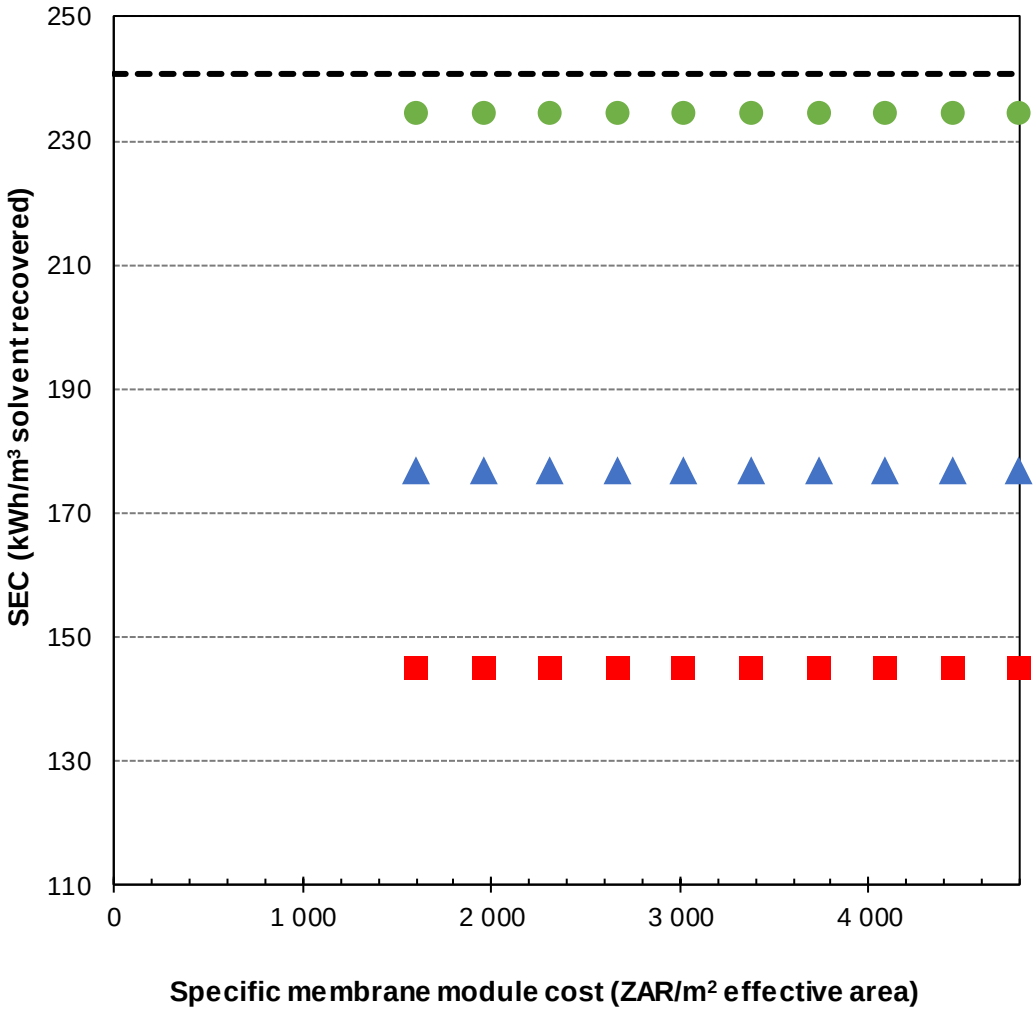

Figure D.9: Specific energy consumption (SEC) of the classical solvent recovery unit (---) compared to a hybrid-OSN unit at a operating pressure of 20 bar (●), 42 bar (▲), and 56 bar (■) for varying specific membrane module cost.

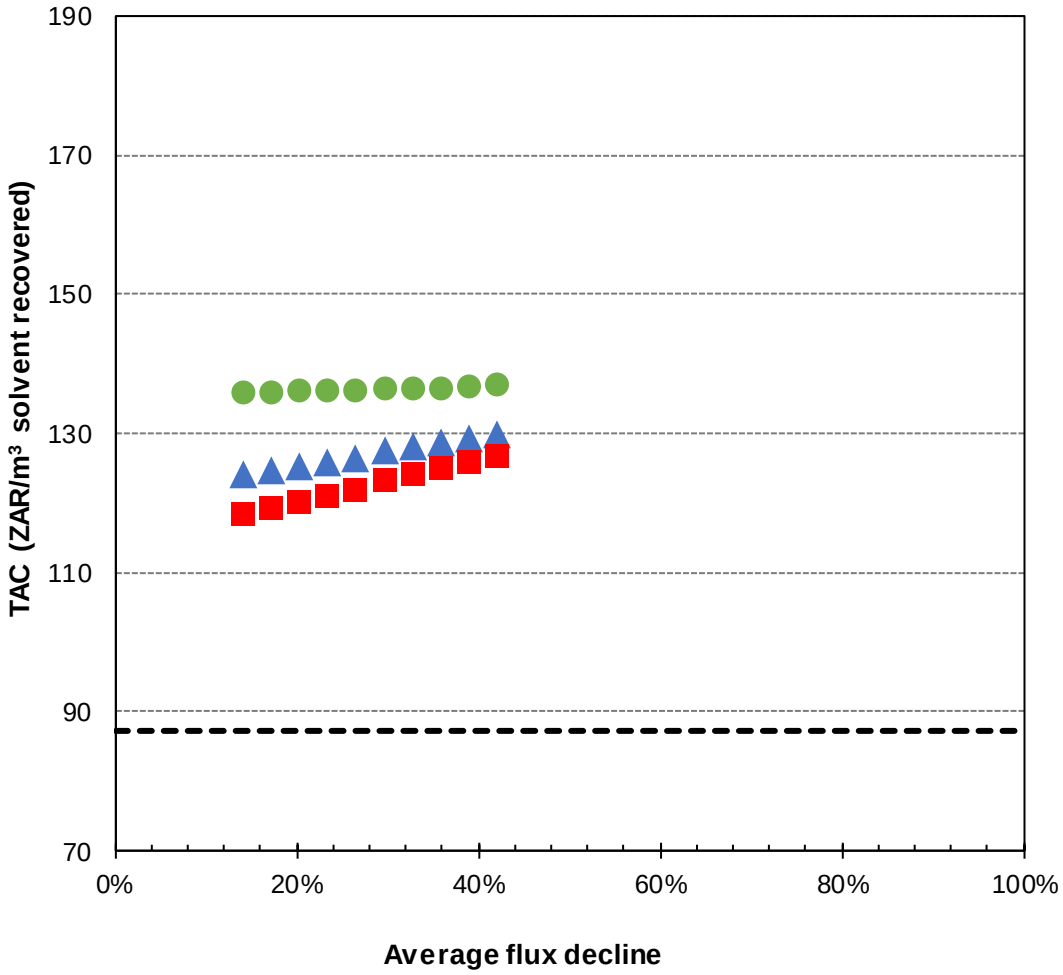

Figure D.10: Total annual cost (TAC) of the classical solvent recovery unit (---) compared to a hybrid-OSN unit at a operating pressure of 20 bar (●), 42 bar (▲), and 56 bar (■) for varying average flux decline over membrane life.

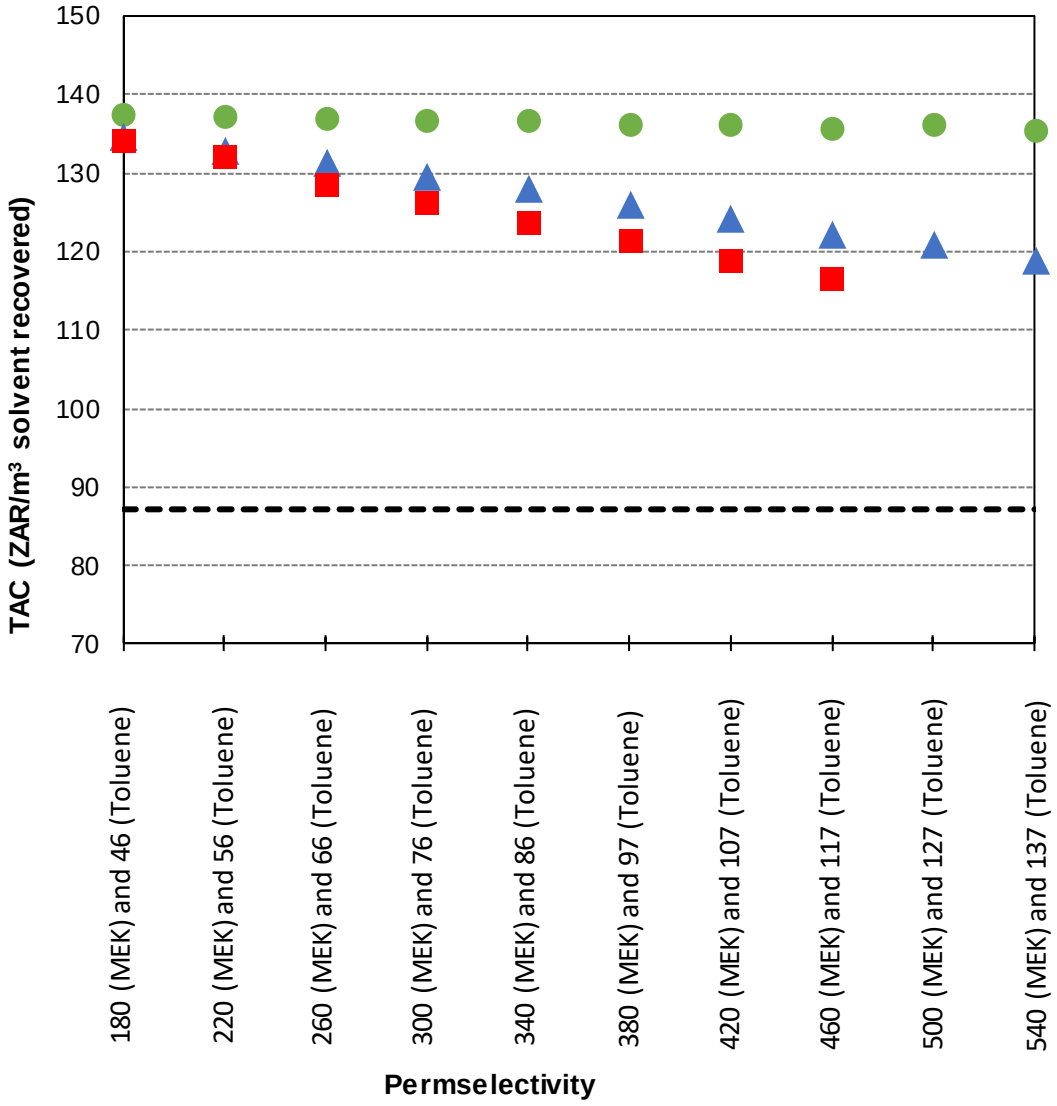

Figure D.11: Total annual cost (TAC) of the classical solvent recovery unit (---) compared to a hybrid-OSN unit at a operating pressure of 20 bar (●), 42 bar (▲), and 56 bar (■) for varying permselectivity.

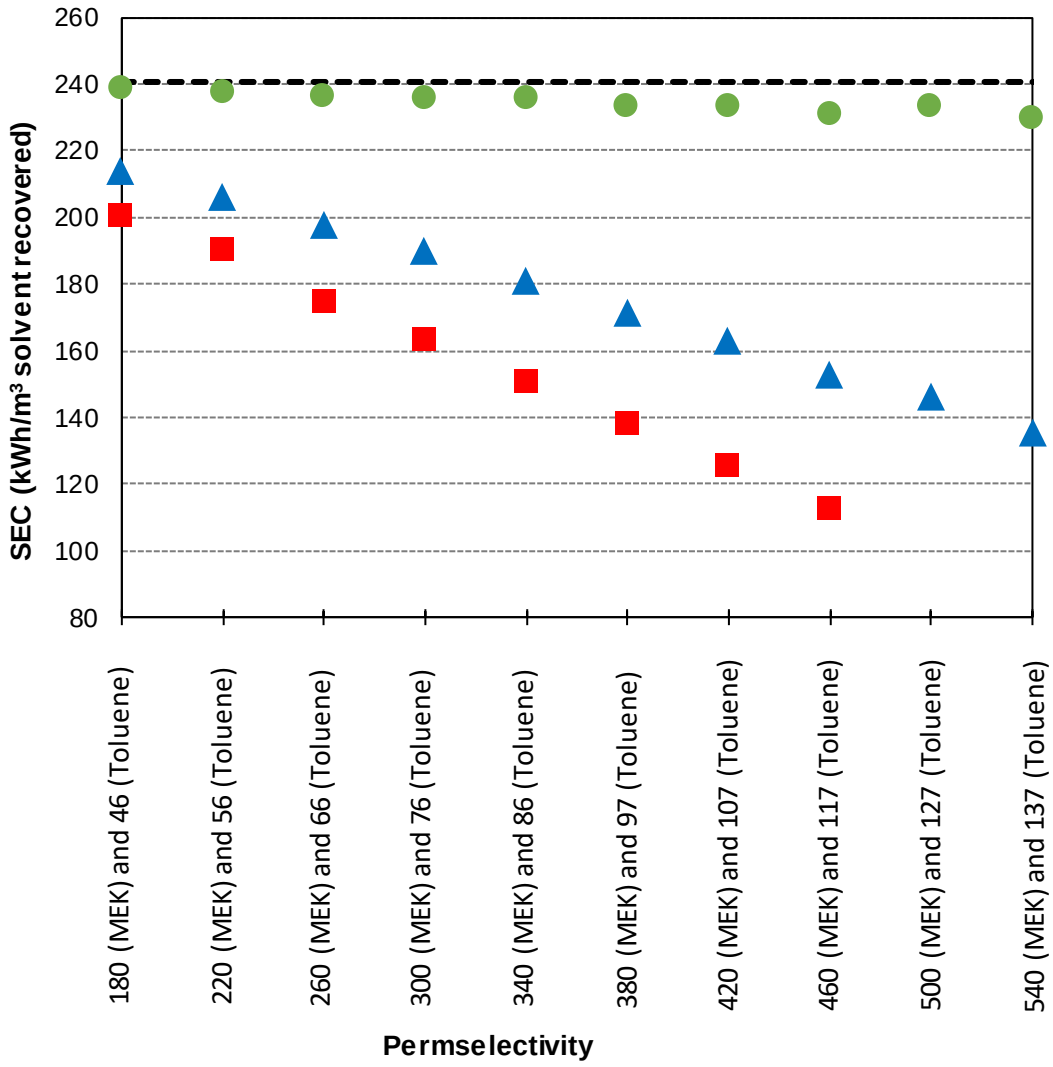

Figure D.12: Specific energy consumption (SEC) of the classical solvent recovery unit (---) compared to a hybrid-OSN unit at a operating pressure of 20 bar (●), 42 bar (▲), and 56 bar (■) for varying permselectivity.

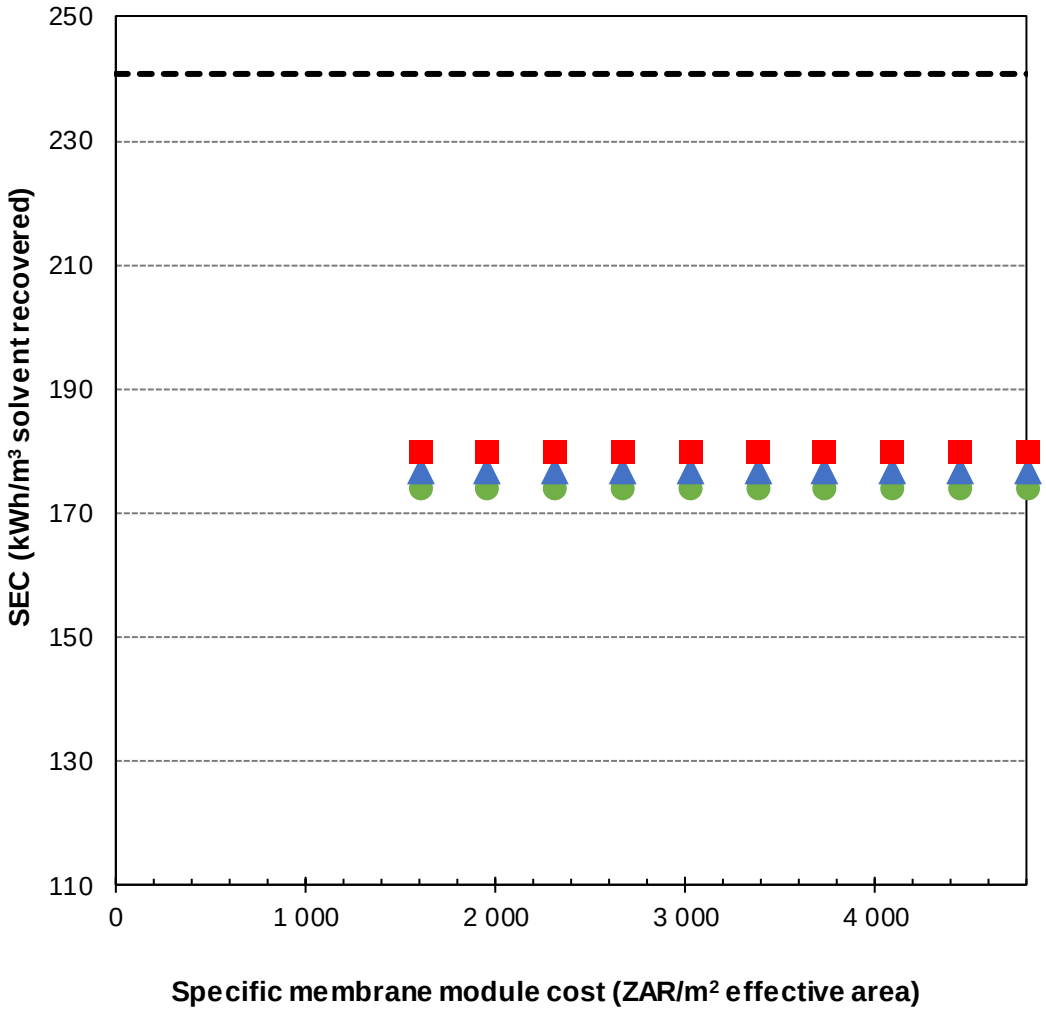

Figure D.13: Specific energy consumption (SEC) of the classical solvent recovery unit (---) compared to a hybrid-OSN unit at a membrane life of 0.5 (●), 2 (▲), and 3.5 years (■) for varying specific membrane module cost.

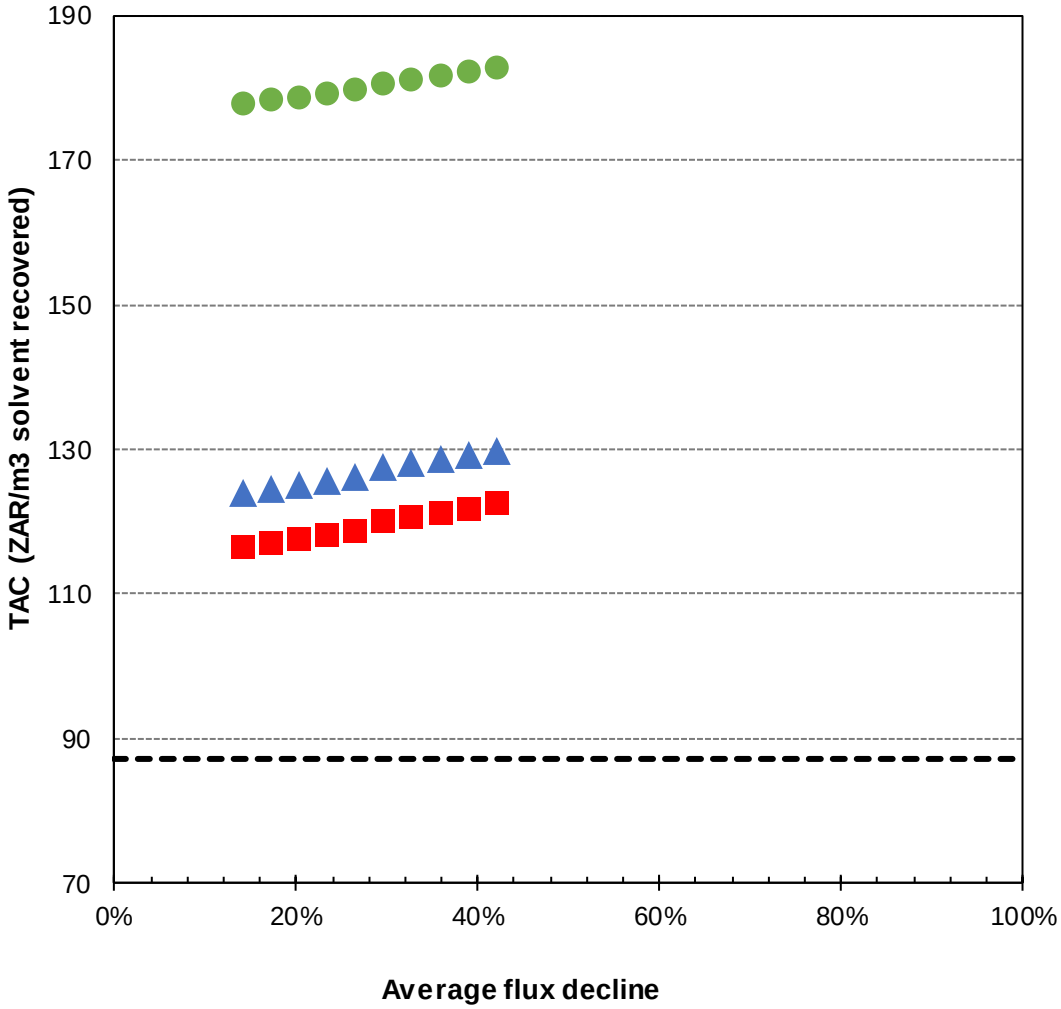

Figure D.14: Total annual cost (TAC) of the classical solvent recovery unit (---) compared to a hybrid-OSN unit at a membrane life of 0.5 (●), 2 (▲), and 3.5 years (■) for varying membrane average flux decline over membrane life**.**

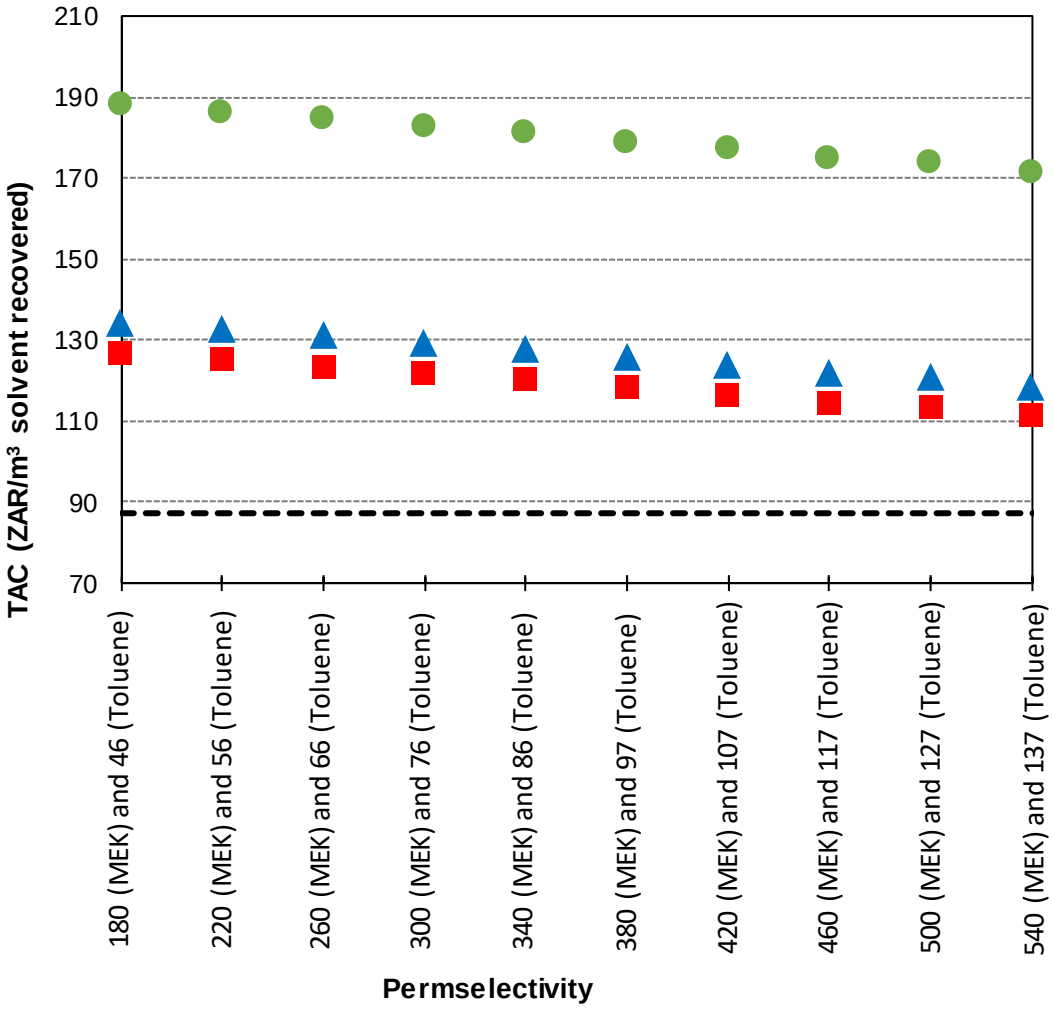

Figure D.15: Total annual cost (TAC) of the classical solvent recovery unit (---) compared to a hybrid-OSN unit at a membrane life of 0.5 (●), 2 (▲), and 3.5 years (■) for varying permselectivity.

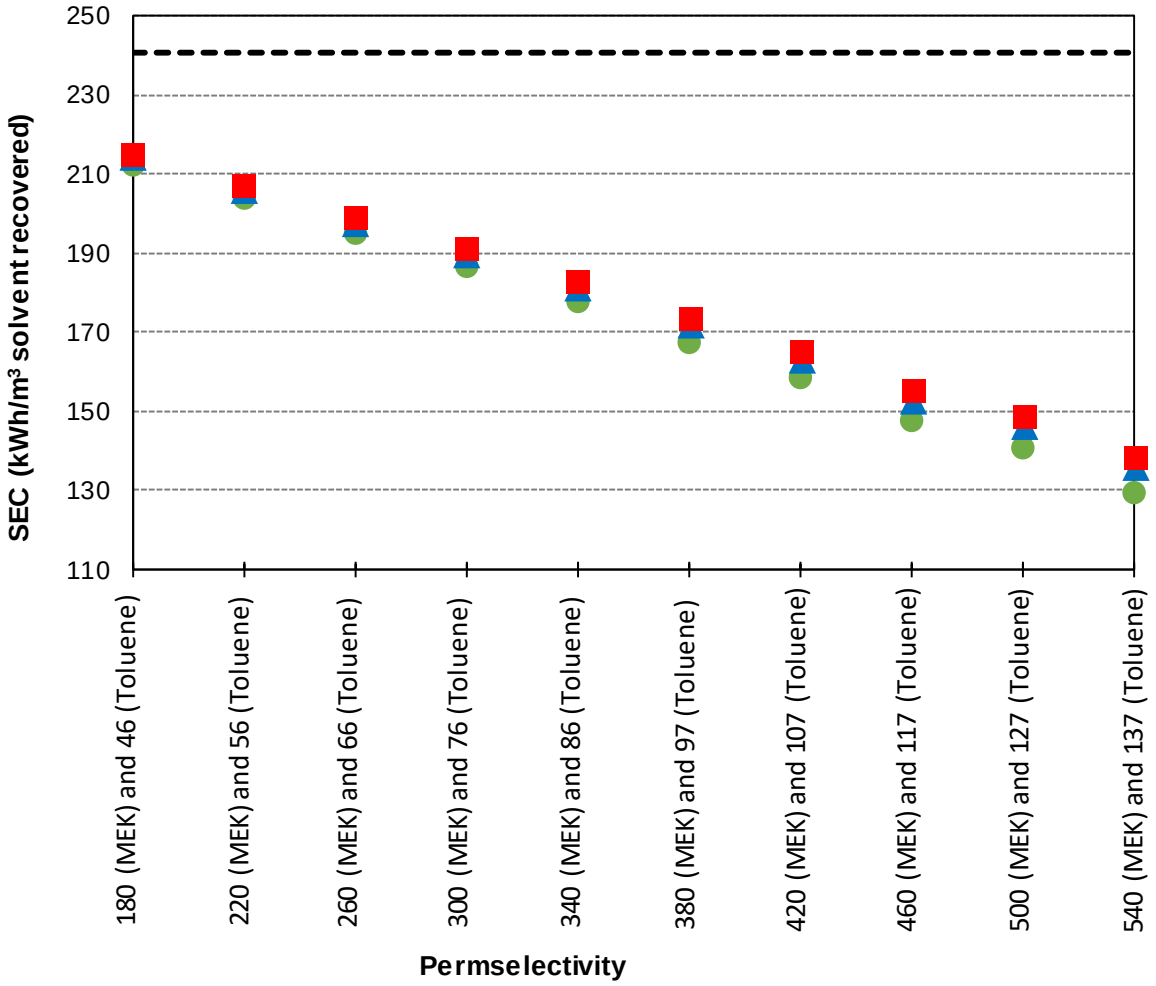

Figure D.16: Specific energy consumption (SEC) of the classical solvent recovery unit (---) compared to a hybrid-OSN unit at a membrane life of 0.5 (●), 2 (▲), and 3.5 years (■) for varying permselectivity.

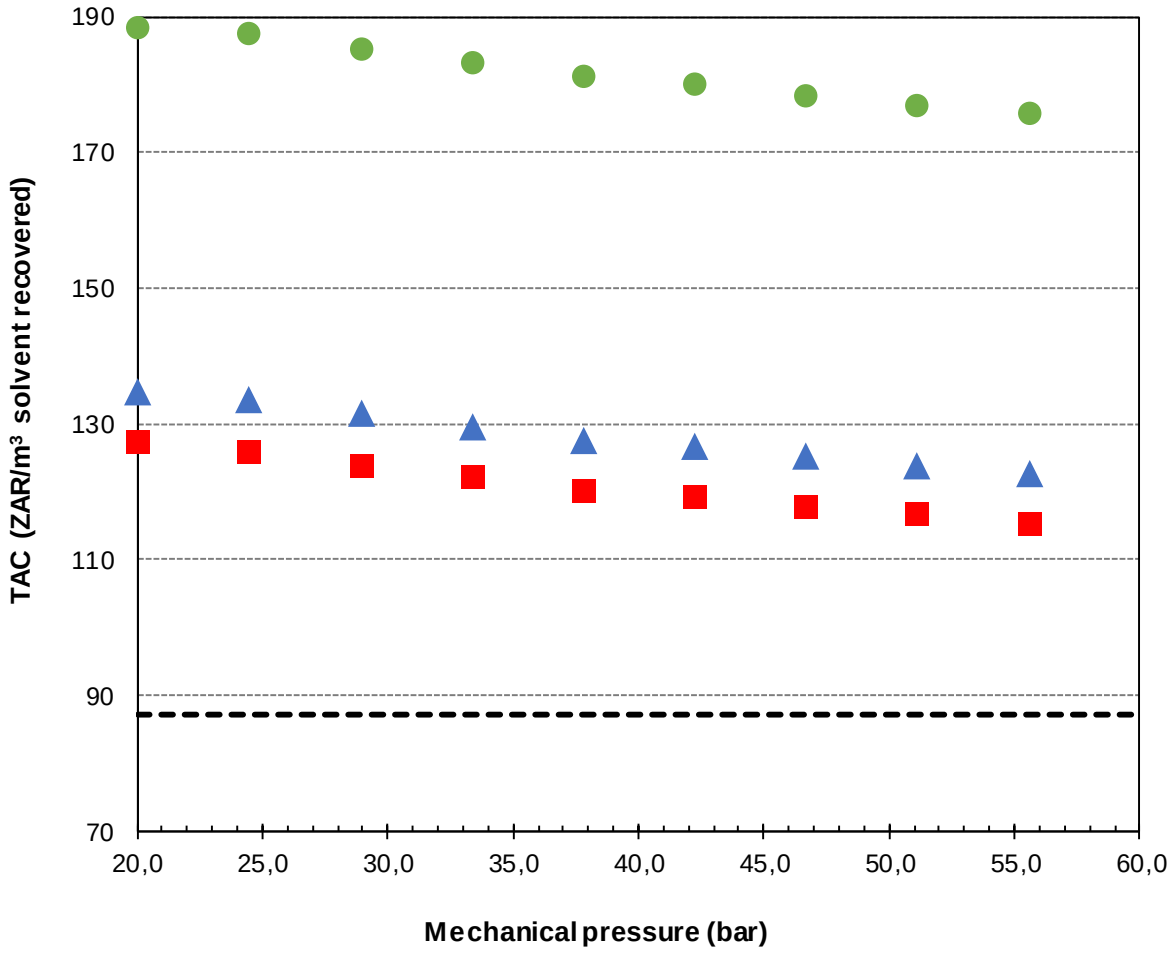

Figure D.17: Total annual cost (TAC) of the classical solvent recovery unit (---) compared to a hybrid-OSN unit at a membrane life of 0.5 (●), 2 (▲), and 3.5 years (■) for varying operating pressure.

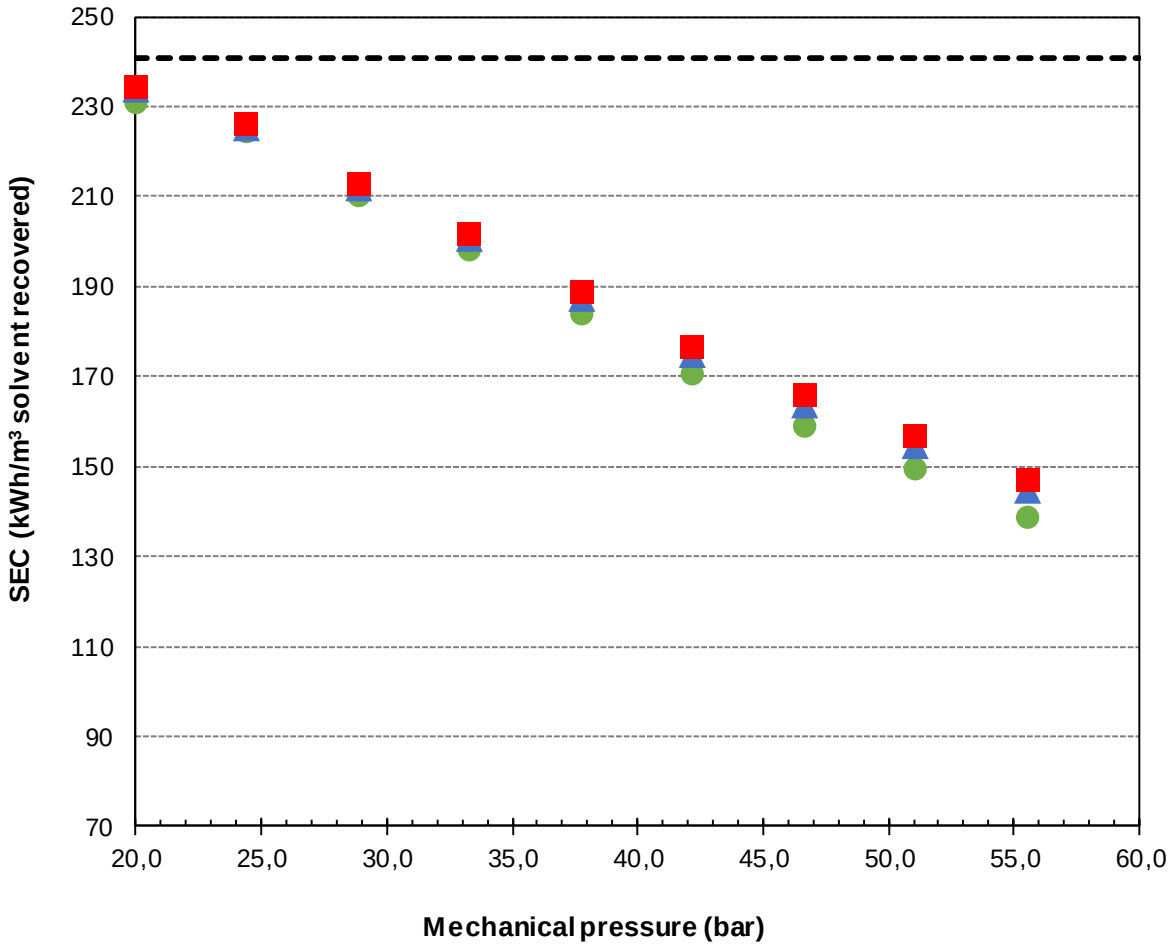

Figure D.18: Specific energy consumption (SEC) of the classical solvent recovery unit (---) compared to a hybrid-OSN unit at a membrane life of 0.5 (●), 2 (▲), and 3.5 years (■) for varying operating pressure**.**

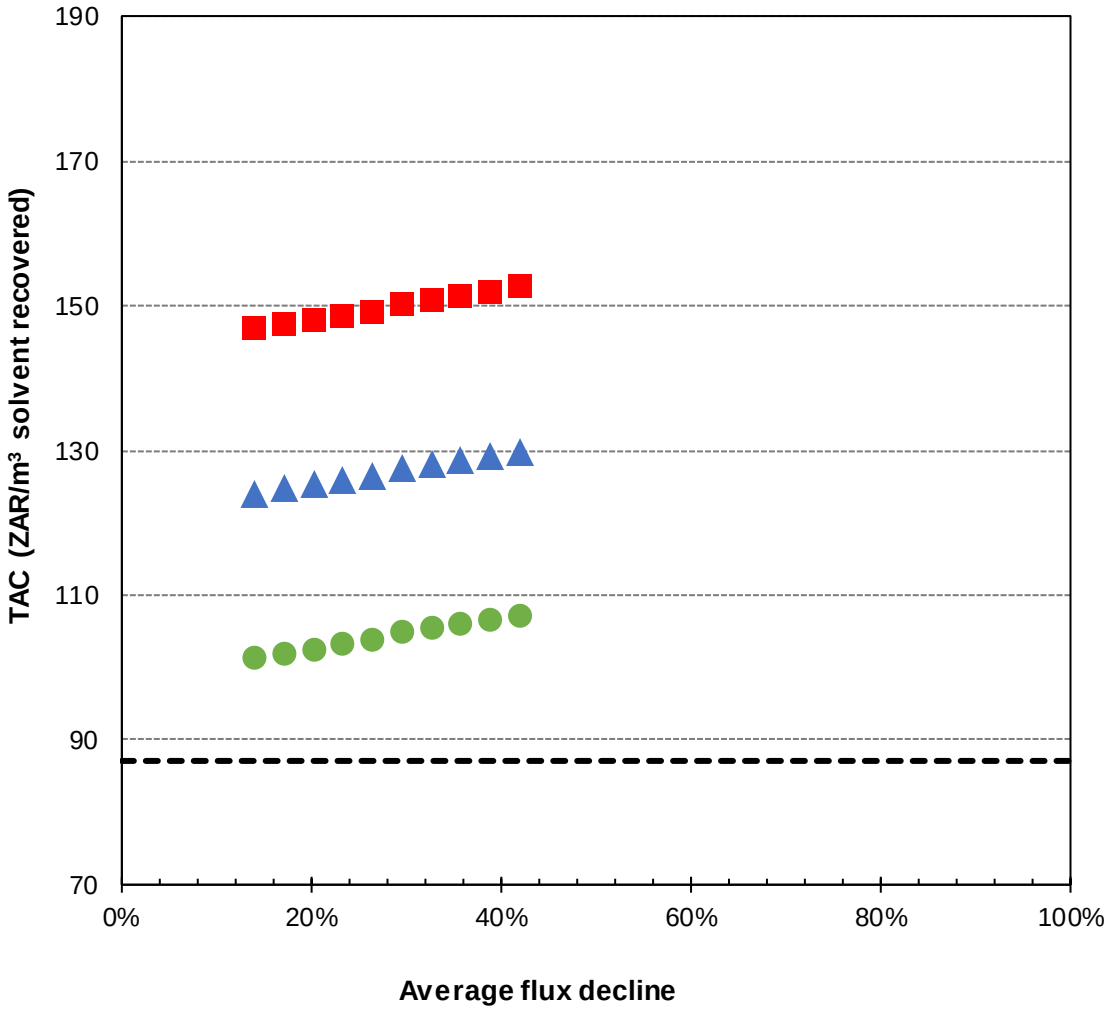

Figure D.19: Total annual cost (TAC) of the classical solvent recovery unit (---) compared to a hybrid-OSN unit at a specific membrane module cost of 1 600 ZAR/m^2 (●), 3 200 ZAR/m^2 (▲), and 4 800 ZAR/m^2 (■) for varying average flux decline over membrane life.

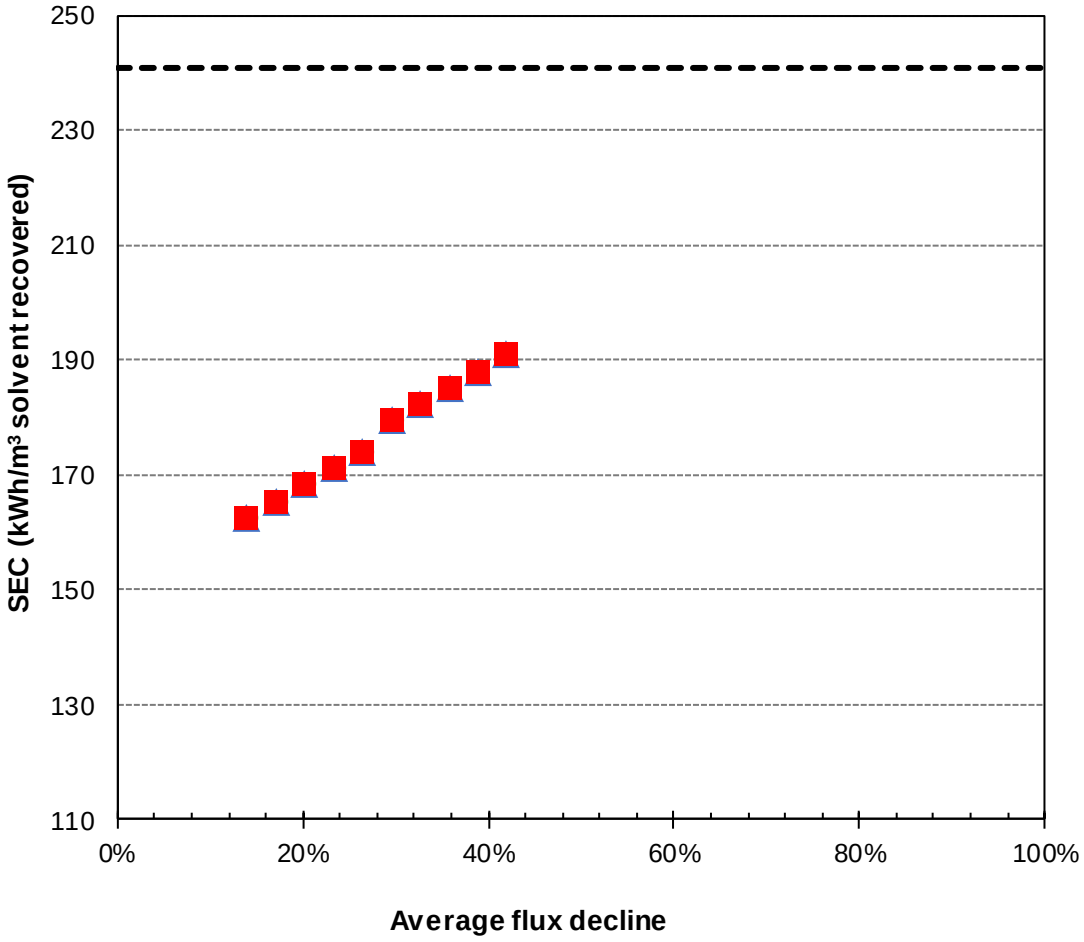

Figure D.20: Specific energy consumption (SEC) of the classical solvent recovery unit (---) compared to a hybrid-OSN unit at a specific membrane module cost of 1 600 ZAR/m^2 (●), 3 200 ZAR/m^2 (▲), and 4 800 ZAR/m^2 (■) for varying average flux decline over membrane life.

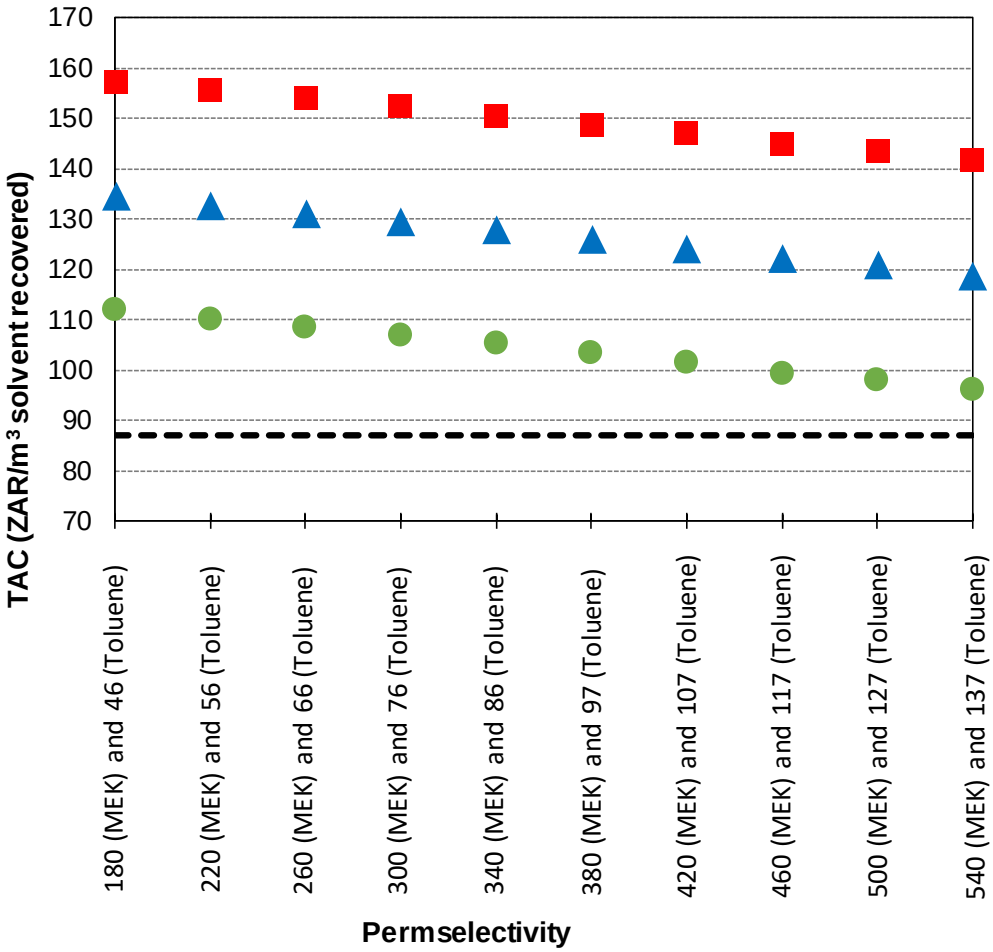

Figure D.21: Total annual cost (TAC) of the classical solvent recovery unit (---) compared to a hybrid-OSN unit at a specific membrane module cost of 1 600 ZAR/m^2 (●), 3 200 ZAR/m^2 (▲), and 4 800 ZAR/m^2 (■) for varying permselectivity.

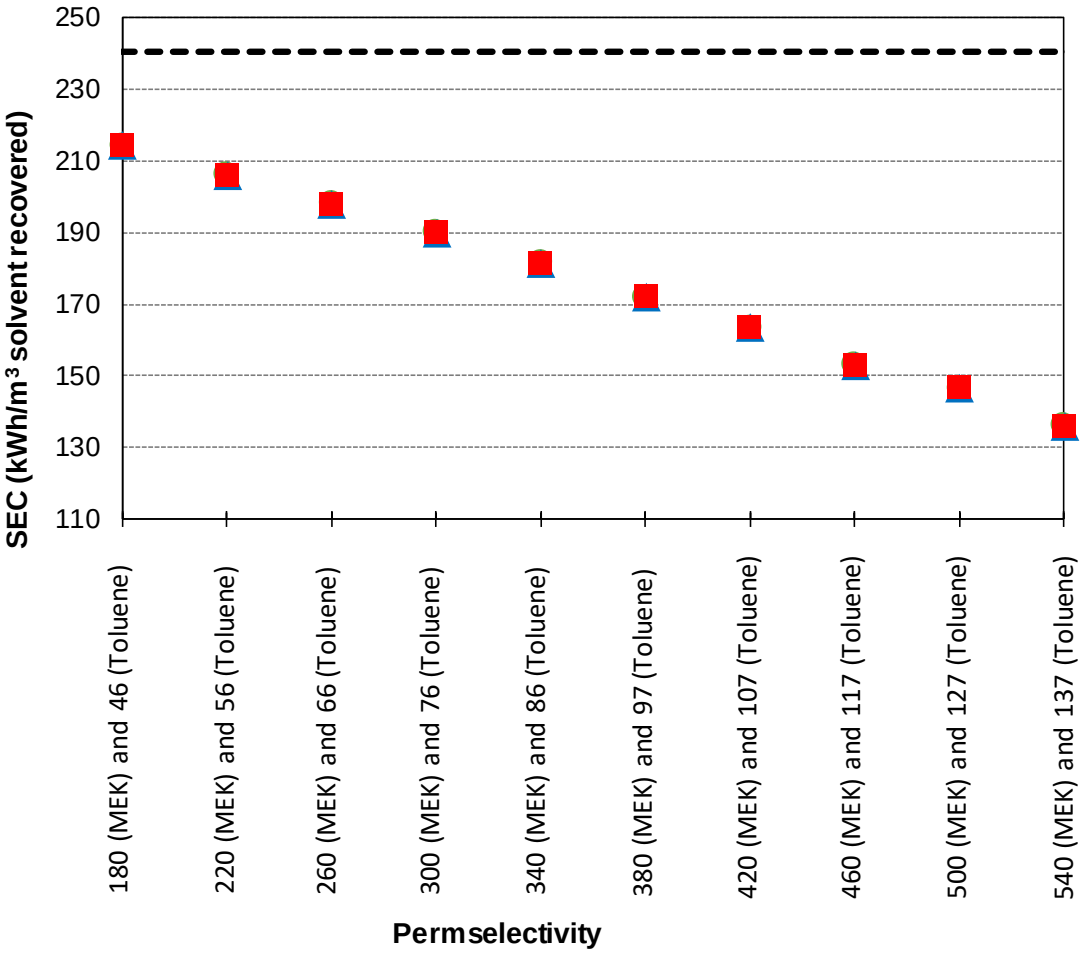

Figure D.22: Specific energy consumption (SEC) of the classical solvent recovery unit (---) compared to a hybrid-OSN unit at a specific membrane module cost of 1 600 ZAR/m^2 (●), 3 200 ZAR/m^2 (▲), and 4 800 ZAR/m^2 (■) for varying permselectivity.

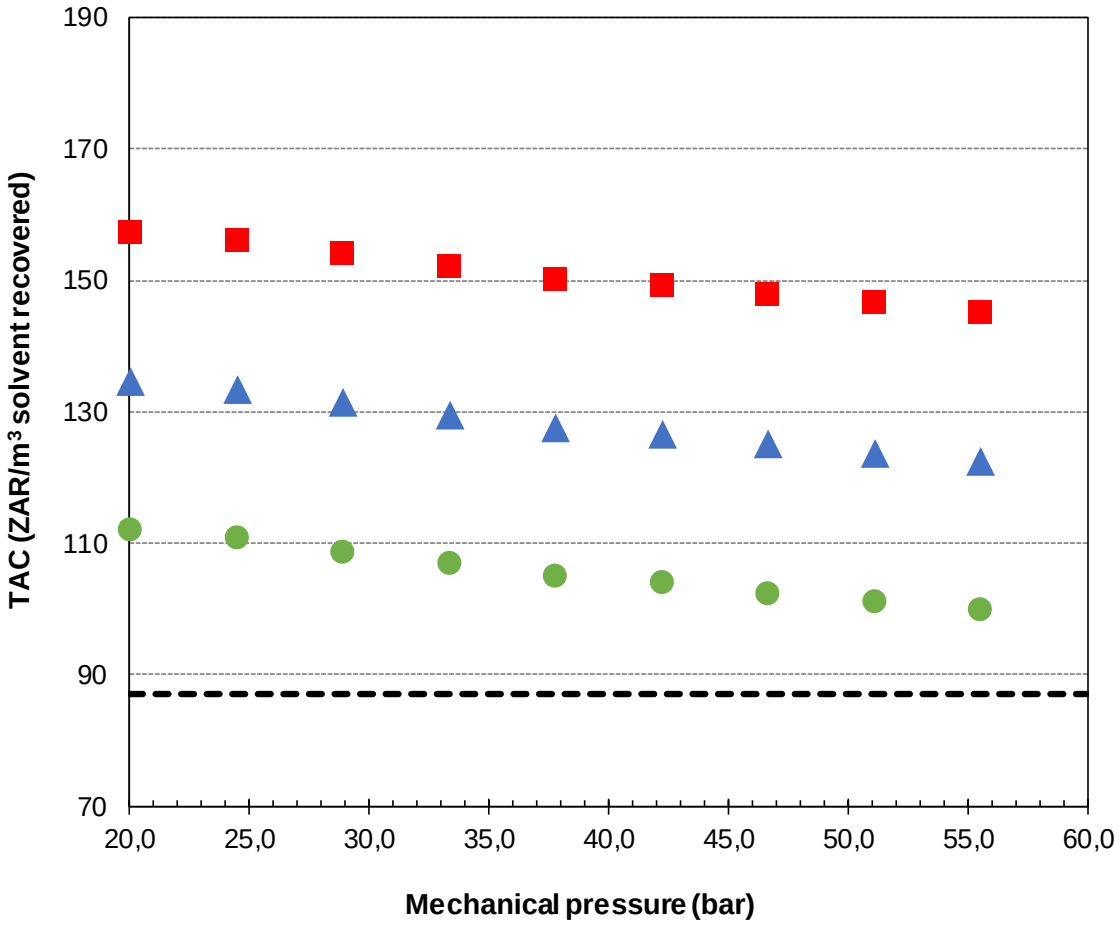

Figure D.23: Total annual cost (TAC) of the classical solvent recovery unit (---) compared to a hybrid-OSN unit at a specific membrane module cost of 1 600 ZAR/m^2 (●), 3 200 ZAR/m^2 (▲), and 4 800 ZAR/m^2 (■) for varying operating pressure.

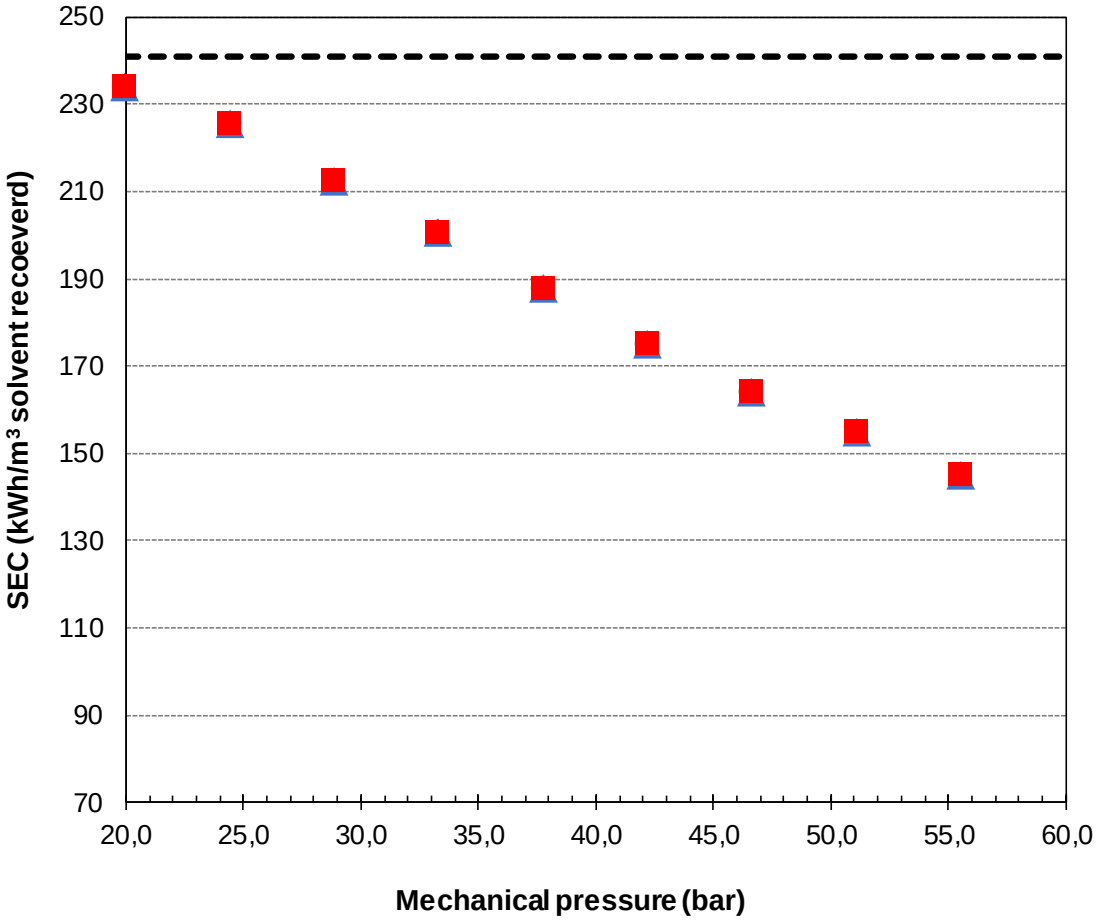

Figure D.24: Specific energy consumption (SEC) of the classical solvent recovery unit (---) compared to a hybrid-OSN unit at a specific membrane module cost of 1 600 ZAR/m^2 (●), 3 200 ZAR/m^2 (▲), and 4 800 ZAR/m^2 (■) for varying operating pressure.

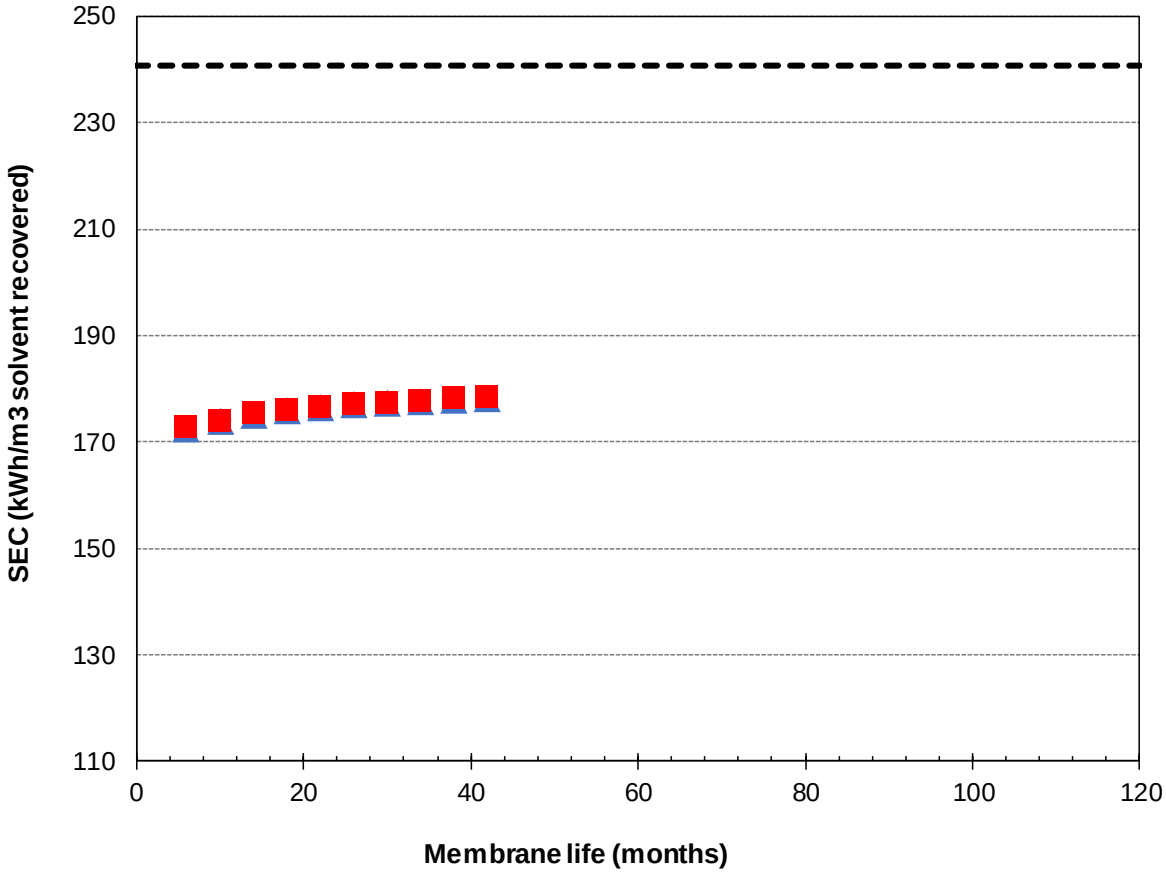

Figure D.25: Specific energy consumption (SEC) of the classical solvent recovery unit (---) compared to a hybrid-OSN unit at a specific membrane module cost of 1 600 ZAR/m^2 (●), 3 200 ZAR/m^2 (▲), and 4 800 ZAR/m^2 (■) for varying membrane life.

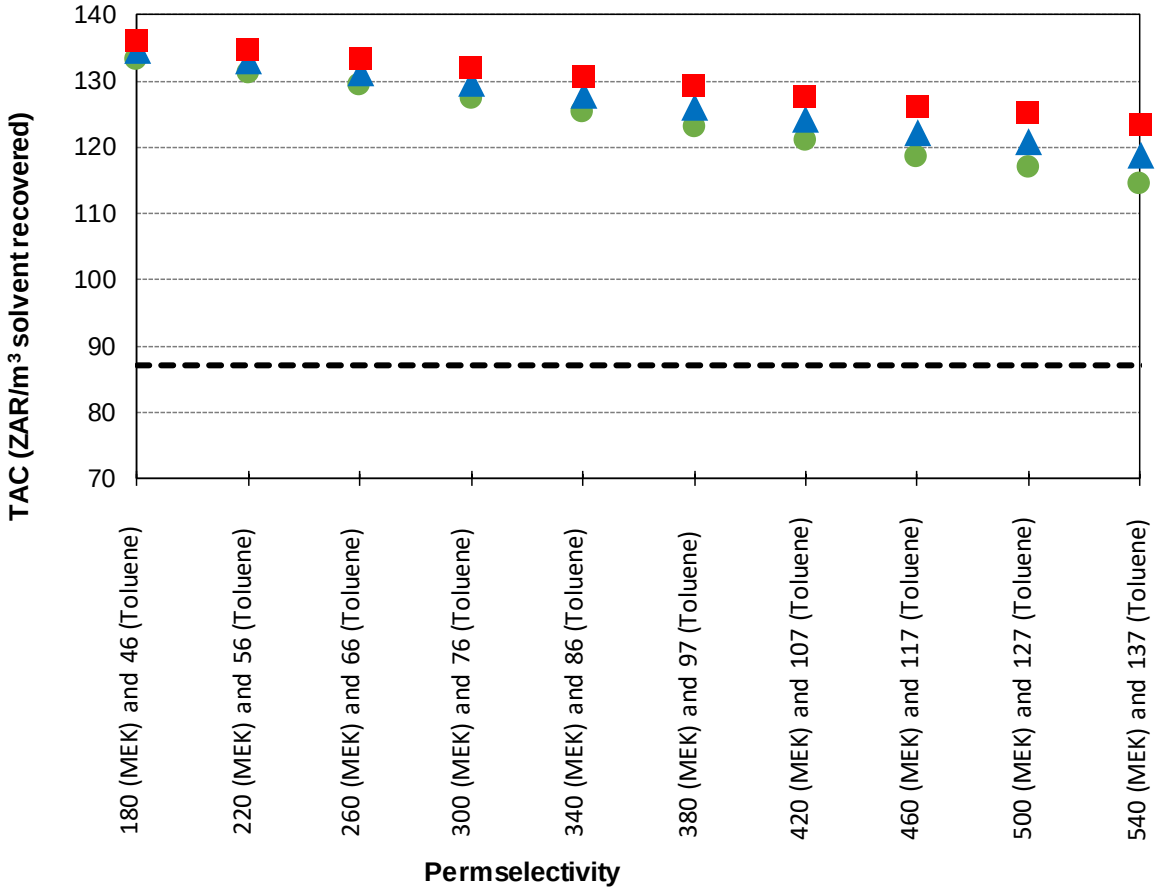

Figure D.26: Total annual cost (TAC) of the classical solvent recovery unit (---) compared to a hybrid-OSN unit at an average flux decline over membrane life of 14% (●), 28% (▲), and 42% (■) for varying permselectivity.

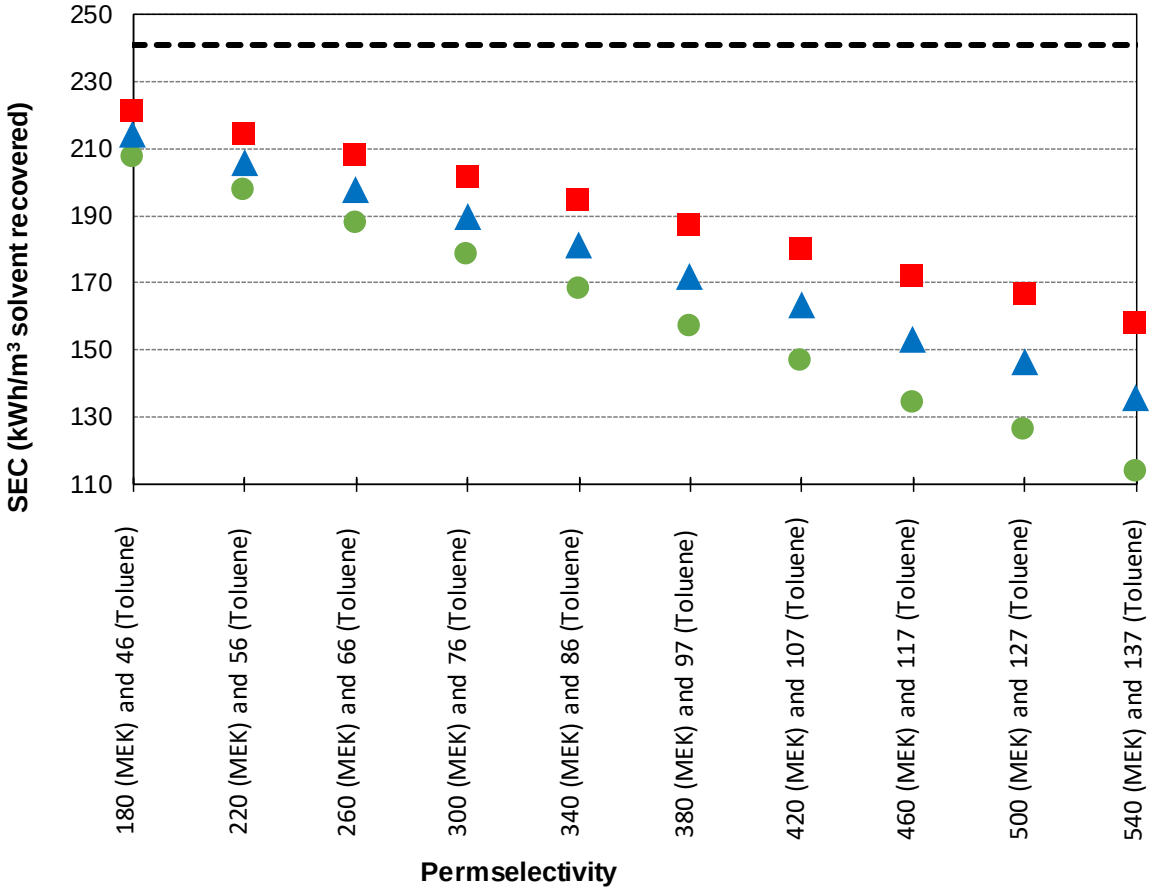

Figure D.27: Specific energy consumption (SEC) of the classical solvent recovery unit (---) compared to a hybrid-OSN unit at an average flux decline over membrane life of 14% (●), 28% (▲), and 42% (■) for varying permselectivity.

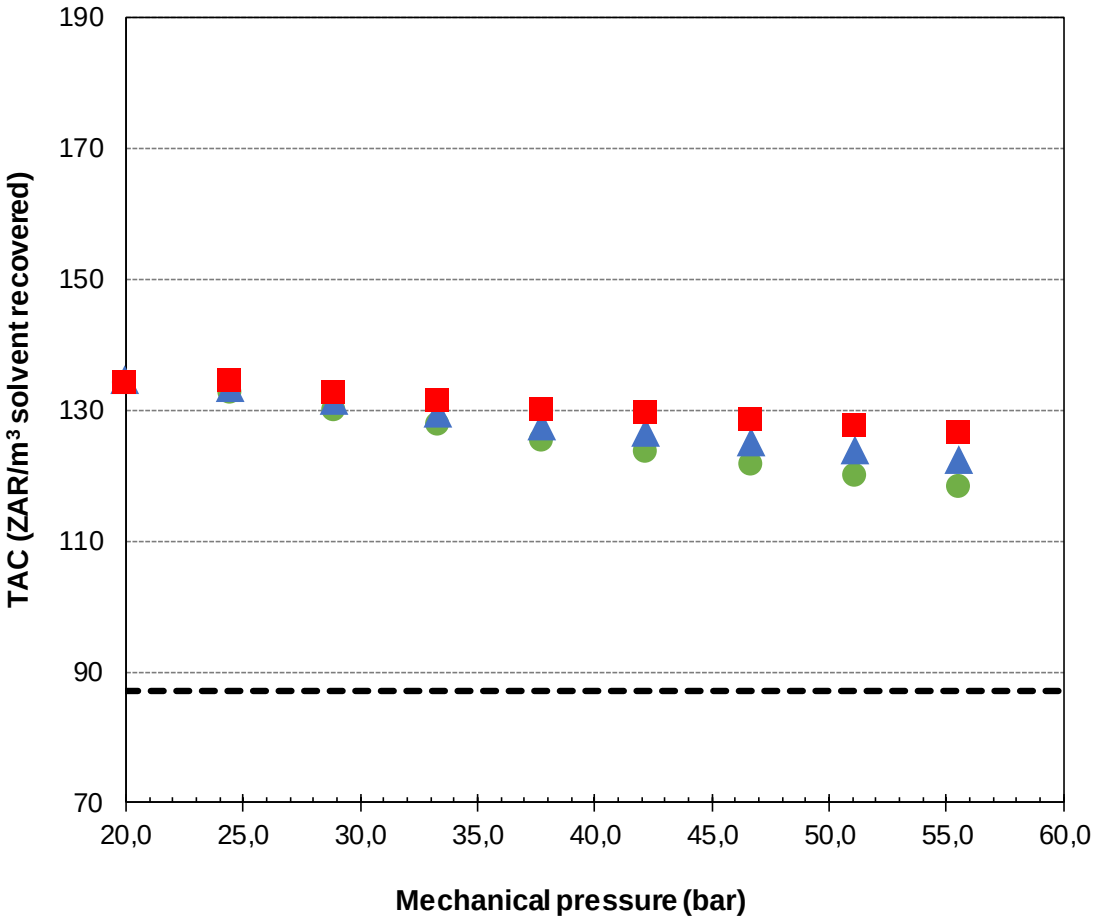

Figure D.28: Total annual cost (TAC) of the classical solvent recovery unit (---) compared to a hybrid-OSN unit at an average flux decline over membrane life of 14% (●), 28% (▲), and 42% (■) for varying operating pressure.

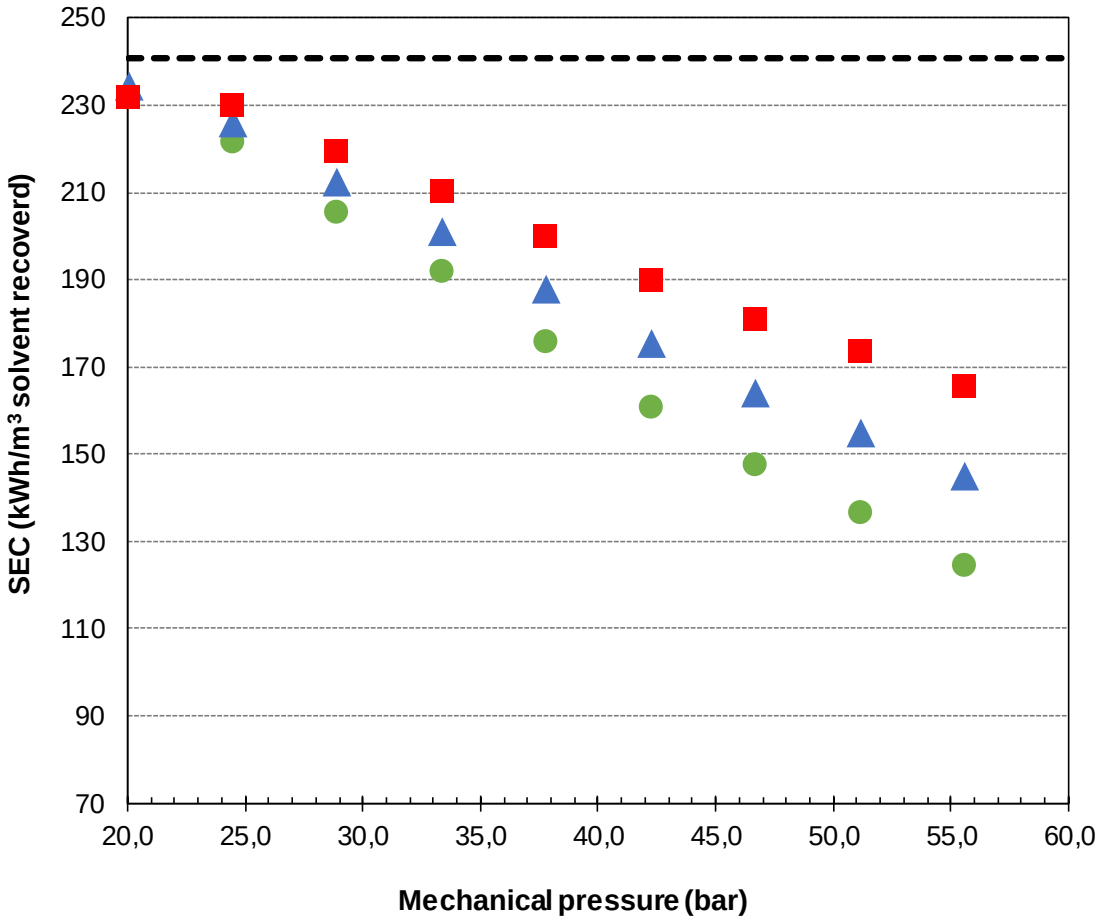

Figure D.29: Specific energy consumption (SEC) of the classical solvent recovery unit (---) compared to a hybrid-OSN unit at an average flux decline over membrane life of 14% (●), 28% (▲), and 42% (■) for varying operating pressure.

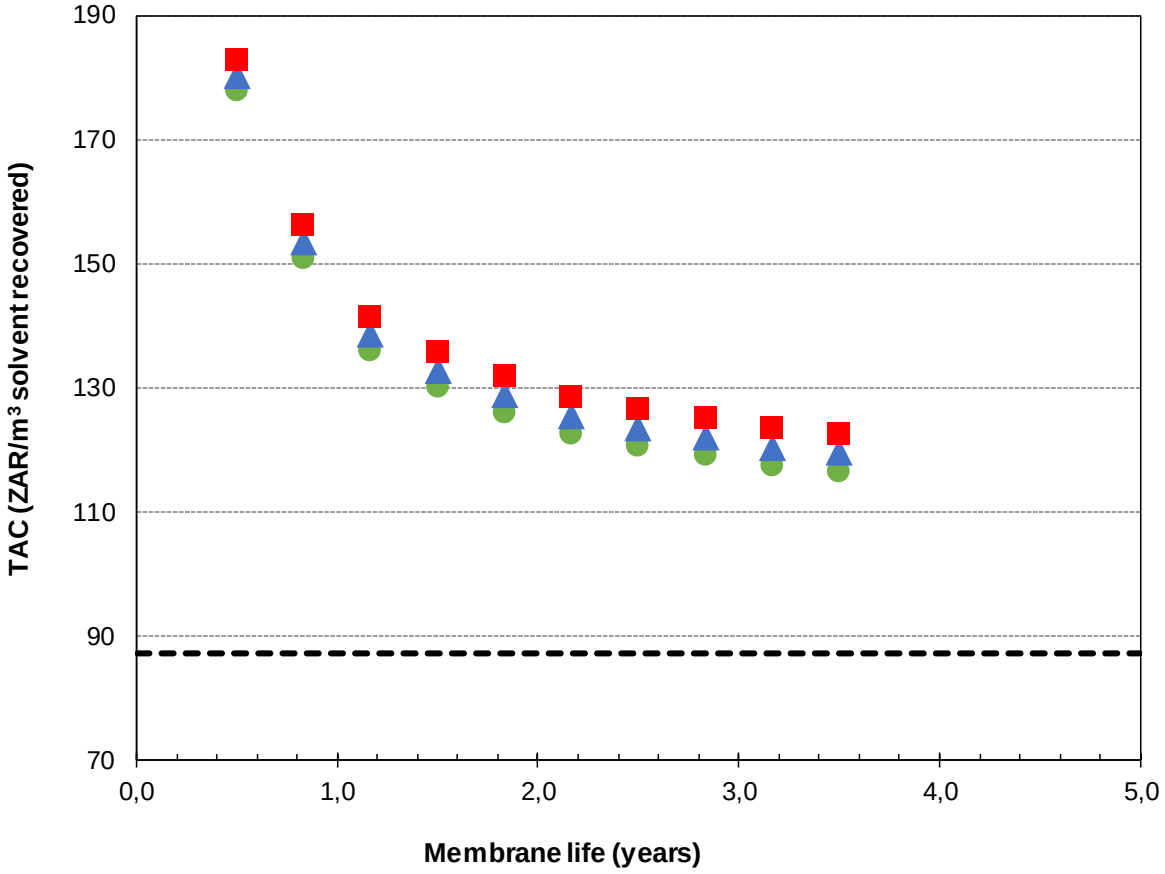

Figure D.30: Total annual cost (TAC) of the classical solvent recovery unit (---) compared to a hybrid-OSN unit at an average flux decline over membrane life of 14% (●), 28% (▲), and 42% (■) for varying membrane life.

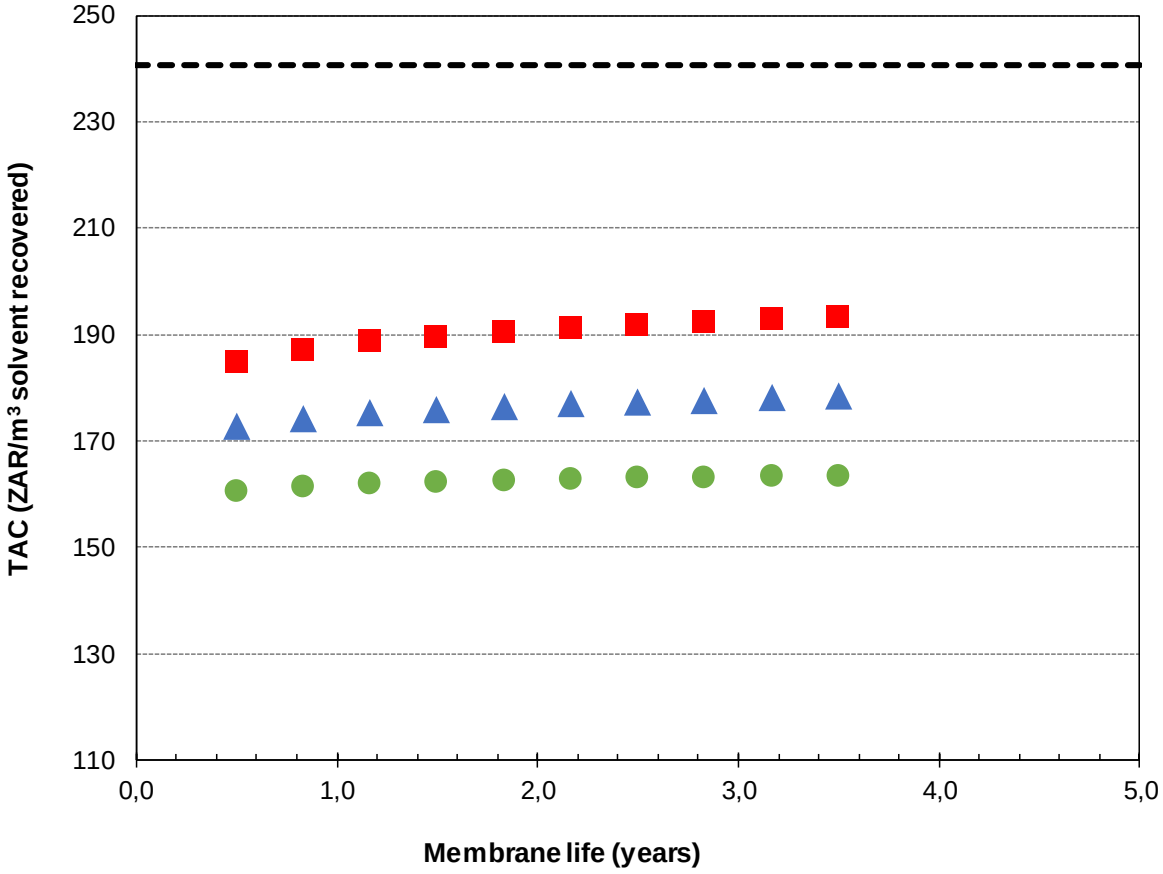

Figure D.31: Specific energy consumption (SEC) of the classical solvent recovery unit (---) compared to a hybrid-OSN unit at an average flux decline over membrane life of 14% (●), 28% (▲), and 42% (■) for varying membrane life.

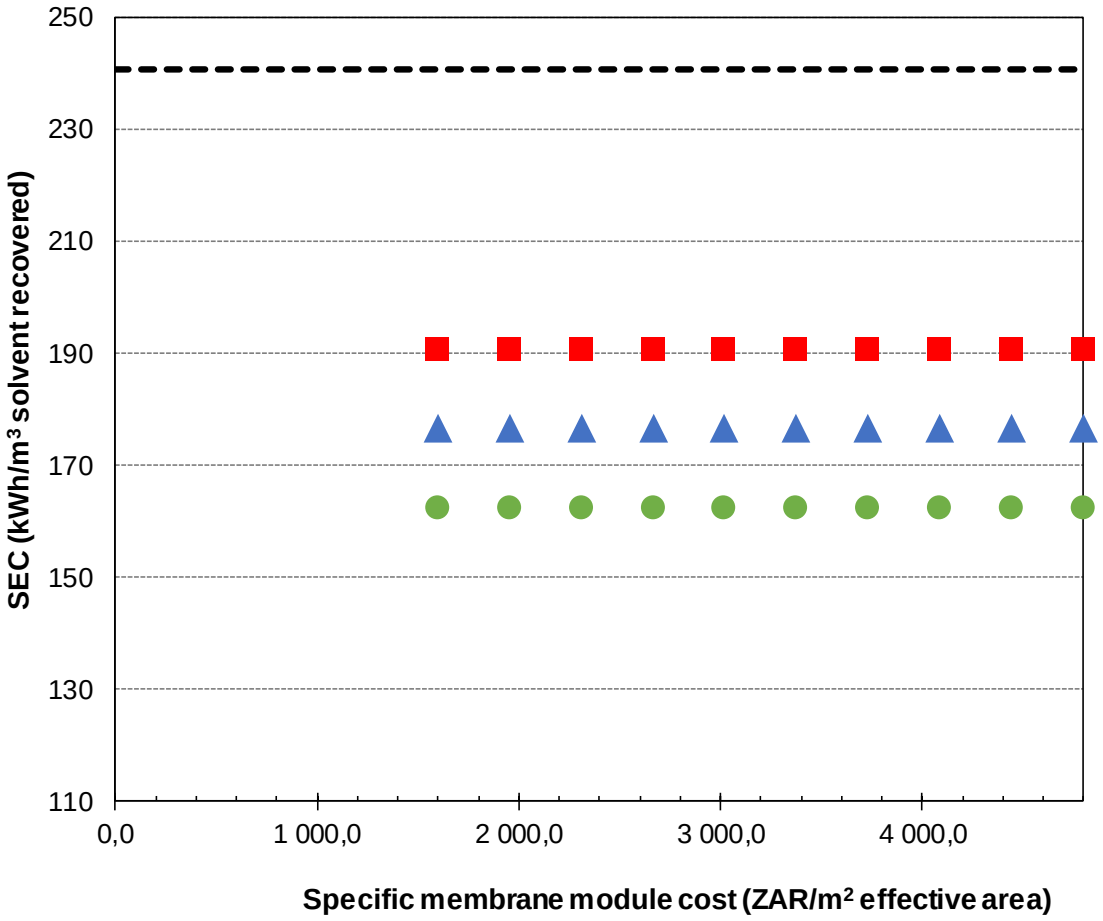

Figure D.32: Specific energy consumption (SEC) of the classical solvent recovery unit (---) compared to a hybrid-OSN unit at an average flux decline over membrane life of 14% (●), 28% (▲), and 42% (■) for varying specific membrane module cost.

APPENDIX E: INTERFACING METHODOLOGY

Spreadsheet Link (MATLAB and Excel):

Information was shared between MATLAB and Excel through the Spreadsheet Link V3.3.2. The link can be accessed in the *exlink* MATLAB toolbox. The link is inserted as an excel add-in and displayed on the ribbon of the workbook. The add-in has built-in Macro (Microsoft Visual Basic for Applications) functions that can export the values of a set of variables as a vector string to MATLAB, initiate a MATLAB function and import values back to Excel. The respective Macro functions are called *MLPutMatix*, *MLEvalString* and *MLGetMatrix*. The VBA code containing the Spreadsheet Link functions is presented in Figure E.1.

```
Public Sub SIMPLE()

Matlabinit      %Start Matlab application

MLPutMatrix "sin", Range("C5:C23")              %Export input vector to Matlab

MLEvalString ("[VFPV,J,xMF1,xMF2,FMF,xP1,xP2,FP,xC1,xC2,FC,VMF,VC,VP,CT,difR,difJ]
=SD_simplified(sin(1),sin(2),sin(3),sin(4),sin(5),sin(6),sin(7),sin(8),sin(9),
sin(10),sin(11),sin(12),sin(13),sin(14),sin(15),sin(16),sin(17),sin(18),sin(19));") %Call SD_simplified function

mlgetmatrix "VFPV", "C41"               %Assign Matlab result to an Excel block
mlgetmatrix "J", "C40"
mlgetmatrix "FMF", "C46"
mlgetmatrix "xMF1", "C43"
mlgetmatrix "xMF2", "C44"
mlgetmatrix "xP1", "C49"
mlgetmatrix "xP2", "C50"
mlgetmatrix "FP", "C52"
mlgetmatrix "xC1", "C55"
mlgetmatrix "xC2", "C56"
mlgetmatrix "FC", "C58"
mlgetmatrix "VC", "C59"
mlgetmatrix "VMF", "C47"
mlgetmatrix "VP", "C53"
mlgetmatrix "CT", "C36"
mlgetmatrix "difJ", "C34"

Matlabrequest           %Print string of results in Excel spreadsheet

End Sub
```

Figure E.1: Microsoft Visual Basic for Application code to transfer information between Excel and MATLAB.

For more information and examples, the reader is directed to *Executing Spreadsheet Link Functions* on the MathWorks forum, available at: https://www.mathworks.com/help/exlink/executing-spreadsheet-link-functions.html.

Aspen Simulation Workbook (Aspen Plus and Excel):

The ASW link is available with Aspen Plus v8.8 as an add-in, automatically included in the v8.8 installer. In the Excel workbook environment, ASW is added as a COM add-in and displayed as an extra tab. The *variable organiser* located in the ribbon of the tab is used to establish the link between an Aspen Plus simulation and Excel spreadsheet. First, the simulation's file location was added to the organiser,

followed by *activating* the simulation case. Once activated, the Aspen Plus window with the simulation case could be made visible if desired. Density and molecular weight were estimated using the UNIFAC method. The input specifications are the flowrate of MEK, toluene and lube-oil, temperature and pressure. The inputs and results were copied to the *variable organiser,* saving the exact location where the inputs were assigned, and results were generated. Once all the variables were added, a *scenario table* was created where new input values can be assigned and resulting properties may be examined.

The stream information and physical properties of the feed solution was simulated in the Aspen Plus process modelling platform. The solution properties involving MW and ρ were predicted with the UNIFAC thermodynamic model so that converting between mass, volume and moles could be possible. In the Aspen Plus environment, OSN plant was represented by a separator block with one feed and two product streams for permeate and final concentrate. The input information shown in Figure 3.6 was transferred to an Excel worksheet using the ASW link. The permeate product of the OSN separator block is defined based on the overall permeate recovered in the plant. Once the OSN block has been defined, process simulation of solvent recovery involving OSN was possible.